Journal of
Medicinal Chemistry

Article

Elucidating the Structural Requirement of Uridylpeptide Antibiotics for Antibacterial Activity

Yuma Terasawa, Chisato Sataka, Toyotaka Sato, Kazuki Yamamoto, Yukari Fukushima, Chie Nakajima, Yasuhiko Suzuki, Akira Katsuyama, Takanori Matsumaru, Fumika Yakushiji, Shin-ichi Yokota, and Satoshi Ichikawa

J. Med. Chem., **Just Accepted Manuscript** • DOI: 10.1021/acs.jmedchem.0c00973 • Publication Date (Web): 28 Jul 2020

Just Accepted

is published by the American Chemical Society. 1155 Sixteenth Street N.W., Washington, DC 20036

Elucidating the Structural Requirement of Uridylpeptide Antibiotics for Antibacterial Activity

Yuma Terasawa,[a] Chisato Sataka,[a] Toyotaka Sato,[b] Kazuki Yamamoto,[a] Yukari Fukushima,[c] Chie Nakajima,[c,d] Yasuhiko Suzuki,[c,d] Akira Katsuyama,[a,e] Takanori Matsumaru,[a,e,†] Fumika Yakushiji,[a,e] Shin-ichi Yokota,[b] and Satoshi Ichikawa[a,e,f*]

[a]*Faculty of Pharmaceutical Sciences, Hokkaido University, Kita-12, Nishi-6, Kita-ku, Sapporo 060-0812, Japan*

[b]*Department of Microbiology, Sapporo Medical University School of Medicine, South-1, West-17, Chuo-ku, Sapporo, 060-8556, Japan*

[c]*Division of Bioresources, Hokkaido University Research Center for Zoonosis Control, Sapporo, 001-0020, Japan*

[d]*Global Station for Zoonosis Control, Global Institution for Collaborative Research and Education (GI-CoRE), Hokkaido University, Kita-20, Nishi-10, Kita-ku, Sapporo, 001-0020, Japan*

[e]*Center for Research and Education on Drug Discovery, Faculty of Pharmaceutical Sciences, Hokkaido University, Kita-12, Nishi-6, Kita-ku, Sapporo 060-0812, Japan*

[f]*Global Station for Biosurfaces and Drug Discovery, Global Institution for Collaborative Research and Education (GI-CoRE), Hokkaido University, Kita-12, Nishi-6, Kita-ku, Sapporo 060-0812, Sapporo, Japan*

[†]*Current affiliation: Department of Chemistry, Faculty of Science and Technology, Keio University, Hiyoshi 3-14-1, Minatokita-ku, Yokohama, 223-8522, Japan*

Abstract

The synthesis and biological evaluation of analogues of uridylpeptide antibiotics were described, and the molecular interaction between the 3′-hydroxy analogue of mureidomycin A (3′-hydroxymureidomycin A) and its target enzyme, MraY, was analyzed in detail. The structure-activity relationship involving MraY inhibition suggests that the side chain at the urea-dipeptide moiety does not affect the MraY inhibition. However, the anti-*Pseudomonas aeruginosa* activity is in great contrast and the urea-dipeptide motif is a key contributor. It is also suggested that the nucleoside peptide permease NppA1A2BCD is responsible for the transport of 3′-hydroxymureidomycin A into the cytoplasm A systematic structure-activity relationship analysis of the urea-dipeptide moiety of 3′-hydroxymureidomycin A was further conducted and determined that the antibacterial activity. This study provides a guide for the rational design of analogues based on uridylpeptide antibiotics.

Introduction

Pseudomonas aeruginosa, which is classified as a Gram-negative bacteria, is a common nosocomial pathogen; healthy individuals are rarely infected by this pathogen because of its low pathogenicity. However, opportunistic and nosocomial infections in

newborns and patients with weakened immunity have become problematic. *P. aeruginosa* also locally infects the urethra, airways and wounds following medical procedures such as surgery and catheterization, in addition to burns, trauma and purulent sites; moreover, infection of patients with cystic fibrosis and chronic respiratory diseases by *P. aeruginosa* can cause increased patient mortality.[1-4] In addition, local infection is followed by systemic infections, such as pneumonia and peritonitis, and it is known that the fatality rate of sepsis due to *P. aeruginosa* in the blood is as high as 80%. Thus, *P. aeruginosa* is among pathogens that must be carefully treated because it worsens the prognosis and mortality of patients. Compared to Gram-positive pathogens, *P. aeruginosa* is inherently less susceptible to antibacterial drugs currently used in the clinic because it possesses an outer membrane that acts as a barrier to prevent their permeation. Furthermore, multi-drug-resistant *P. aeruginosa*, which is resistant to all carbapenems, aminoglycosides, and fluoroquinolones used for the treatment of *P. aeruginosa* infection, has emerged in the clinic. The fatality rate caused by its infection is high because of the very limited number of effective drugs and is the cause of a severe global health problem. Consequently, development of new drugs for multi-drug-resistant *P. aeruginosa* is an urgent task for worldwide health care.[5-7] In choosing novel antibacterial agents, the target must be

essential for their growth, and the agent's mechanism of action should be different from those of existing drugs.[8-12]

Uridylpeptide antibiotics are nucleoside natural products sharing a common structural feature; a 3′-deoxyuridine with a *Z*-enamide linkage is attached to a tetrapeptide moiety with a urea linkage reversing the direction of the *N*- and *C*-termini, with α,β-diaminobutylic acid playing a pivotal role by connecting the *N*-terminal amino acid, the urea-dipeptide, and the 3′-deoxyuridine moieties (Figure 1).[13-14] The class includes mureidomycins (MRDs),[15] napsamycins,[16] pacidamycins (PCDs),[17] and sansanmycins.[18] Uridylpeptide antibiotics are a growing class of nucleoside natural products, and their chemical structures vary with various amino acid residues. Among the class of uridylpeptide antibiotics, the MRDs, isolated from *Streptomyces flavidoviridens* SANK 60486, have been reported to show the most potent antibacterial activity against strains of *Pseudomonas* (minimum inhibitory concentration (MIC) 1.5–12.5 μg/mL) *in vitro* and can also protect mice against *P. aeruginosa* infection.[15b,c] The MRDs and PCDs have been reported to inhibit the formation of lipid II and peptidoglycan and are strong inhibitors of the phospho-MurNAc-pentapeptide transferase (MraY),[19,20] which is responsible for the formation of lipid I in the peptidoglycan biosynthesis pathway.[19-24] Since MraY is an essential enzyme in bacteria, it is a potential target for the development

of general antibacterial agents.[25] A narrow antibacterial spectrum is characteristic of

uridylpeptide antibiotics.[15b,c] They exhibit highly selective antibacterial activity against

P. aeruginosa but not against other Gram-negative and Gram-positive bacterial pathogens.

Different from Gram-positive bacteria, Gram-negative bacteria possess an outer

membrane, which acts as a physiological barrier preventing antibacterial drugs from

reaching the periplasm. Only limited nutrients and ions necessary for bacterial growth

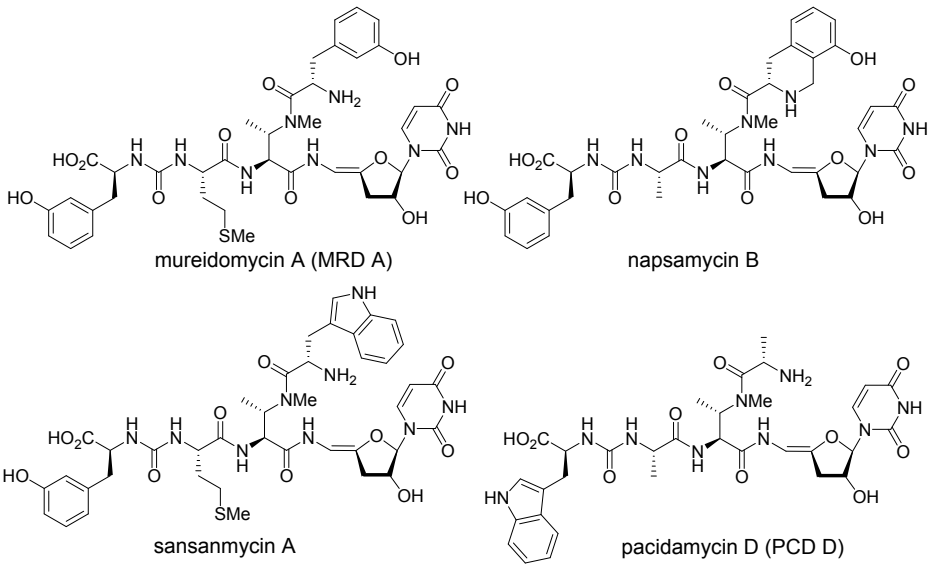

Figure 1. Structures of Uridylpeptide Natural Products

can be incorporated through specific transporters. The observed narrow spectrum of uridylpeptides indicates that they utilize a transporter specifically expressed on *P. aeruginosa*.[26] We have recently investigated the MraY inhibitory and anti-*P.aeruginosa* activities of synthetic pacidamycin D (PCD D) and its 3′-hydroxy analogue **1** (3′-hPCD D, Figure 2).[27,28] They exhibited potent MraY inhibitory activity with IC_{50} values of 22 nM for PCD D and 42 nM for **1** and moderate antibacterial activity against *P. aeruginosa.* The existence of a hydroxyl group at the 3′-position of the uridine moiety does not interfere with either the MraY inhibition or the antibacterial activity. The 3′-hydroxy analogues of uridylpeptide antibiotics are a good starting point to investigate a structure-activity relationship (SAR) of uridylpeptide antibiotics since the 3′-hydroxy analogues are more accessible from a chemical synthesis point of view. Judging from the data

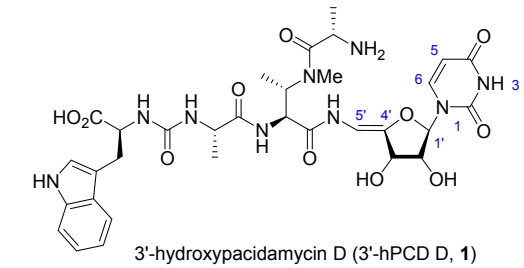

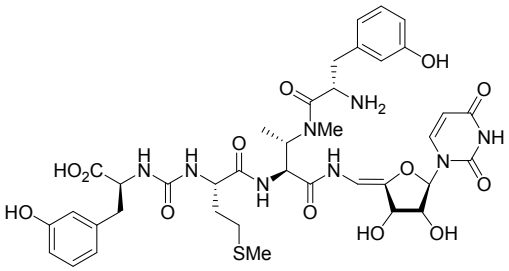

Figure 2. Structures of 3'-hydroxyuridylpeptide analogues

reported in the literature, among the uridylpeptide antibiotics shown in Figure 1, those possessing the L-*m*-tyrosine (L-*m*Tyr) on both *N*- and *C*-termini, namely, the MDRs, seem to exhibit the strongest antibacterial activity against *P. aeruginosa*. Although SAR studies of antibacterial activity of this class of natural products have independently been conducted,[29-39] the strains tested were not uniform. Therefore, a side-by-side comparison of the impact of each amino acid residue on both MraY inhibition and antibacterial activity must be performed to understand the molecular basis of uridylpeptide antibiotics. Very recently, we reported a complex structure of 3′-hydroxymureidomycin A (3′-hMRD A, **2**, Figure 2) bound to MraY from *Aquifex aeolicus* ($MraY_{AA}$).[40] Here, we describe the detailed synthesis, biological evaluation and further SAR of **2**. In addition, a transporter responsible for uptake of **2** is also proposed. The aim of this study is to elucidate the structural requirements of **2** for both MraY inhibition and antibacterial activity against *P. aeruginosa* to gain insight into future drug design based on uridylpeptide antibiotics.

Results and discussion

Synthesis of 3′-hydroxymureidomycin A. We have previously accomplished the total synthesis of PCD D and **1** featuring a stereoselective construction of the *Z*-oxy-acyl enamide architecture by copper-catalyzed *C*-*N* cross-coupling.[27,28] We have also developed the second-generation synthesis of **1** via a Ugi four-component reaction.[38] This

Scheme 1

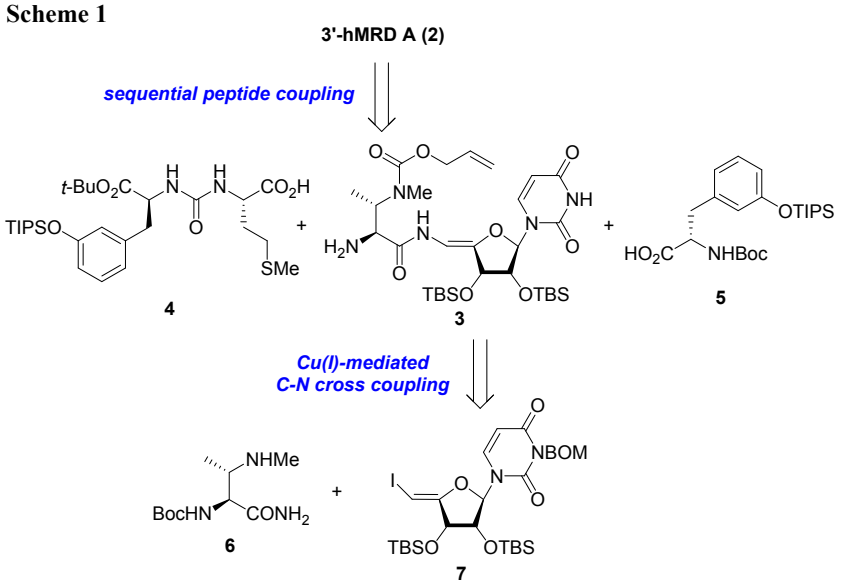

second-generation synthesis is a convergent method to provide a range of analogues. However, it also provided an undesired and inactive diastereomer at the 2,3-diaminobutanoic acid residue. Therefore, we developed a more efficient third-generation synthesis to investigate the systematic SAR of uridylpeptide antibiotics. Our retrosynthetic analysis of **2** is shown in Scheme 1. The 2,3-diaminobutanoic acid residue linking to the uridine moiety with a *Z*-enamide linkage plays a role as a branching scaffold and both the urea-dipeptide and the amino acid are linked to two nitrogen atoms by forming primary and secondary carboxamide linkages. Thereby, **2** was disconnected from these components, **3**-**5**. Thus, a range of analogues suitable for investigating the SAR regarding the urea-dipeptide and the amino acids on both termini could be attained in the last stage of the synthesis. A uridine derivative connected to diaminobutanoic acid via an

enamide linkage **3** was disconnected from the 2,3-diaminobutancarboxamide **6** and the *Z*-vinyl iodide **7** by copper-catalyzed *C*-*N* cross-coupling.

Scheme 2

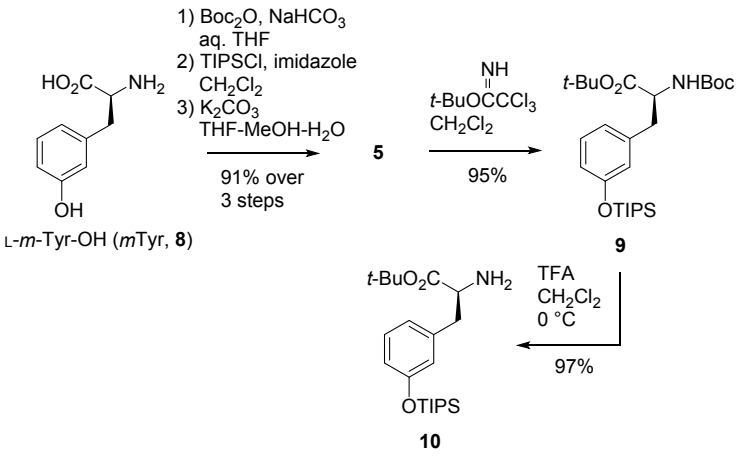

Suitably protected L-*m*Tyr derivatives **5** and **10** were prepared starting from commercially available L-*m*Tyr as shown in Scheme 2. Solution phase synthesis has thus far been used for synthesis of urea-dipeptide; however, it sometimes causes a decrease in the yield of the desired urea-dipeptide due to homodimer formation. Therefore, solid phase synthesis was applied, in which an asymmetric urea-dipeptide can be selectively and easily synthesized a simple purification procedure (Scheme 3).[41] Fmoc-L-methionine immobilized on 2-chlorotrityl resin was treated with piperidine, and the resulting amine was converted to the corresponding carbonylimidazolidate, which was reacted with **10** in the presence of *i*-Pr_2NEt to yield urea **12**. Finally, removal of the urea-dipeptide from the resin by treatment with 1% TFA in CH_2Cl_2 cleanly provided **4** with a 78% yield over four

steps from **11**. This method is suitable for the comprehensive preparation of a variety of urea-dipeptides.

Scheme 3

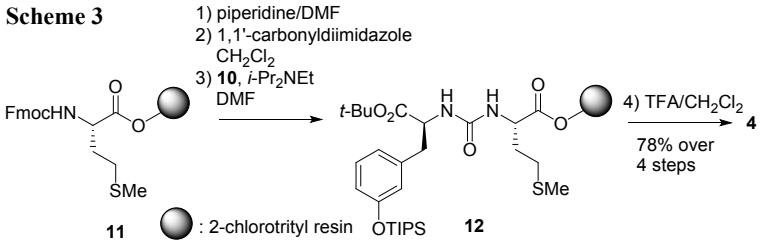

With **4** and **5** in hand, synthesis of **2** was investigated as shown in Scheme 4. The

carboxylic acid **13**, which was readily prepared from L-threonine in six steps in large

quantity by using a previous procedure,[31] was converted to the carboxamide **14** in 81%

yield (NH_4Cl, HATU, *i*-Pr_2NEt, DMF). After cleavage of the *N*-*O* bond of **14** by catalytic hydrogenolysis (H_2, $Pd(OH)_2$, MeOH), the liberated amine **6** was directly coupled with

Scheme 4

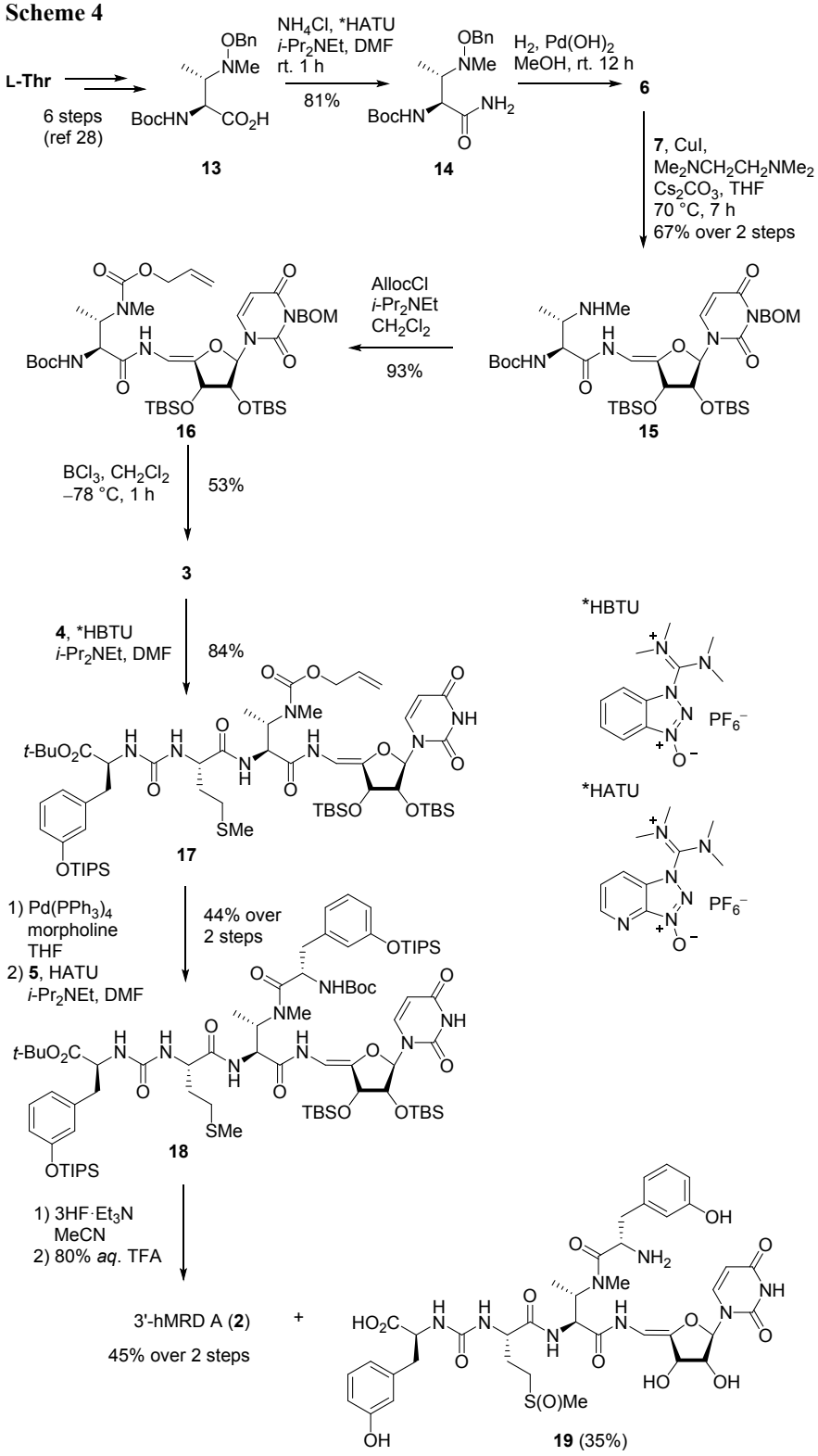

the iodide **7**[27,28] under the conditions using CuI, $MeNHCH_2CH_2NHMe$, and Cs_2CO_3 in THF at 70 °C to give the desired *Z*-enamide **15** in 67% yield. Cross coupling of **7** and **14** also proceeded to produce the corresponding *Z*-enamide in good yield, however the following *N*-*O* bond cleavage was unsuccessful. After protection of the *N*-methylamine of the carboxamide **6** with an allyloxycarbonyl (Alloc) group, the corresponding *N*-Alloc carboxamide was used for the coupling. In this case, an unknown byproduct was mainly generated, and the desired **16** was not obtained at all. This problem was solved by simply changing the order of the cross coupling and Alloc protection reactions. After the *N*-methyamino group of **15** was protected by the Alloc group to give **16** in 93% yield, simultaneous deprotection of the benzyloxymethyl (BOM) and Boc groups was achieved with BCl_3 in CH_2Cl_2 at −78 °C to afford **3** in 53% yield. The primary amine **3** was condensed with the urea-dipeptide **4** (HBTU and *i*-Pr_2NEt in DMF) to give **17** in 84% yield. Removal of the Alloc group at the *N*-terminus of **17** was conducted by the use of conventional conditions ($Pd(PPh_3)_4$, morphorine, THF), and the resulting *N*-methylamine was condensed with **5** in the presence of HATU and *i*-Pr_2NEt in DMF to afford the fully protected 3′-hMRD A **18** in 44% yield over two steps. Finally, deprotection of the TBS groups ($3HF \cdot Et_3N$, MeCN) followed by the Boc and *t*-Bu groups (80% *aq*. TFA) successfully provided 3′-hMRD A (**2**) in 45% yield over two steps. During 80% *aq*. TFA

treatment, the methythio group was oxidized, and the corresponding sulfoxide **19** was also obtained in 35% yield, which was easily separated by reverse-phase column chromatography.

Biological activity of 2. The MraY inhibition of **2** was evaluated with fluorescence-

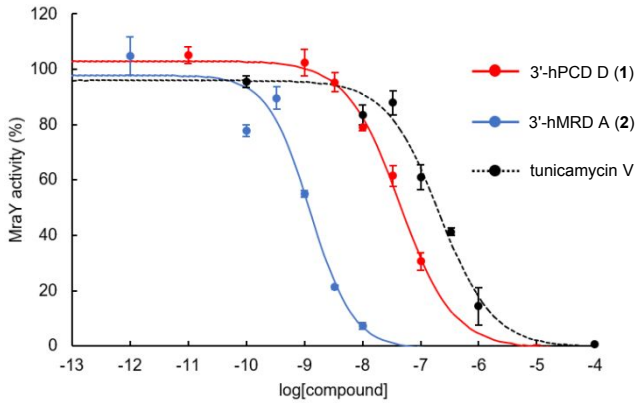

Figure 3. MraY inhibitory activity of analogues. [a]The inhibitory activities of the compounds against purified MraY from *S. aureus*. Reaction was conducted with 50 mM Tris-HCl (pH 7.6), 50 mM KCl, 25 mM $MgCl_2$, 0.2% Triton X-100, 8% glycerol, 50 μM C55-P, 10 μM UDP-MurNAc-dansylpentapeptide, and MraY enzyme (55 ng/5 μL/well). After 3-4 h incubation at room temperature, the formation of dansylated lipid I was monitored by fluorescence enhancement (excitation at 355 nm, emission at 535 nm). The data were obtained from three independent experiments.

based MraY inhibitory assay[42] using the purified MraY enzyme (*S. aureus*, $MraY_{SA}$) and

dansylated Park's nucleotide that was prepared by dansylation of Park's nucleotide

chemically synthesized with our method.[43] The data were obtained from three

independent experiments. As shown in Figure 3 and Table 1, **2** exhibits a strong $MraY_{SA}$ inhibitory activity, with an IC_{50} value of 1.3±0.2 nM, and is 34-fold more potent than **1**. The antibacterial activity of **2** against a range of *P. aeruginosa* strain, including a variety

Table 1. Biological activity of 1 and 2

		1	**2**
IC_{50} for $MraY_{SA}$ (nM)[a]		44 ± 4	1.3 ± 0.2
IC_{50} for HepG2 (μM)[b]		>100	>100
strains		MIC (μg/mL)[a]	
PAO1		16-32	4-16
ATCC27853		32-128	4-16
MDRP62	multi-drug resistant	>128	16-32
1483	clinical isolate	>128	8-32
1485	clinical isolate	16-64	4-8
2867	clinical isolate	32-128	8-32
2931	clinical isolate	>128	16
9728b	clinical isolate	>128	32
IID1001	serotype A	>128	64-128
IID1002	serotype B	>128	16
IID1007	serotype B	>128	32-128
IID1013	serotype B	>128	>128
IID5004	serotype B	64-128	8-16
IID1021	serotype C	16-64	8-32
IID1004	serotype D	>128	8-16
IID1130	serotype E	>128	16-32
IID1006	serotype F	>128	>128
IID1020	serotype G	>128	8-16
IID1009	serotype H	32-128	8-32
IID1010	serotype I	>128	32-128
IID1011	serotype J	>128	16-32
IID1012	serotype K	64-128	16-64
IID5141	serotype L	32	4-16
IID1015	serotype M	>128	16-32
IID5018	serotype M	>128	>128

[a]The inhibitory activities of the compounds against purified MraY from *S. aureus* was determined in a manner similar to the experiments shown in Figure 3. [b]HepG2 cells were seeded in 96-well tissue culture plates at a $1x10^5$ cells/well. After 24 h, cells were treated with varying concentrations of compounds for 48 h. After the treatment, the cell viability was measured by WST-8 assay. In there experiments, tunicamycin exhibited cytotoxicity with the IC_{50} value of 38.6 μM. [c]MICs were determined by a microdilution broth method as recommended by the CLSI. The data were obtained from three independent experiments described as a range of the values.

of clinical isolates and serotypes was then investigated. The data were obtained from three independent experiments, and MIC values for each compound are within four-fold, which are described as a range of these values. 3′-Hydroxymureidomycin (**2**) exhibits a potent antibacterial activity over a wide range of *P. aeruginosa* strains with MIC values ranging from 4-128 μg/mL, which are lower than those of **1**. It is noteworthy that **2** is effective against multi-drug-resistant *P. aeruginosa* (MDRP62) with an MIC value of 16-32 μg/mL. Improvement of the $MraY_{SA}$ inhibitory activity of **2** over **1** is correlated with the anti-*P. aeruginosa* activity, and it was revealed that **2** possesses superior properties in terms of both $MraY_{SA}$ inhibitory activity and anti-*P. aeruginosa* activity. Overall, the replacement of amino acid resides at both *C*- and *N*-termini with L-*m*Tyrs improved the biological activity, confirming **2** as a superior candidate, as expected from the literature review.[13-20] Selective toxicity is an important issue in chemotherapy for infectious disease. Accordingly, the cytotoxicity of **2** against human hepatocellular carcinoma (HepG2) cells was then evaluated. Tunicamycins were also tested as a positive control and showed evidence of cytotoxicity, with an IC_{50} of 38.6 μM. Under these conditions, **2** exhibited no cytotoxicity (IC_{50} >100 μM). This result indicates that **2** showed selective toxicity against bacterial strains. The observed high therapeutic index is a desirable

property for antibacterial agents. Thus, **2** was confirmed to be a selective anti-*P. aeruginosa* agent.

Elucidating the interaction between MraY and 2. The X-ray crystal structure of a complex of muraymycin D2 (MRY D2), other class of nucleoside natural product and a strong MraY inhibitor, bound to MraY from *Aquifex aeolicus* ($MraY_{AA}$) has been elucidated (PDB code 5CKR, 2.95 Å).[44] It is also revealed that $MraY_{AA}$ undergoes a large conformational change upon binding to MRY D2 by comparing the structure with the apo$MraY_{AA}$ structure (PDB code 4J72) (Figure 4b, d, f).[45] With **2** possessing better properties, the X-ray crystal structure of a complex of **2** bound to $MraY_{AA}$ (PDB code 6OZ6, 3.832–3.70 Å) was solved by our collaborative study to understand the molecular basis of the interaction of **2** and $MraY_{AA}$ (Figure 4a, c, e).[40] The complex of **2** bound to $MraY_{AA}$ is similar to that of MRY D2. Using the alignment of the sequence of $MraY_{SA}$ and MraY from *P. aeruginosa* ($MraY_{PA}$) (Figure 5, for larger image, see Supporting Information) on the crystal structure of $MraY_{AA}$ bound to **2** as a template, in this study, we developed homology models of $MraY_{SA}$ and $MraY_{PA}$ (Figure 6) using SwissModel[46] to predict the molecular basis of **2** interacting with $MraY_{SA}$, which is used for enzymatic assays, and $MraY_{PA}$ expressed in *P. aeruginosa*, the target bacteria. These models reveal that overall, the three-dimensional structures of the $MraY_{SA}$ and $MraY_{PA}$ models are quite

similar to that of $MraY_{AA}$, and the amino acid residues and their interacting modes are

almost identical among $MraY_{AA}$, $MraY_{SA}$, and $MraY_{PA}$ (Figures 4a, 6a,b). Conserved

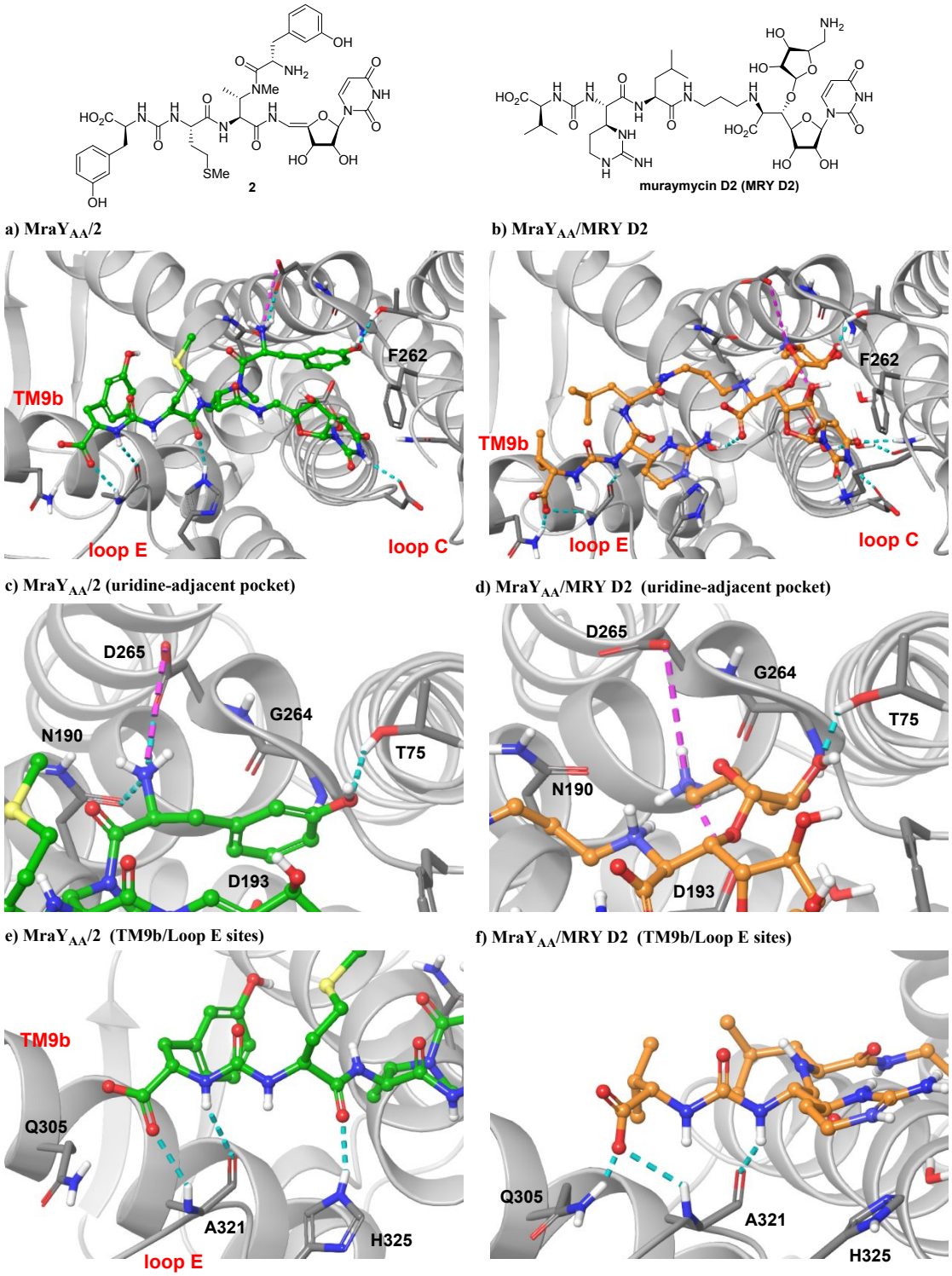

Figure 4. X-ray crystal structures of MraY$_{AA}$ bound to 2 and MRY D2. Carbons of **2** and MRY D2 are shown in green and orange, respectively. Hydrogen bond and salt bridge are indicated by cyan and magenda dash lines, respectively. a) An overall view of the complex bound to **2**. b) An overall view of the complex bound to MRY D2. c) A zoomed-in view of the uridine-adjacent pocket bound to L-*m*Tyr residue of **2**. d) A zoomed-in view of the uridine-adjacent pocket bound to aminoribose moiety of MRD D2. e) A zoomed-in view of the TM9b/Loop E sites interacting to urea-dipeptide motif of **2**. d) A zoomed-in view of the TM9b/Loop E sites interacting to urea-dipeptide motif of MRY D2.

residues in Loop C of the cytoplasmic faces of both MraY$_{SA}$ and MraY$_{PA}$ form a

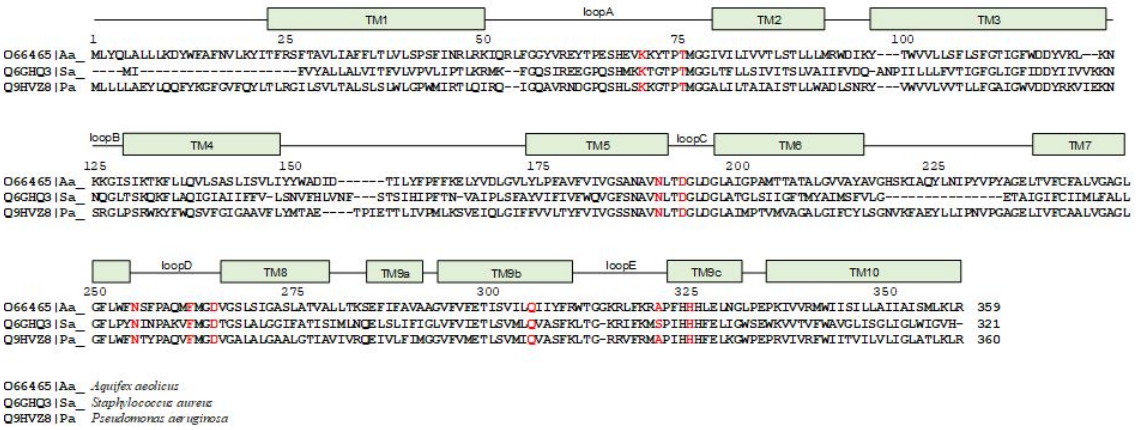

Figure 5. Sequence alignment of MraY. For detail, see Supporting Information.

hydrogen-bonding network around the uracil moiety of **2**, which is further stabilized by a

π-π stacking interaction with Phe226 in $MraY_{SA}$ and Phe264 in $MraY_{PA}$ (Figures 6a, b).

A similar interaction with Phe262 was observed in the $MraY_{AA}$-MRY D2 complex

(Figure 4b). The *N*-terminal L-*m*Tyr residue of **2** interacts with the conserved residues

Thr49 in $MraY_{SA}$, Thr73 in $MraY_{PA}$ (Thr75 in $MraY_{AA}$), and Asn172 in $MraY_{SA}$, Asn195

in $MraY_{PA}$ (Asn190 in $MraY_{AA}$), which create a shallow pocket adjacent to the uracil

binding pocket (Figures 6c,d). In the $MraY_{AA}$/MRY D2 complex, this interaction is

formed by the 5′-aminoribose moiety (Figure 4d). In detail, the amino group at the L-

*m*Tyr residue of **2** forms a hydrogen bond with Asp229 in $MraY_{SA}$ and Asp267 in $MraY_{PA}$

(Asp265 in $MraY_{AA}$), among the most conserved and essential residues in the enzymatic

activity of MraY. Of note is the interaction of the hydroxy group at the L-*m*Tyr residue.

The hydroxy group interacts with Thr49 in $MraY_{SA}$ and Thr73 in $MraY_{PA}$ (Thr75 in

$MraY_{AA}$) as in the hydroxy group at the aminoribose moiety of MRY D2. 3′-

Hydroxypacidamycin **1** has an L-alanine residue at the corresponding site, which lacks the hydroxy group. This structural analysis revealed the reason for the improved $MraY_{SA}$ inhibitory activity of **2** over **1**. Observations that the 5′-amino-4′,5′-didehydro-5′-

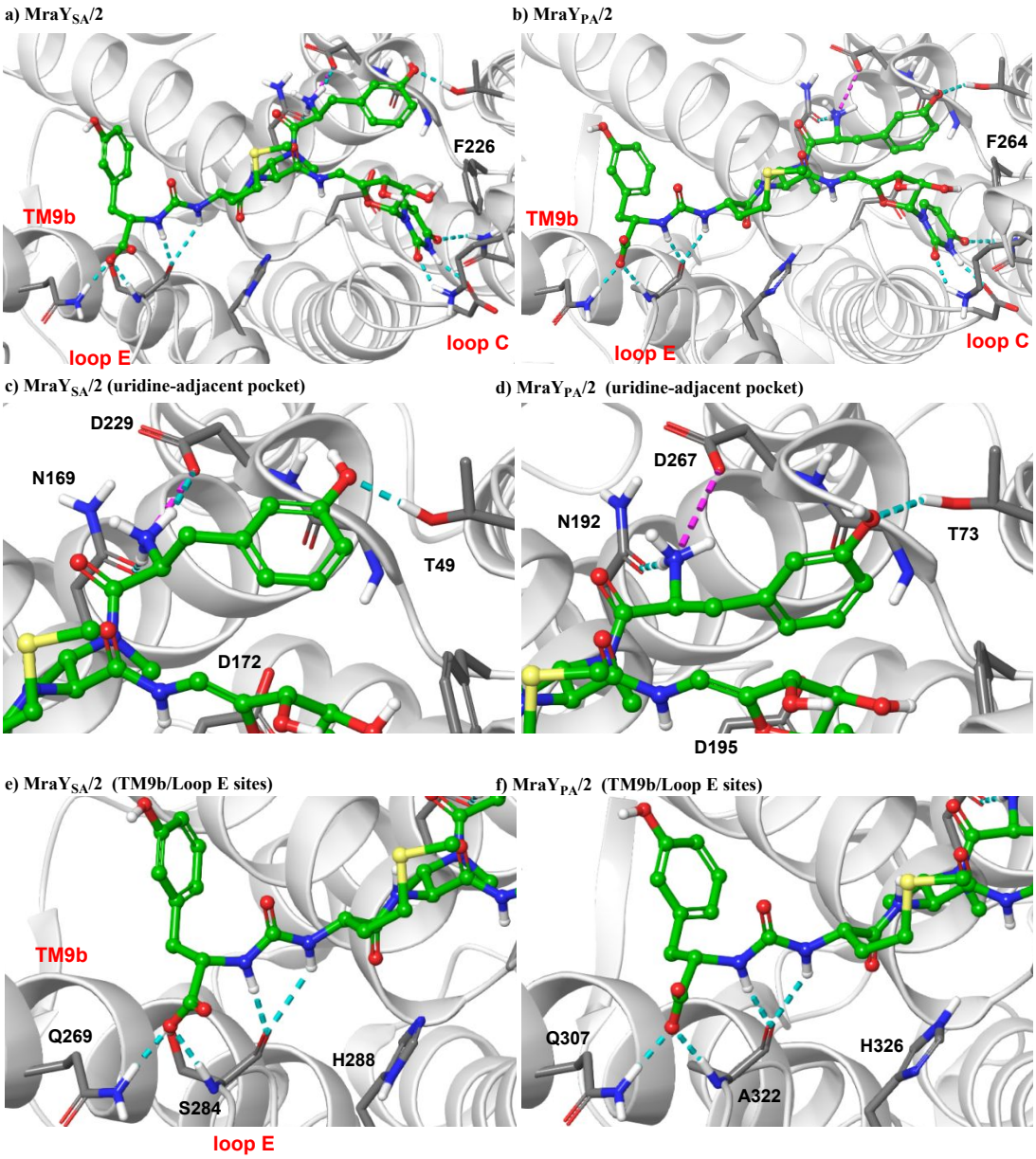

Figure 6. Docking model structures of $MraY_{SA}$ and $MraY_{PA}$ bound to 2. Carbons of **2** are shown in green. Hydrogen bond and salt bridge are indicated by cyan and magenda dash lines, respectively. a) An overall view of the complex of a homology modelled for MraY from *S. aureus* ($MraY_{SA}$) docked to **2**. b) An overall view of the complex a homology modelled for MraY from *P. aeruginosa* ($MraY_{PA}$) docked to **2**. c) A zoomed-in view of the uridine-adjacent pocket of $MraY_{SA}$ bound to L-*m*Tyr residue of **2**. d) A zoomed-in view of the uridine-adjacent pocket bound to aminoribose moiety of $MraY_{PA}$ bound to L-*m*Tyr residue of **2**. e) A zoomed-in view of the TM9b/Loop E sites of $MraY_{SA}$ interacting to urea-dipeptide motif of **2**. d) A zoomed-in view of the TM9b/Loop E sites of $MraY_{PA}$ interacting to urea-dipeptide motif of **2**.

deoxyribofuranose moiety does not directly interact with MraY and the 3′-hydroxy group of **2** is exposed toward a solvent accessible area are in good accordance with our previous results where existence of the hydroxyl group at the 3′-position of the uridine moiety of **1** does not interfere with MraY inhibition.[28]

3′-Hydroxymureidomycin A (**2**) and MRY D2 share a urea-dipeptide moiety in their chemical structure, though the amino acid residues constituting the urea-dipeptide moiety are different between **2** and MRY D2. The moieties of each extend toward transmembrane (TM) 9b and Loop E, forming an interaction with the essential residue His288 in $MraY_{SA}$ and His326 in $MraY_{PA}$ (His324 in $MraY_{AA}$) in the Loop E helix (Figures 6e,f). One of the two hydrogens in the urea-motif of **2** forms a hydrogen bond with the carbonyl oxygen of the Ala321 in the $MraY_{AA}$ crystal structure (Figure 4f). However, both hydrogens in the urea-motif of **2** are suggested to form hydrogen bonds with the carbonyl oxygen of the Ser284 in the $MraY_{SA}$ model and the Ala322 in the $MraY_{PA}$ model upon minimization of the complex structures (Figures 6e,f). In all cases, the carboxylate in the *C*-terminus of **2** interacts with Gln269 in $MraY_{SA}$ and Gln307 in $MraY_{PA}$ (Gln305 in $MraY_{AA}$). Contrary to the interaction observed for the urea-motif of **2** and MRY D2, none of side chains in the urea-dipeptide moiety interacts with any MraY (Figures 4e,f and 6e,f). Our previous SAR study of MRY D2 regarding the urea-dipeptide moiety indicated that the observed

interaction between the urea-dipeptide moiety and TM 9b and Loop E is not necessary

for $MraY_{SA}$ inhibition.[47,48] Namely, truncation of the urea-dipeptide moiety of the

lipophilic analogue **20**, which is a membrane-permeable analogue of MRY D2, did not

diminish the inhibitory activity at all and the truncated analogue **21** still showed a potent

MraY inhibitory activity comparable to that of MRY D2 and **20** (Figure 7). It is suggested

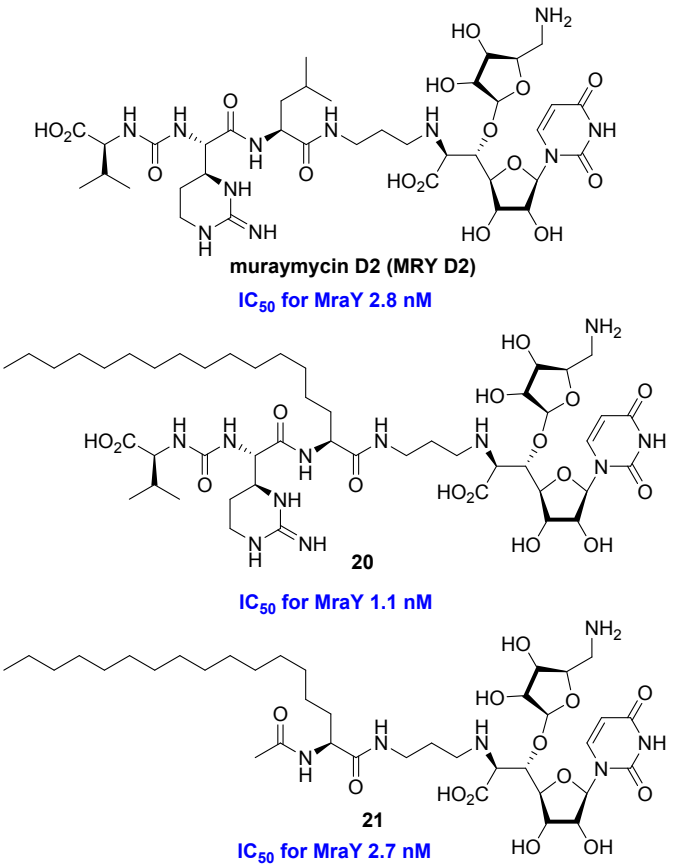

Figure 7. Structures and biological activity of muraymycin D2 and its lipophilic analogues

that the binding affinity of MRYs is mainly contributed by the aminoribosyluridine

moiety, which is superimposable to the uridine and L-*m*Tyr moieties in **2**, and the urea-

dipeptide moiety plays a role as an accessory motif. To see the impact of the urea-peptide

moiety in the case of **2**, several truncated analogues **22-24** (Figure 8), which lack the urea-

motif, were synthesized (Schemes S1, 2), and their $MraY_{SA}$ inhibitory activity was

evaluated (Table 2). As a result, truncation of the urea-motif of **2** led to a complete loss

of inhibitory activity, in a great contrast to the results observed for MRY_{SA}. These results

clearly indicate that the urea-dipeptide motif is also a key contributor in **2**, in addition to

Table 2. Biological activity of analogues

	19	22	23	24
IC_{50} (nM)[a]	4.7	>1000	>1000	>1000
MIC (μg/mL)[b]	32	n.a.	n.a.	n.a.

[a]The inhibitory activities of the compounds against purified MraY from *S. aureus* was determined in a manner similar to the experiments shown in Figure 3. [b]MICs for *P. aeruginosa* were determined by a microdilution broth method as recommended by the CLSI. n.a.:not analyzed.

the uridine and L-*m*Tyr moieties. The fact that **23** has a carboxamide functionality with only one hydrogen suggests that both hydrogens in the urea-motif likely form hydrogen bonds with the carbonyl oxygen of the Ser284 in the $MraY_{SA}$ and the Ala322 in the $MraY_{PA}$, as predicted by modeling (Figure 6). However, it is also true that only the C-terminal carboxylic acid moiety could be important for MraY inhibition. Such kind of analogues has never tested and the possibility remains to be elucidated. Brandish *et al*., through kinetic analysis of the enzymatic reaction, revealed that MRD A inhibits the

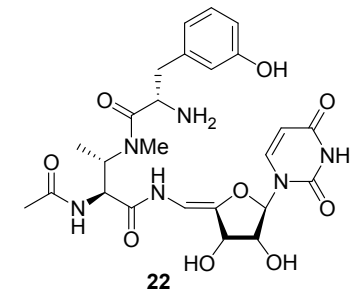

22

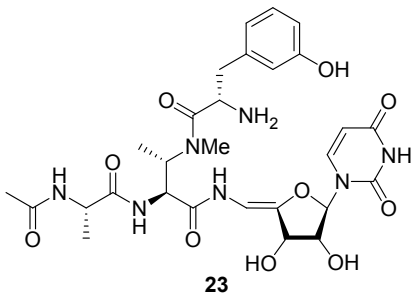

23

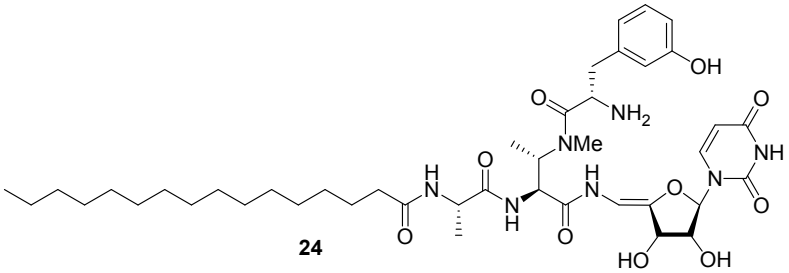

24

Figure 8. Structures of truncated and lipophilic analogues

function of MraY in a concentration- and time-dependent manner, and thus is a slow-binding inhibitor.[49] Initially, this was proposed to be a reaction with an unusual enamide functional group, although the enamide was later found not to be an essential pharmacophore.[50] Presumably, the urea-dipeptide motif, uridine and L-*m*Tyr moieties cooperatively interact with MraY during the course of the conformational change, allowing the urea-dipeptide moiety of **2** to bind to the side of TM9b and loop E to form a more stable conformation although more detailed analyses will be necessary to support this hypothesis.

Identification of the protein associated with 3′-hydroxymureidomycin A resistance. Our initial SAR study with **1**, **2**, and **22-24** suggests that their amino acid composition has a great impact on antibacterial activity. The active site of MraY faces the cytoplasm and these inhibitors must be incorporated into the cytoplasm to reach the active site. It is unlikely that they pass through the outer and inner membranes by passive diffusion, considering the hydrophilic chemical structures of uridylpeptide antibiotics and the analogues investigated in this study. In conjunction with the narrow spectrum of uridylpeptide antibiotics, it is suggested that they utilize a transporter specifically expressed on *P. aeruginosa*; therefore, it is very important to understand how they are taken up by *P.aeruginosa*. It is known that both *E. coli* and *P. aeruginosa* show intrinsic

resistance to uridylpeptide antibiotics. Gotoh *et al.* reported that the resistance of *E. coli*

to MRDs A and C is attributed to efflux by extrusion via the AcrAB-TolC pump.[51] Recently, Mistry *et al.* and Pletzer *et al.* independently found that the resistance of *P. aeruginosa* to PCD 4 and D is primarily due to a loss of function of uptake into the cell mediated by peptide ABC transporters belonging to the nucleoside peptide permease (Npp) family, NppA1A2BCD, which is encoded in the *P. aeruginosa* genome and was previously designated the oligopeptide transport system.[26] The latter reports are in good accordance with the selective antibacterial activity of uridylpeptide antibiotics only against *P. aeruginosa*. Considering these reports, it is presumed that the transporter recognizes chemical structures and/or sequence compositions of the amino acid residues involved in uridylpeptide antibiotics. We briefly investigated whether the synthetic analogue **2**, which possesses the extra hydroxy group at the 3′-position of the parent MRD A, behaves similarly. Exposure of *P. aeruginosa* PAO1 to **2** resulted in emergence of

Table 3. Properties of *P. aeruginosa* mutants resistant to 2

mutants	MIC of **2** (μg/mL)	products	coding region change	amino acid change	CDS*	gene*
MRD1	>64	ABC transporter	insertion of GAAGG in 1164_1165	Asp389 frame shift	NP_250501.1	**PA1810**
		ABC transporter	G→ T of conversion in 1534	Gly512Cys	NP_250501.1	**PA1810**
		aminomethyltransferase	G→ T of conversion in 569	Gly190Val	NP_251132.1	*gcvT2*
MRD2	>64	ABC transporter	insertion of GAAGG in 1164_1165	Asp389 frame shift	NP_250501.1	**PA1810**
		ABC transporter	G→ T of conversion in 1534	Gly512Cys	NP_250501.1	**PA1810**
MRD30	>64	bifunctional diguanylate cyclase/phosphodiesterase	A→ C of conversion in 806	Asp269Ala	NP_253704.1	PA5017
		ABC transporter	insertion of GAAGG in 1164_1165	Asp389 frame shift	NP_250501.1	**PA1810**
		phage coat protein A	A→ G of conversion in 569	Asp190Gly	NP_249415.1	PA0724
		phage coat protein A	G→ A of conversion in 559	Gly187Ser	NP_249415.1	PA0724
		phage coat protein A	insertion of GCG in 634_635	Gly insertion in Gly211_Asp212	NP_249415.1	PA0724

*CDS and Genes were annotated by *P. aeruginosa* PAO1 genome (Accession number, NC_002516.2)

resistant mutants with an 8-fold increase of the MIC values within a day. Among thirty resistant mutants obtained in this study, and the full genome sequences of the three mutants MRD1, 2 and 30 were determined by next-generation genome sequencing, and the sequences obtained were compared with those of wild-type *P. aeruginosa* PAO1 (Table 3). Several nucleotide mutations were found in the genes encoding NppA1A2BCD (PA1810) as reported previously, and five nucleotides insertions attribute to functional disruption of NppA1A2BCD was commonly detected in MRD1, 2 and 30. These results support previous reports[26] that NppA1A2BCD is responsible for transport of **2** into the cytoplasm. To confirm whether NppA1A2BC transporter of *P. aeruginosa* PAO1 is truly required for uptake of **2** across the inner membrane, antimicrobial susceptibility of two transposonmutants *P. aeruginosa* PW4182 and PW4181 (Table 4), which have functional disruptions of NppA1A2BCD via transposon insertion into the encoding gene, was investigated. As expected, two mutants were totally resistance to **2** (MIC >128 μg/mL), and therefore, NppA1A2BCD transporter is responsible for uptake of **2** in *P. aeruginosa* PAO1. Since NppA1A2BCD transports peptides, the observed difference in the antibacterial activity of analogues synthesized in this study (Table 2) may be attributed to the mode of recognition of the amino acid sequence of analogues by NppA1A2BCD.

Table 4. Properties of transposonmutants *P. aeruginosa* mutants

mutants	MIC of **2** (μg/mL)	ORF	putative ORF function	position in ORF	gene position	transposon
PW4181	>128	**PA1810**	probable binding protein component of ABC transporter	747 (1848)	1966872	ISlacZ/hah
PW4182	>128	**PA1810**	probable binding protein component of ABC transporter	799 (1848)	1966820	ISphoA/hah

Detailed structure-activity relationship regarding the urea-dipeptide moiety. Uridylpeptide antibiotics have a dual nature as antibacterial agents: they must be a substrate of a transporter, one of the candidates of which is suggested to be NppA1A2BCD, as well as an inhibitor of MraY. Therefore, it has proved difficult to design analogues of these antibiotics that retain both MraY inhibition and antimicrobial activity.[52] NppA1A2BCD transports peptides with a certain selectivity for the length and sequence; however, the details of the selectivity and sequence preference remain unclear.[26] It was revealed that the L-*m*Tyr at the *N*-terminus of **2** largely contributes to MraY inhibition and none of side chains in the urea-dipeptide moiety of **2** interacts with $MraY_{AA}$ in the X-ray crystal structure or with $MraY_{SA}$ and $MraY_{PA}$ constructed by homology modeling. These results prompted us to see the impact of the side chains on MraY inhibition and antibacterial activity through a systematic SAR of the urea-dipeptide moiety. In a different study, Bugg *et al.* proposed a structural link between two aromatic residues (L-Trp or L-*m*Tyr at the *C*-terminus and L-*m*Tyr at the *N*-terminus) in the MDR/PCD structures, and an Arg-Trp-x-x-Trp motif on the lysis

protein E of bacteriophage ϕX174,[53] which inhibits MraY via a protein-protein interaction

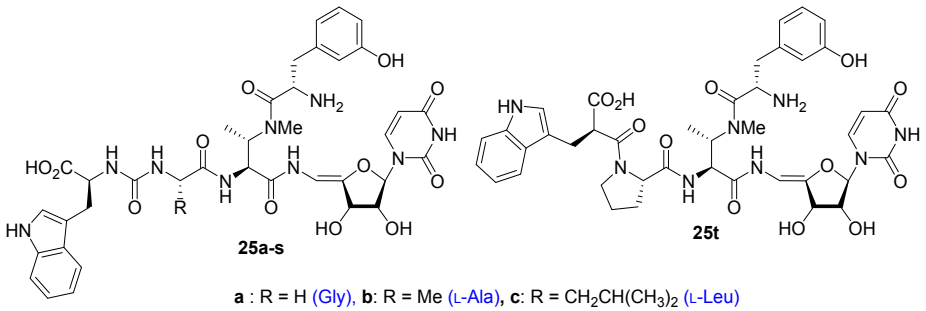

a : R = H (Gly), **b**: R = Me (L-Ala), **c**: R = $CH_2CH(CH_3)_2$ (L-Leu)
d: R = $CH(CH_3)CH_2CH_3$ (L-Ile), **e**: R = $CH(CH_3)_2$ (L-Val)
f: R = CH_2SH (L-Cys), g: R = $CH_2CH_2SCH_3$ (L-Met), **h**: R = CH_2Ph (L-Phe),
i: R = CH_2(p-hydroxyphenyl) (L-Tyr), **j**: R = CH_2(2-indole) (L-Trp)
k: R = CH_2(4-imidazole) (L-His), **l**: R = CH_2CO_2H (L-Asp)
m: R = $CH_2CH_2CO_2H$ (L-Glu), **n**: R = $CH_2CH_2CH_2CH_2NH_2$ (L-Lys)
o: R = $CH_2CH_2CH_2NHC(=NH)NH_2$ (L-Arg), **p**: R = CH_2OH (L-Ser)
q: R = $CH(OH)CH_3$ (L-Thr), **r**: R = CH_2CONH_2 (L-Asn)
s: R = $CH_2CH_2CONH_2$ (L-Gln)

Figure 9. Structures of analogues modified at the urea-dipeptide moiety

remote from the active site [54] and suggested that two aromatic residues in the

MDR/PCD are important for uptake into the cell via a hydrophobic channel

present in the structure of MraY. Therefore, the impact of the internal amino acid

residue at the urea-dipeptide moiety on antibacterial activity was investigated as the index

of NppA1A2BCD transport by using a set of analogues **25a-t**. L-Tryptophan was chosen for the *C*-terminal amino acid instead of L-*m*Tyr (Figure 9). These analogues were prepared by a modified synthetic route for **2**. Namely, L-*m*Tyr at the *N*-terminus was introduced to **15** to give **27** prior to connecting the urea-dipeptide moiety **29a-t** to reduce the synthetic steps (Scheme 5). The attempt to prepare a free primary amine obtained by deprotection of **27** by BCl_3 failed because the free amine underwent decomposition resulting in removal of the Fmoc group at the *N*-terminus. Therefore, the free amine was

Scheme 5

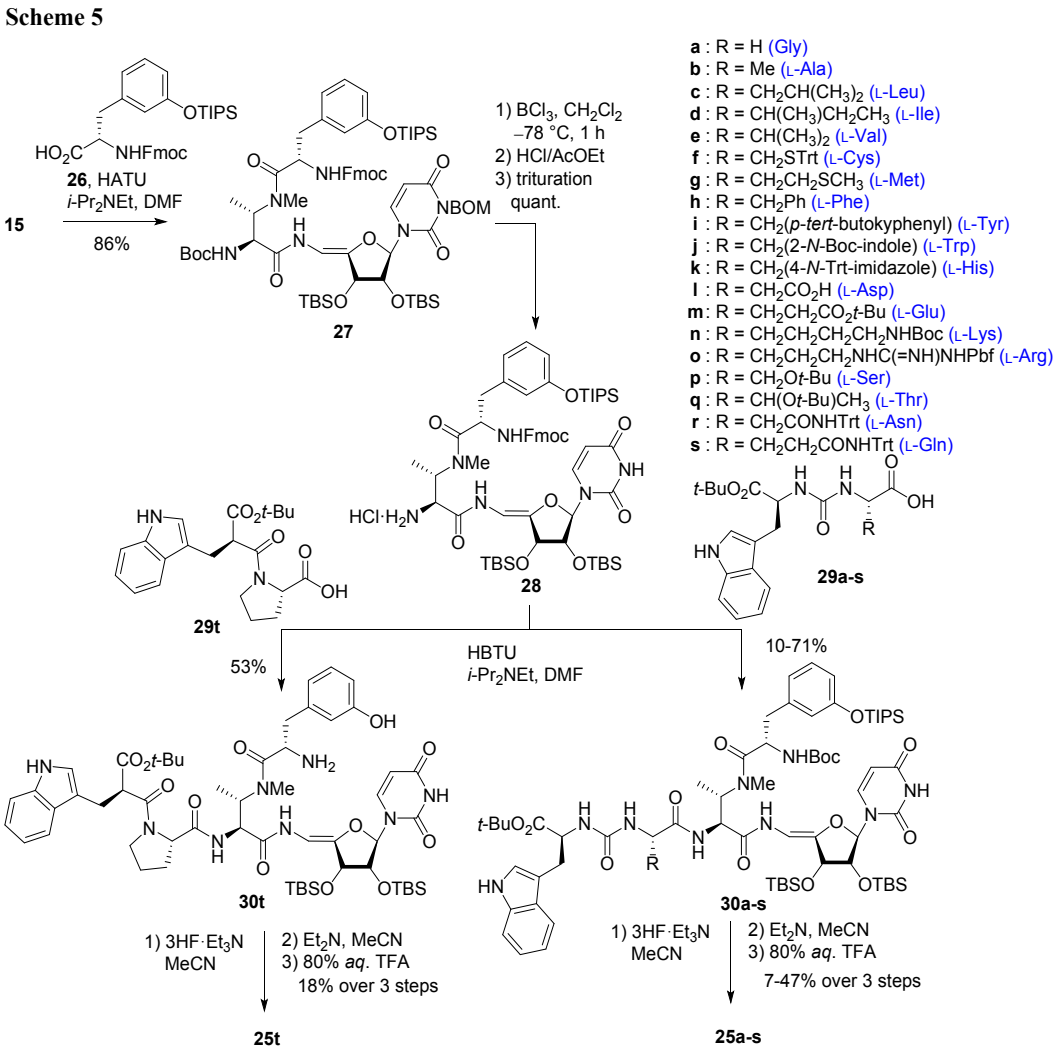

converted to the corresponding hydrochloride salt **28**, which is stable and can be stored, immediately after deprotection of the protecting groups. Except for **29t**, solid-phase parallel synthesis of urea-dipeptides is suitable for rapid access to the urea-dipeptide carboxylic acids **29a-s**. Condensation of **28** and **29a-t** followed by deprotection afforded **25a-t**.

The IC_{50} values for the $MraY_{SA}$ inhibitory activities of **25a-s** were essentially within a similar range (0.22±0.07 -7.6±1.6 nM), and a variety of amino acid residues with various physicochemical properties including negative or positive charges are acceptable for MraY inhibition. Analogues **1** and **25b** share the same urea-dipeptide moiety, with a structural difference of a single amino acid replacement at the *N*-terminus (L-Ala vs. L-*m*Tyr). The fact that this replacement resulted in a significant, 32-fold, increase in $MraY_{SA}$ inhibition supported the hypothesis that the L-*m*Tyr at the *N*-terminus largely contributes to the inhibitory activity, as was expected in the interactions in uridine-adjacent pocket (Figures 5c, d). Analogues possessing aromatic residues tend to exhibit a stronger inhibitory activity among **25a-s**, and the L-Tyr analogue **25i** showed the strongest $MraY_{SA}$ inhibitory activity with an IC_{50} value of 0.22±0.07 nM. One exception is the L-Pro analogue **25t**, which largely decreased the inhibitory activity with an IC_{50} value of >500 nM. Replacement with L-Pro consequently results in a deficit of one of the two hydrogens

in the urea-motif, and the decrease in inhibitory activity of **25t** is consistent with the SAR

for the truncated analogues **22**-**24**. Overall, the SAR of **25a**-**t** regarding MraY inhibition

is in good accordance with the structural features observed for the X-ray crystal structure

of the complex of **2** bound to $MraY_{AA}$. The antibacterial activities of analogues against *P. aeruginosa* PAO1, which may reflect the selectivity for their cellular uptake by NppA1A2BCD, were next investigated. Different from $MraY_{SA}$ inhibitory activity, it was found that the side chains in the urea-dipeptide largely affected the antibacterial activity. Except for the L-Leu analogue **25c**, analogues possessing hydrophobic residues such as L-Ile, L-Val, and L-Met (**25d**, **25e**, **25g**, respectively) and aromatic residues such as L-Phe, L-Tyr, and L-Trp (**25h**, **25i**, **25j**, respectively) exhibited a comparable antibacterial activity against *P. aeruginosa* PAO1 to **2** with MICs ranging from 16-128 μg/mL. The L-Val analogue is the best in terms of antibacterial activity against *P. aeruginosa* among those tested in this study (MIC 16 μg/mL for **25e**). Analogues containing less hydrophobic residues such as L-Gly (**25a**), charged residues, such L-Asp, L-Glu, L-Lys, and L-Arg (**25l**, **25m**, **25n**, and **25o**, respectively), and polar residues such as L-His, L-

Table 5. Biological activity of analogues 25a-t

	25a Gly	**25b** L-Ala	**25c** L-Leu	**25d** L-Ile	**25e** L-Val	**25f** L-Cys	**25g** L-Met	**25h** L-Phe	**25i** L-Tyr	**25j** L-Trp	**25k** L-His
		hydrophobic					*aromatic*				
IC_{50} (nM)[a]	4.2±1.2	1.3±0.2	4.0±1.3	1.4±0.4	1.5±0.2	1.6±0.2	1.0±0.2	0.60±0.15	0.22±0.07	0.44±0.10	2.8±0.6
MIC (μg/mL)[b]	>128	64	32-128	16-32	16	128	32-64	16-32	16-32	32	>128

	25l L-Asp	**25m** L-Glu	**25n** L-Lys	**25o** L-Arg	**25p** L-Ser	**25q** L-Thr	**25r** L-Asn	**25s** L-Gln	**25t** L-Pro
	acidic		*basic*		*hydrogen bonding*				
IC_{50} (nM)[a]	7.6±1.6	3.3±0.6	1.8±0.5	3.4±0.5	1.8±0.4	1.8±0.4	2.1±0.4	1.3±0.2	>500
MIC (μg/mL)[b]	>128	128	>128	>128	>128	32-64	>128	128	>128

[a]The inhibitory activities of the compounds against purified MraY from *S. aureus* was determined in a manner similar to the experiments shown in Figure 3. [b]MICs for *P. aeruginosa* were determined by a microdilution broth method as recommended by the CLSI. The data were obtained from three independent experiments described as a range of the values.

Ser, L-Asn, and L-Gln (**25k**, **25p**, **25r**, and **25s**, respectively), which can form a hydrogen bonding, decreased the antibacterial activity to a large extent. These results suggest that polar amino acid residues at the internal amino acid residue of the urea-dipeptide moiety are not preferred but hydrophobic residues are preferred for incorporation. Of interest is antibacterial activity of **25d**, **25e**, and **25q**. Namely, the analogues containing β-branched amino acid residues such as L-Ile, L-Val, L-Thr tend to exhibit better antibacterial activity.

Conclusion

Development of a novel lead effective against multi drug-resistant *P. aeruginosa* is urgently needed worldwide. Intrigued by the specific antibacterial activity and potent MraY inhibitory activity of uridylpeptide antibiotics, the SAR of the 3'-hydroxy derivative of mureidomycin A (**2**) was conducted to elucidate its structural requirement for both MraY inhibition and antibacterial activities against *P. aeruginosa*. First, a synthetic method capable of providing a range of analogues suitable for investigating the SAR was established as the third-generation synthesis, where the urea-dipeptide moiety and *N*-terminal amino acid are introduced in the last stage of the synthesis. Design and synthesis of analogues guided by X-ray crystal structure analysis of **2** bound to $MraY_{AA}$ was conducted to elucidate the mode of MraY inhibition. The SAR of analogues **25a-t** suggests that hydrophobic residues at the internal amino acid residue of the urea-dipeptide

moiety are a better substrate for bacterial incorporation. It was suggested that the interaction of the urea-motif is essential for the strong MraY inhibitory activity and that the amino acid residues in the motif did not contribute to the inhibition. The SAR regarding anti-*P. aeruginosa* activity is in great contrast to that for MraY inhibition, as anti-*P. aeruginosa* activity is greatly affected by the amino acid residues. As shown in this study, a side-by-side comparison of the impact of each amino acid residue on both MraY inhibition and antibacterial activity enabled us to evaluate more reliable SAR of uridylpeptide antibiotics and their analogues. A summary of the SAR of uridylpeptide antibiotics revealed by this study includes the following: 1) L-*m*Tyr at the *N*-terminus is favored to increase the MraY inhibitory activity, 2) the interaction of the urea-dipeptide motif is indispensable for the MraY inhibitory activity, 3) the side chain at the urea-dipeptide moiety does not affect the MraY inhibition, and 4) the antibacterial activity of uridylpeptide antibiotics depends on their amino acid composition, presumably because selectivity for cellular uptake by NppA1A2BCD. As for antibacterial activity, analogues possessing hydrophobic residues and aromatic residues exhibited a comparable antibacterial activity against *P. aeruginosa* PAO1 to **2.** There are parallel trends between these data and those reported in previous studies.[33,39] With this SAR information in hand, future optimization of the amino acid residues would improve the antibacterial activity

against *P. aeruginosa*. Thus, it will be necessary to understand the structural requirements of uridylpeptide antibiotics in NppA1A2BCD recognition in much more detail with future SAR analyses. Uridylpeptide antibiotics have a dual nature as an antibacterial agent and it is challenging to design analogues that retain both MraY inhibition and antimicrobial activity. This study provides a guide for the rational design of analogues based on uridylpeptide antibiotics.

Experimental Section

General experimental methods. NMR spectra were reported in parts per million (δ) relative to tetramethylsilane (0.00 ppm) as internal standard otherwise noted. Coupling constant (*J*) was reported in herz (Hz). Abbreviations of multiplicity were as follows; s: singlet, d; doublet, t: triplet, q: quartet, m: multiplet, br: broad. Data were presented as follows; chemical shift (multiplicity, integration, coupling constant). Assignment was based on ^{1}H–^{1}H COSY, HMBC and HMQC NMR spectra. Purity of all the compounds tested for biological evaluation was confirmed to be >95% by LC-MS analysis as shown in Supporting Information.

(*S*)-2-[(*tert*-Butoxycarbonyl)amino]-3-(3-hydroxyphenyl)propanoic acid (5). A mixture of H-L-*m*Tyr-OH (**8**) (1.50 g, 8.28 mmol) and $NaHCO_3$ (1.04 g, 12.4 mmol) in

THF (40 mL) and H_2O (40 mL) was treated with Boc_2O (1.99 g, 9.11 mmol) at 0 ºC, and the mixture was stirred at room temperature for 17 h. The mixture was partitioned between AcOEt and 1 M *aq*. HCl. The organic phase was washed with brine, dried (Na_2SO_4), filtered and concentrated *in vacuo* to afford a crude carboxylic acid. A solution of the crude carboxylic acid and imidazole (3.38 g, 49.7 mmol) in CH_2Cl_2 (83 mL) was treated with TIPSCl (5.26 mL, 24.8 mmol) at 0 ºC, and the mixture was stirred at room temperature for 44 h. The mixture was partitioned between AcOEt and 1 M *aq*. HCl, and the organic phase was washed with water and brine, dried over Na_2SO_4, filtered and concentrated *in vacuo*. A solution of the residue in THF/MeOH (2/1, 83 mL) and H_2O (13 mL) was treated with K_2CO_3 (1.60 g, 11.6 mmol) at room temperature for 2 h. The mixture was partitioned between AcOEt and 1 M *aq*. HCl, and the organic phase was washed with water and brine, dried (Na_2SO_4), filtered and concentrated *in vacuo*. The residue was purified by silica gel column chromatography (50% AcOEt/hexane) to afford **5** (3.30 g, 7.54 mmol, 91%) as a colorless oil. ^{1}H NMR ($CDCl_3$, 400 MHz) δ 7.15 (dd, 1H, H-5-*m*Tyr, $J_{5\text{-}m\text{Tyr, }4\text{-}m\text{Tyr}} = J_{5\text{-}m\text{Tyr, }6\text{-}m\text{Tyr}} = 7.7$ Hz), 6.80-6.68 (m, 3H, H-2-*m*Tyr, H-4-*m*Tyr, H-6-*m*Tyr), 4.89 (br d, 1H, NH-*m*Tyr, $J_{\text{NH-}m\text{Tyr, }\alpha\text{-}m\text{Tyr}} = 7.4$ Hz), 4.57 (m, 1H, H-α-*m*Tyr), 3.12 (dd, 1H, H-β-*m*Tyr, $J_{\beta\text{-}m\text{Tyr, }\alpha\text{-}m\text{Tyr}} = 4.6$, $J_{\text{gem}} = 13.7$ Hz), 3.03 (dd, 1H, H-β-*m*Tyr, $J_{\beta\text{-}m\text{Tyr, }\alpha\text{-}m\text{Tyr}} = 6.3$, $J_{\text{gem}} = 13.7$ Hz), 1.42 (s, 9H, ^{t}Bu), 1.24 (m, 3H, Si[C*H*$(CH_3)_2]_3$),

1.10 (s, 12H, Si[CH(CH_3)$_2$]$_3$), 1.08 (s, 6H, Si[CH(CH_3)$_2$]$_3$); ^{13}C NMR ($CDCl_3$, 100 MHz) δ 176.8, 156.3, 137.3, 129.7, 122.1, 121.2, 118.8, 80.4, 54.3, 37.6, 28.4, 18.1, 12.8; ESIMS-LR *m/z* 438 [(M+H)$^+$]; ESIMS-HR *m/z* calcd for $C_{23}H_{39}NO_5SiNa$ 460.2490, found 460.2503; $[\alpha]^{24}_D$ +13.7 (*c* 0.44, MeOH).

***tert*-Butyl (*S*)-2-[(*tert*-Butoxycarbonyl)amino]-3-{3-[(triisopropylsilyl)oxy] phenyl}-propanoate (9).** A solution of **5** (2.51 g, 5.74 mmol) in CH_2Cl_2 (57 mL) was treated with *O*-*tert*-butyl 2,2,2-trichloroacetmidate (5.14 mL, 28.7 mmol) at room temperature. The mixture was then warmed to 45 ºC and stirred for 2 h. Additional *O*-*tert*-butyl 2,2,2-trichloroacetmidate (5.14 mL, 28.7 mmol) was added to the mixture, which was stirred for 2 h. The mixture was concentrated *in vacuo*, and the residue was purified by silica gel column chromatography (3% AcOEt/hexane) to afford **9** (2.70 g, 5.47 mmol, 95%) as a colorless oil. ^{1}H NMR ($CDCl_3$, 400 MHz) δ 7.11 (dd, 1H, H-5-*m*Tyr, $J_{5\text{-}m\text{Tyr, 4-}m\text{Tyr}} = J_{5\text{-}m\text{Tyr, 6-}m\text{Tyr}} = 8.0$ Hz), 6.75-6.70 (m, 3H, H-2-*m*Tyr, H-4-*m*Tyr, H-6-*m*Tyr), 4.96 (br d, 1H, NH-*m*Tyr, $J_{\text{NH-}m\text{Tyr, α-}m\text{Tyr}} = 8.2$ Hz,), 4.43 (dd, 1H, H-α-*m*Tyr, $J_{\alpha\text{-}m\text{Tyr, NH}} = 8.2$, $J_{\alpha\text{-}m\text{Tyr, β-}m\text{Tyr}} = 6.0$ Hz), 3.00 (d, 2H, H-β-*m*Tyr, $J_{\beta\text{-}m\text{Tyr, α-}m\text{Tyr}} = 6.0$ Hz), 1.42 (s, 9H, Boc-^{t}Bu), 1.41 (s, 9H, ^{t}Bu), 1.29-1.19 (m, 3H, Si[C*H*(CH$_3$)$_2$]$_3$), 1.10 (d, 18H, *J* = 6.9 Hz, H-Si[CH(CH_3)$_2$]$_3$); ^{13}C NMR ($CDCl_3$, 100 MHz) δ 171.0, 156.1, 155.2, 137.8,

129.3, 122.4, 121.4, 118.3, 82.1, 79.7, 54.8, 38.3, 28.5, 28.1, 18.1, 12.8; ESIMS-LR *m/z* calcd for $C_{27}H_{48}NO_5Si$ 494.33, found 494.00.

***tert*-Butyl (*S*)-2-Amino-3-[3-(triisopropylsilyloxy)phenyl)]propanoate trifluoro acetate salt (10).** Compound **9** (2.60 g, 5.27 mmol) was treated with 10% TFA/CH_2Cl_2 (53 mL) at room temperature for 1.5 h. The mixture was concentrated *in vacuo*, and the residue was purified by silica gel column chromatography (3% MeOH/$CHCl_3$ containing 0.1% TFA) to afford **10** (2.60 g, 5.30 mmol, 97%) as a colorless oil. ^{1}H NMR (CD_3OD, 400 MHz) δ 7.24 (dd, 1H, H-5-*m*Tyr, $J_{5\text{-}m\text{Tyr, }4\text{-}m\text{Tyr}} = J_{5\text{-}m\text{Tyr, }6\text{-}m\text{Tyr}} = 7.8$ Hz), 6.88-6.80 (m, 3H, H-2-*m*Tyr, H-4-*m*Tyr, H-6-*m*Tyr), 4.12 (dd, 1H, H-α-*m*Tyr, $J_{\alpha\text{-}m\text{Tyr, }\beta\text{-}m\text{Tyr}} = 7.8$, $J_{\alpha\text{-}m\text{Tyr, }\beta\text{-}m\text{Tyr}} = 6.9$ Hz), 3.11 (m, 2H, H-β-*m*Tyr), 1.42 (s, 9H, ^{t}Bu), 1.29 (m, 3H, Si[C*H*$(CH_3)_2]_3$), 1.13 (s, 12H, Si[CH($CH_3)_2]_3$), 1.11 (s, 6H, Si[CH($CH_3)_2]_3$); ESIMS-LR *m/z* calcd for $C_{22}H_{40}NO_3Si$ 394.28, found 394.0.

(*S*)-1-(*tert*-Butoxy)-1-oxo-3-{[3-(triisopropylsilyloxy)phenyl]propan-2-yl-carbamoyl}-L-methionine (4). 2-Chlorotrityl chloride resin (1.6 mmol/g, 200 mg) was placed in a 10 mL polypropylene syringe fitted with a polyethylene filter disc. The resin was washed with CH_2Cl_2 (2 mL), and a solution of Fmoc-Met-OH (356 mg, 960 μmol) and ^{i}Pr$_2$NEt (334 μL, 1.92 mmol) in CH_2Cl_2 (2 mL) was then added. After the mixture was agitated at room temperature for 3 h, the solvent and reagents were removed by

suction. The resin was subjected to the following washing treatments with CH_2Cl_2/MeOH/$^{i}Pr_2NEt$ (17/2/1, 2 mL × 3), DMF (2 mL × 2) and CH_2Cl_2 (2 mL × 2). The resin was treated with piperidine/DMF (1/4, 5 min, then 1/9, 15 min) to remove the Fmoc group at room temperature and washed with DMF (2 mL × 3) and CH_2Cl_2 (2 mL × 3). A solution of 1,1′-carbonyldiimidazole (156 mg, 960 μmol) and *N*-methylmorpholine (211 mg, 1.92 μmol) in CH_2Cl_2 (2 mL) was added to each resin. After the mixture was agitated at room temperature for 1 min, solvent and reagents were removed by suction. This procedure was repeated for 5 times. The resin was washed with CH_2Cl_2 (2 mL × 3). Then, a solution of **10** (189 mg, 480 μmol) and $^{i}Pr_2NEt$ (167 μL, 960 μmol) in DMF (2 mL) was added to the resins. The mixture was agitated at room temperature for 3 h, and solvent and reagents were removed by suction. The resin was washed with DMF (2 mL × 3) and CH_2Cl_2 (2 mL × 3). The resin was treated with 1% TFA/CH_2Cl_2 to cleaved the urea-dipeptide from the resin, and the filtrate was partitioned between AcOEt and H_2O. The organic phase was washed with brine, dried (Na_2SO_4), filtrated and concentrated *in vacuo* to afford **4** (141 mg, 248 μmol, 78 %) as a colorless oil. ^{1}H NMR (CD_3OD, 400 MHz) δ 7.14 (dd, 1H, H-5-*m*Tyr, $J_{5\text{-}m\text{Tyr},\ 4\text{-}m\text{Tyr}} = J_{5\text{-}m\text{Tyr},\ 6\text{-}m\text{Tyr}} = 7.9$ Hz), 6.82 (d, 1H, H-6-*m*Tyr, $J_{6\text{-}m\text{Tyr},\ 5\text{-}m\text{Tyr}} = 7.9$ Hz), 6.76-6.73 (m, 2H, H-4-*m*Tyr, H-2-*m*Tyr), 4.42-4.38 (m, 2H, H-α-*m*Tyr,, H-α-Met), 2.95 (d, 2H, H-β- *m*Tyr, $J_{\beta\text{-}m\text{Tyr},\ \alpha\text{-}m\text{Tyr}} = 6.8$ Hz), 2.56-2.52 (m, 2H, H-

γ-Met), 2.12-2.08 (m, 1H, H-β-Met), 2.08 (s, 3H, SC*H*$_3$), 1.94-1.84 (m, 1H, H-β-Met), 1.40 (s, 9H, ^{t}Bu), 1.28-1.19 (m, 3H, Si[C*H*(CH$_3$)$_2$]$_3$), 1.11 (d, 18H, Si[CH(C*H*$_3$)$_2$]$_3$, J = 7.3 Hz); ^{13}C NMR (CD$_3$OD, 100 MHz) δ 176.8, 173.1, 159.7, 157.3, 139.7, 130.3, 123.6, 122.1, 119.1, 82.8, 56.2. 53.2, 39.3, 33.4, 31.0, 28.3, 18.4, 15.3, 13.9; ESIMS-HR *m/z* calcd for $C_{28}H_{49}N_2O_6SSi_2$ 569.3075, found 569.3064.

(2*S*,3*S*)-2-[(*tert*-Butoxycarbonyl)amino]-3-[(*N*-benzyloxy-*N*-methyl)amino]-butanamide (14). A mixture of (2*S*,3*S*)-2-[(*tert*-butoxycarbonyl)amino]-3-[(*N*-benzyloxy-*N*-methyl)amino]butanoic acid (**13**, 7.6 g, 22.3 mmol), NH_4Cl (11.9 g, 223 mmol), HATU (11.0 g, 29.0 mmol), and *N*-methylmorpholine (31.9 mL, 290 mmol) in DMF (220 mL) was stirred at 0 °C for 1 h. The reaction mixture was diluted with H_2O and extracted with AcOEt. The combined organic layers were washed with 0.2 M *aq*. HCl and brine, dried (Na_2SO_4), filtrated and concentrated *in vacuo*. The residue was crystallized from AcOEt to afford **14** (6.1 g, 18.1 mmol, 81%) as a white solid. ^{1}H NMR (CD$_3$OD, 400 MHz) δ 7.38-7.26 (m, 5H, OCH$_2$*C$_6$H$_5$*), 4.66 (d, 1H, O*CH*$_2$Ph, J_{gem} = 10.7 Hz), 4.63 (d, 1H, O*CH*$_2$Ph, J_{gem} = 10.7 Hz), 4.49 (dr s, 1H, H-α), 3.16 (qd, 1H, H-β, $J_{\beta,\gamma}$ = $J_{\beta,\alpha}$ = 6.8 Hz), 2.61 (s, 3H, H-NC*H*$_3$), 1.46 (s, 9H, Boc), 1.07 (d, H-γ, $J_{\gamma,\beta}$ = 6.8 Hz); ^{13}C NMR (CD$_3$OD, 100 MHz) δ 176.8, 158.0, 138.6, 130.1, 129.3, 128.9, 80.8, 75.6,

64.4, 57.6, 42.3, 28.7, 11.1; ESIMS-HR *m/z* calcd for $C_{17}H_{28}N_3O_4$ 338.2074, found 338.2078.; $[\alpha]^{25}_D$ –8.5 (*c* 0.87, MeOH)

Compound 15. A mixture of **14** (2.55 g, 6.78mmol) and $Pd(OH)_2$ (1.1 g) in MeOH (68 mL) was vigorously stirred at room temperature for 3 h under H_2 atmosphere. The catalyst was filtered off through a Celite pad, and the filtrate was concentrated *in vacuo* to afford a crude carboxamide. The crude carboxamide, **7** (4.75g, 6.78 mmol), CuI (1.25 g, 8.14 mmol) and Cs_2CO_3 (13.1 g, 10.2 mmol) were added to a flask. Dried THF (68 mL) and *N*,*N*-dimethyl-1,2-ethylendiamine (2.8 mL, 16.3 mmol) were added to the mixture, which was heated on 70 °C for 7 h. The reaction mixture was diluted with AcOEt, and the insoluble substances were filtered off through a Celite pad, and the filtrate was washed with H_2O and brine, dried (Na_2SO_4), and concentrated *in vacuo*. The residue was purified by silica gel column chromatography ($CHCl_3$/MeOH = 6-10 %) to afford **15** (3.65 g, 4.53 mmol, 67 %) as a white foam. ^{1}H NMR ($CDCl_3$, 400 MHz) δ 9.15 (br s, 1H, NH), 7.38-7.27 (m, 5H, $NCH_2OCH_2C_6H_5$), 7.17 (d, 1H, H-6-uridine, $J_{6,5}$ = 8.2 Hz), 6.30 (s, 1H, H-5′-uracil), 6.29 (d, 1H, H-1′-uridine, $J_{\text{H-1′-uridine, H-2′-uridine}}$ = 6.0 Hz), 5.86 (d, 1H, H-5-uridine, $J_{\text{H-5-uridine, H-6-uridine}}$ = 8.2 Hz), 5.50 (d, 2H, NCH_2OBn, J_{gem} = 6.4 Hz), 4.69 (s, 2H, NCH_2OCH_2Ph), 4.40 (d, 1H, H-3′-uridine, $J_{\text{H-3′-uridine, H-2′-uridine}}$ = 4.1 Hz), 4.17 (dd, 1H, H-2′-uridine, $J_{\text{H-2′-uridine, H-1′-uridine}}$ = 6.0, $J_{\text{H-2′-uridine, H-3′-uridine}}$ = 4.1 Hz), 4.05 (dd, 1H, H-

α-DABA, $J_{\text{H-α-DABA, H-β-DABA}}$ = 6.9 Hz), 2.74 (dq, 1H, H-β-DABA, $J_{\text{H-β-DABA, H-α-DABA}}$ = 6.9, $J_{\text{H-β-DABA, H-γ-DABA}}$ = 6.4 Hz), 2.38 (s, 3H, NCH_3), 1.41 (s, 9H, Boc-^{t}Bu), 1.13 (d, 3H, H-γ-DABA, $J_{\text{H-γ-DABA, H-β-DABA}}$ = 6.4 Hz), 0.90 (s, 9H, SiC(CH_3)$_3$), 0.83 (s, 9H, SiC(CH_3)$_3$), 0.11 (s, 3H, ^{t}BuSi(CH_3)$_2$), 0.09 (s, 3H, ^{t}BuSi(CH_3)$_2$), 0.03 (s, 3H, ^{t}BuSi(CH_3)$_2$), –0.03 (s, 3H, ^{t}BuSi(CH_3)$_2$); ^{13}C NMR ($CDCl_3$, 100 MHz) δ 168.4, 162.4, 156.5, 151.2, 141.4, 138.3, 137.8, 128.4, 127.8, 103.2, 100.9, 89.6, 75.8, 72.2, 71.2, 70.5, 33.8, 28.4, 25.9, 25.7, 18.3, 18.0, 16.2, –4.1, –4.4, –4.9; ESIMS-LR *m/z* calcd for $C_{39}H_{66}N_5O_9Si_2$ 804.44, found 805.0; ESIMS-HR *m/z* calcd for $C_{39}H_{66}N_5O_9Si_2$ 804.4394, found 804.4399; $[\alpha]^{19}_D$ –28.1 (*c* 0.75, $CHCl_3$).

Compound 16. A mixture of **15** (2.62 g, 3.25 mmol) and AllocCl (414.8 μmol, 3.90 mmol) in THF/*sat*. *aq*. $NaHCO_3$ (1/1, 40 mL) was vigorously stirred at 0 °C for 5 h. The reaction was quenched with MeOH, and the organic solvents were removed under reduced pressure. The resulting aqueous phase was extracted with AcOEt, which was washed with H_2O and brine, dried (Na_2SO_4), filtrated and concentrated *in vacuo*. The residue was purified by silica gel column chromatography (ϕ 5 × 10 cm, hexane/AcOEt = 10-30%) to afford **16** (2.7 mg, 3.0 μmol, 92%) as a white foam. ^{1}H NMR (CD_3OD, 500 MHz, 1:1 mixture of rotamers) δ 7.70 (d, 1H, H-6-uridine, $J_{\text{H-6-uridine, H-5-uridine}}$ = 8.0 Hz), 7.68 (d, 1H, H-6-uridine, $J_{\text{H-6-uridine, H-5-uridine}}$ = 8.0 Hz), 7.33-7.28 (m, 5H,

$NCH_2OCH_2C_6H_5$), 6.40 (d, 1H, H-1′-uridine, $J_{\text{H-1′-uridine, H-2′-uridine}}$ = 6.3 Hz), 6.35 (d, 1H, H-1′-uridine, $J_{\text{H-1′-uridine, H-2′-uridine}}$ = 6.9 Hz), 6.25 (s, 1H, H-5′-uridine), 5.97-5.88 (m, 2H, H-5-uridine, C*H*-Alloc), 5.48 (s, 5H, CH_2OBn), 5.31, 5.29 (each d, 1H, C*H*-Alloc, *J* = 17.2, 16.6 Hz), 5.18 (d, 1H, C*H*-Alloc, *J* = 10.3 Hz), 4.65 (s, 2H, NCH_2OCH_2Ph), 4.58-4.51 (m, 4H, H-2′-uridine, H-3′-uridine, CH_2-Alloc), 4.44-4.28 (m, 1H, H-α-DABA,), 4.37 (m, 1H, H-β-DABA), 2.81 (s, 3H, NCH_3), 1.42 (s, 9H, Boc-^{t}Bu), 1.21 (m, 3H, H-γ-DABA), 0.94 (s, 9H, $SiC(\underline{CH_3})_3$), 0.85 (s, 9H, $SiC(\underline{CH_3})_3$), 0.17 (s, 3H, ^{t}BuSi(CH_3)$_2$), 0.14 (s, 3H, ^{t}BuSi(CH_3)$_2$), 0.08 (s, 3H, ^{t}BuSi(CH_3)$_2$), –0.02 (s, 3H, ^{t}BuSi(CH_3)$_2$); ^{13}C NMR (CD_3OD, 125 MHz, 1:1 mixture of rotamers) δ 169.7, 164.2, 157.6, 152.8, 144.0, 141.4, 141.2, 139.1, 134.2, 129.3, 128.8, 128.7, 117.9, 117.6, 1103.7, 103.5, 101.4, 101.3, 91.0, 90.3, 81.0, 76.5, 76.1, 73.0, 72.7, 71.5, 67.6, 67.3, 58.4, 54.5, 30.4, 28.7, 26.4, 26.2, 19.1, 18.8, 15.2, 14.3, –3.9. –4.2, –4.3, –4.8; ESIMS-LR *m/z* calcd for $C_{43}H_{70}N_5O_{11}Si_2$ 888.46, found 888.4; ESIMS-HR *m/z* calcd for $C_{43}H_{70}N_5O_{11}Si_2$ 888.4605, found 888.4598; $[\alpha]^{24}_D$ –0.65 (*c* 1.06, $CHCl_3$).

Compound 17. A solution of **16** (444 mg, 500 μmol) in CH_2Cl_2 (10 mL) was treated with 1 M BCl_3 in CH_2Cl_2 (5 mL, 5 mmol) at –78 °C for 30 min followed by at 0 °C for 15 min. After *sat*. *aq*. $NaHCO_3$ was added to the mixture, the resulting biphasic mixture was vigorously stirred for 15 min. The mixture was extracted with CH_2Cl_2, which was

washed with *sat*. *aq*. $NaHCO_3$, H_2O and brine. The organic layer was dried (Na_2SO_4), filtrated and concentrated *in vacuo*. The residue was semi-purified by silica gel column chromatography (ϕ 2 × 10 cm, $CHCl_3$/MeOH = 0-1-2-5%) to afford amine (177.9 mg, 266.3 μmol, 53%) as a white foam. This amine was immediately used to the next reaction. A mixture of the amine (47.3 mg, 70.7 μmol), ureadipeptide **4** (60.4 mg, 106.1 μmol), HOBt (14.3 mg, 106.1 μmol) and $^{i}Pr_2NEt$ (37.0 μL, 212.2 μmol) in CH_2Cl_2 (1 mL) was treated with EDCI (20.4 mg, 106.1 mmol) at room temperature for 12 h. The reaction mixture was diluted with AcOEt and washed with 0.1 M *aq*. HCl, *sat*. *aq*. $NaHCO_3$, H_2O and brine. The organic layer was dried (Na_2SO_4), filtrated and concentrated *in vacuo*. The residue was purified by flash silica gel column chromatography (ϕ 1.5 × 10 cm, $CHCl_3$/MeOH = 0-1-2%) to afford **17** (64.2 mg, 53 μmol, 75%) as a colorless amorphous solid. ^{1}H NMR (CD_3OD, 500 MHz, 1:1 mixture of rotamers) δ 7.68, 7.61 (each d, 1H, H-6, $J_{6,\,5}$ = 8.0, 8.0 Hz), 7.14 (dd, 1H, H-5-*m*Tyr, $J_{5\text{-}m\text{Tyr},\,4\text{-}m\text{Tyr}} = J_{5\text{-}m\text{Tyr},\,6\text{-}m\text{Tyr}}$ = 7.6 Hz), 6.80 (d, 1H, H-6-*m*Tyr, $J_{6\text{-}m\text{Tyr},\,5\text{-}m\text{Tyr}}$ = 7.6 Hz), 6.74 (s, 1H, H-2-*m*Tyr), 6.74 (d, 1H, H-4-*m*Tyr, $J_{4\text{-}m\text{Tyr},\,5\text{-}m\text{Tyr}}$ =7.6 Hz), 6.38 (d, 1H, H-1′-uridine, $J_{\text{H-1′-uridine, H-2′-uridine}}$ = 6.9 Hz), 6.33 (d, 1H, H-1′-uridine, $J_{\text{H-1′-uridine, H-2′-uridine}}$ = 6.9 Hz), 6.26 (s, 1H, H-5′-uridine), 6.24 (s, 1H, H-5′-uridine), 5.94 (ddt, 1H, C*H*-Alloc, *J* = 16.6, 10.9, 5.7 Hz), 5.86 (d, 1H, H-5-uridine, $J_{\text{H-5-uridine, H-6-uridine}}$ = 8.0 Hz), 5.80 (d, 1H, H-5-uridine, $J_{\text{H-5-uridine, H-6-uridine}}$ = 8.0 Hz), 5.31

(d, 1H, C*H*-Alloc, J = 16.6 Hz), 5.28 (d, 1H, C*H*-Alloc, J = 16.6 Hz), 5.18 (d, 1H, C*H*-Alloc, J = 10.9 Hz), 4.71(d, 1H, H-α-DABA, $J_{\text{H-α-DABA, H-β-DABA}}$ = 8.0 Hz), 4.63 (d, 1H, H-α-DABA, $J_{\text{H-α-DABA, H-β-DABA}}$ = 10.3 Hz), 4.58-4.52(m, 3H, H-3′-uridine, CH_2-Alloc), 4.48-4.37 (m, 2H, H-2′-uridine, H-β-DABA), 4.41 (t, 1H, H-α-*m*Tyr, $J_{\text{α-}m\text{Tyr, β-}m\text{Tyr}}$ = 6.9 Hz), 4.35 (m, 1H, H-α-Met) , 2.92 (d, 2H, H-β-*m*Tyr, $J_{\text{β-}m\text{Tyr, α-}m\text{Tyr}}$ = 6.9Hz), 2.81 (s, 3H, NCH_3), 2.80 (s, 3H, H-NCH_3), 2.47 (m, 2H, H-γ-Met), 2.04 (s, 3H, SCH_3-Met), 1.98 (dddd, 1H, H-β-Met, $J_{\text{gem}} = J_{\text{β-Met, α-Met}}$ = 14.2, $J_{\text{β-Met, γ-Met}}$ = 6.9, 2.3 Hz), 1.83 (ddd, 1H, H-β-Met, $J_{\text{gem}} = J_{\text{β-Met, α-Met}}$ = 14.2, $J_{\text{β-Met, γ-Met}}$ = 8.0 Hz), 1.39 (s, 9H, ^{t}Bu), 1.29-1.24 (m, 3H, Si[C*H*$(CH_3)_2]_3$), 1.21 (d, 3H, H-γ-DABA, $J_{\text{H-γ-DABA, H-β-DABA}}$ = 6.9 Hz), 1.10 (d, 18H, Si[CH(C$H_3)_2]_3$, J = 7.5 Hz), 0.92 (s, 9H, SiC(C$\underline{H_3}$)$_3$), 0.88 (s, 9H, SiC(C$\underline{H_3}$)$_3$), 0.15 (s, 3H, ^{t}BuSi(C$H_3)_2$), 0.12 (s, 3H, ^{t}BuSi(C$H_3)_2$), 0.08 (s, 3H, ^{t}BuSi(C$H_3)_2$), 0.01 (s, 3H, ^{t}BuSi(C$H_3)_2$); ^{13}C NMR (CD_3OD, 125 MHz, 1:1 mixture of rotamers) δ 174.6, 173.0, 169.1, 168.9, 165.5, 159.4, 157.3, 152.3, 152.3, 144.1, 144.0, 142.1, 139.7, 134.3, 130.3, 123.5, 122.1, 119.0, 118.0, 117.6, 104.0, 101.3, 89.3, 82.8, 76.6, 76.3, 72.7, 67.6, 67.3, 56.7, 56.2, 54.6, 54.1, 39.4, 33.7, 30.9, 30.5, 28.3, 27.9, 26.3, 26.2, 19.0, 18.8, 18.5, 15.4, 14.5, 13.9 ,−3.9, −4.2, −4.3, −4.9; ESIMS-LR *m/z* calcd for $C_{58}H_{100}N_7O_{13}SSi_3$ 1218.64, found 1218.7; ESIMS-HR *m/z* calcd for $C_{58}H_{100}N_7O_{13}SSi_3$ 1218.6402, found 1218.6417; $[\alpha]^{23}_D$ +15.5 (*c* 0.89, $CHCl_3$).

Compound 18. A solution of **17** (44.6 mg, 36.6 μmol) and morpholine (12.6 μL, 146.4 μmol) in THF (400 μL) was treated with $Pd(PPh_3)_4$ (21.1 mg, 18.3 μmol) at room temperature for 2 h. After SH silica gel was added to the mixture, the whole was stirred for 1 h. The SH silica gel was filtered off, and the filtrate was concentrated *in vacuo*. A mixture of the crude amine, Boc-*m*Tyr(TIPS)-OH (**5**) (32.0 mg, 73.2 μmol) and $^{i}Pr_2NEt$ (25.6 μL, 146.4 μmol) in DMF (400 μL) was treated with HATU (27.8 mg, 73.2 μmol) at room temperature for 5 h. The reaction mixture was diluted with AcOEt/hexane (4/1), which was washed with 0.1 M *aq*. HCl, *sat*. *aq*. $NaHCO_3$, H_2O and brine. The organic layer was dried (Na_2SO_4), filtrated and concentrated *in vacuo*. The residue was purified by flash silica gel column chromatography (ϕ 1 × 10 cm, $CHCl_3$/MeOH = 0-1-2-5%, then hexane/AcOEt = 50%) to afford **18** (24.8 mg, 16.0 μmol, 44%) as a colorless amorphous solid. ^1H NMR (CD_3OD, 500 MHz, 3:2 mixture of rotamers, selected date for the major rotamer) δ 7.38 (d, 1H, H-6-uridine, $J_{\text{H-6-uridine, H-5-uridine}}$ = 8.0 Hz), 7.18-7.11 (m, 2H, H-5-*m*Tyr), 6.88 (d, 1H, H-4-*m*Tyr, $J_{\text{4-}m\text{Tyr, 5-}m\text{Tyr}}$ = 7.5 Hz), 6.83 (br s, 1H, H-2-*m*Tyr), 6.81-6.68 (m, 4H, H-2-*m*Tyr, H-4-*m*Tyr, H-6-*m*Tyr), 6.49 (d, 1H, NH-*m*Tyr, $J_{\text{NH-}m\text{Tyr, α-}m\text{Tyr}}$ = 8.6 Hz), 6.24 (s, 1H, H-5′-uridine), 6.19 (d, 1H, H-1′-uridine, $J_{\text{H-1′-uridine, H-2′ -uridine}}$ = 7.5 Hz), 5.73 (d, 1H, H-5-uridine, $J_{\text{H-5-uridine, H-6-uridine}}$ = 8.0 Hz), 4.91-4.84 (m, 1H, H-β-DABA), 4.71 (d, 1H, H-α-DABA, $J_{\text{H-α-DABA, H-β-DABA}}$ = 8.0 Hz), 4.68 (ddd, 1H, H-α-

*m*Tyr, $J_{\alpha\text{-}m\text{Tyr, }\beta\text{-}m\text{Tyr}}$ = 10.3, $J_{\alpha\text{-}m\text{Tyr, NH-}m\text{Tyr}}$ = 8.6, $J_{\alpha\text{-}m\text{Tyr, }\beta\text{-}m\text{Tyr}}$ =3.4 Hz), 4.49 (d, 1H, H-3′-uridine, $J_{\text{H-3′-uridine, H-2′-uridine}}$ = 4.0 Hz), 4.42-4.47 (m, 2H, H-2′-uridine, H-α-*m*Tyr), 4.37-4.30 (m, 1H, H-α-Met), 3.07 (s, 3H, NC*H*$_3$), 2.92 (d, 1H, H-β-*m*Tyr, $J_{\beta\text{-}m\text{Tyr, }\alpha\text{-}m\text{Tyr}}$ = 6.9 Hz), 2.90-2.85 (m, 2H, H-β-*m*Tyr, H-β′-*m*Tyr), 2.59 (dd, 1H, H-β-*m*Tyr, J_{gem} = 14.3, $J_{\beta\text{-}m\text{Tyr, }\alpha\text{-}m\text{Tyr}}$ = 10.3 Hz), 2.51-2.45 (m, 2H, H-γ-Met), 2.05 (s, 3H, SC*H*$_3$-Met), 2.02-1.95 (m, 1H, H-β-Met), 1.87-1.80 (m, 1H, H-β-Met), 1.39 (s, 9H, ^{t}Bu), 1.34 (s, 9H, Boc-^{t}Bu), 1.31-1.20 (m, 9H, H-γ-DABA, Si[C*H*$(CH_3)_2]_3$), 1.12-1.10 (d, 36H, Si[CH$(CH_3)_2]_3$), 0.90 (s, 9H, SiC($\underline{CH_3}$)$_3$), 0.85 (s, 9H, SiC($\underline{CH_3}$)$_3$), 0.12 (s, 3H,^{t}BuCSi$(CH_3)_2$), 0.10 (s, 3H, ^{t}BuSi$(CH_3)_2$), 0.01 (s, 3H, ^{t}BuSi$(CH_3)_2$), –0.05 (s, 3H, ^{t}BuSi$(CH_3)_2$); ^{13}C NMR (CD_3OD, 125 MHz, 1:1 mixture of rotamers) δ 174.8, 174.7, 174.4, 174.0, 173.1, 173.0, 168.7, 165.6, 165.5, 159.5, 159.4, 157.6, 157.5, 157.4, 157.3, 115.2, 143.9, 143.7, 142.5, 140.4, 139.7, 139.7, 139.4, 130.7, 130.5, 130.4, 123.6, 123.4, 123.2, 122.2, 122.1, 122.1, 104.0, 101.5, 101.4, 91.0, 82.8, 80.9, 80.5, 76.5, 75.9, 72.9, 72.6, 56.9, 56.6, 56.2, 56.1, 55.8, 54.3, 53.7, 53.0, 52.3, 40.3, 39.5, 39.3, 38.4, 33.5, 33.3, 31.0, 30.8, 28.9, 28.7, 28.6, 28.3, 26.4, 26.3, 26.2, 19.1, 18.8, 18.5, 18.5, 18.2, 18.5, 15.4, 14.3, 14.2, 13.9, 13.7, −3.8, −4.1, −4.2, −4.9, −4.9; ESIMS-LR *m/z* calcd for $C_{77}H_{133}N_8O_{15}SSi_2$ 1553.87, found 1554.6; ESIMS-HR *m/z* calcd for $C_{77}H_{133}N_8O_{15}SSi_2$ 1553.8683, found 1553.8624; $[\alpha]^{20}_D$ +26.1 (*c* 0.70, $CHCl_3$).

3′-Hydroxymureidomycin A (2) and sulfoxide analogue 19. A solution of **18** (17.0 mg, 10.9 μmol) in MeCN (1 mL) was treated with 3HF·Et_3N (71.3 μL, 437.5 μmol) at room temperature for 50 h. The reaction mixture was concentrated, and the residue was diluted with AcOEt. The organic layer was washed with *sat*. *aq*. $NaHCO_3$, H_2O and brine, dried (Na_2SO_4), filtered and concentrated *in vacuo*. The resulting residue was treated with 80% *aq*. TFA at room temperature for 2 h. After toluene was added, the mixture was concentrated *in vacuo*. The residue was triturated with Et_2O, and the precipitate was collected and purified by ODS column chromatography (H_2O/MeCN = 0-30%, containing 0.1% TFA) to afford 3′-hydroxymureidomycin A (**2**) (4.2 mg, 4.9 μmol, 45% over 2 steps) and sulfoxide analogue **19** (3.3 mg, 3.8 μmol, 35% over 2 steps) as a white powder after lyophilization. ^{1}H NMR (D_2O, 500 MHz, 3:1 mixture of rotamers, selected date for the major rotamer) δ 7.30 (1H, H-5-*m*Tyr, H-5′-*m*Tyr, $J_{5\text{-}m\text{Tyr},\ 6\text{-}m\text{Tyr}} = J_{5'\text{-}m\text{Tyr},\ 6'\text{-}m\text{Tyr}} = J_{5\text{-}m\text{Tyr},\ 4\text{-}m\text{Tyr}} = J_{5\text{-}m\text{Tyr},\ 4'\text{-}m\text{Tyr}}$ = 7.5 Hz), 7.22 (1H, H-5-*m*Tyr, H-5′-*m*Tyr, $J_{5\text{-}m\text{Tyr},\ 6\text{-}m\text{Tyr}} = J_{5'\text{-}m\text{Tyr},\ 6'\text{-}m\text{Tyr}} = J_{5\text{-}m\text{Tyr},\ 4\text{-}m\text{Tyr}} = J_{5\text{-}m\text{Tyr},\ 4'\text{-}m\text{Tyr}}$ = 7.5 Hz), 7.10 (d, 1H, H-6-uridine, $J_{\text{H-6-uridine, H-5-uridine}}$ = 8.0 Hz), 6.87-6.73 (m, 6H, H-6-*m*Tyr, H-4-*m*Tyr, H-2-*m*Tyr), 6.23 (s, 1H, H-5′-uridine), 6.06 (d, 1H, H-1′-uridine, $J_{\text{H-1′-uridine, H-2′-uridine}}$ = 5.2 Hz), 5.65 (d, 1H, H-5-uridine, $J_{\text{H-5-uridine, H-6-uridine}}$ = 8.0 Hz), 4.95 (dq, 1H, H-β-DABA, $J_{\text{H-β-DABA, H-α-DABA}}$ = 9.7, $J_{\text{H-β-DABA, H-γ-DABA}}$ = 6.9 Hz), 4.72 (d, 1H, H-3′-uridine, $J_{\text{H-3′-uridine, H-2′-uridine}}$ = 5.2 Hz),

4.63 (d, 1H, H-α-DABA, $J_{\text{H-α-DABA, H-β-DABA}}$ = 9.2 Hz), 4.58 (dd, 1H, H-α-*m*Tyr, $J_{\text{α-}m\text{Tyr, β-}m\text{Tyr}}$ = 10.0, $J_{\text{α-}m\text{Tyr, β-}m\text{Tyr}}$ = 4.0 Hz), 4.36 (dd, 1H, H-α-*m*Tyr, $J_{\text{α-}m\text{Tyr, β-}m\text{Tyr}}$ = 8.3, $J_{\text{α-}m\text{Tyr, β-}m\text{Tyr}}$ = 5.7 Hz), 4.27 (dd, 1H, H-α-Met, $J_{\text{H-α-Met, H-β-Met}}$ = 8.0, $J_{\text{H-α-Met, H-β-Met}}$ = 5.7 Hz), 4.24 (dd, 1H, H-2′-uridine, $J_{\text{H-2′-uridine, H-3′-uridine}}$ = $J_{\text{H-2′-uridine, H-1′-uridine}}$ = 5.2 Hz), 3.06 (s, 3H, H-NC*H*$_3$), 3.10-3.05 (m, 1H, H-β-*m*Tyr), 3.02 (dd, 1H, H-β-*m*Tyr, J_{gem} = 14.3, $J_{\text{β-}m\text{Tyr, α-}m\text{Tyr}}$ = 5.7 Hz), 2.88 (dd, 1H, H-β-*m*Tyr, J_{gem} = 14.2, $J_{\text{β-}m\text{Tyr, α-}m\text{Tyr}}$ = 8.3 Hz), 2.73-2.66 (m, 1H, H-β-*m*Tyr), 2.55-2.42 (m, 2H, H-γ-Met), 2.06 (s, 3H, SC*H*$_3$-Met), 2.00-1.95 (m, 2H, H-β-Met), 1.23 (d, 3H, H-γ-DABA, $J_{\text{H-γ-DABA, H-β-DABA}}$ = 6.9 Hz); ESIMS-LR *m/z* 857.1 [(M+H)$^+$]; ESIMS-HR *m/z* calcd for $C_{38}H_{49}N_8O_{13}S$ 857.3134, found 857.3122; $[\alpha]^{19}_{D}$ −13.4 (*c* 0.15, H_2O). ^{1}H NMR (D_2O, 500 MHz, a mixture of diastereomers) δ 7.27 (1H, H-5-*m*Tyr), 7.20 (1H, H-5-*m*Tyr), 7.02 (m, 1H, H-6), 6.82-6.70 (m, 6H, H-6-*m*Tyr, H-4-*m*Tyr, H-2-*m*Tyr), 6.19 (s, 1H, H-5′-uridine), 6.00 (m, 1H, H-1′-uridine), 5.58 (m, 1H, H-5-uridine), 4.91 (m, 1H, H-β-DABA), 4.72 (m, 1H, H-3′-uridine), 4.55 (m, 2H, H-α-DABA, H-α-*m*Tyr), 4.38-4.15 (m, 3H, H-α-*m*Tyr, H-α-Met, H-2′-uridine), 3.08-3.05 (m, 1H, H-β-*m*Tyr), 3.05 (s, 3H, NC*H*$_3$), 2.94-2.80 (m, 4H, H-β-*m*Tyr, H-γ-Met), 2.71-2.65 (m, 1H, H-β-*m*Tyr,), 2.65 (s, 3H, SOC*H*$_3$-Met), 2.13-1.97 (m, 2H, H-β-Met), 1.18 (m, 3H, H-γ-DABA); ESIMS-LR *m/z* calcd for $C_{38}H_{49}N_8O_{14}S$ 873.31, found 873.1 [(M+H)$^+$]; ESIMS-HR *m/z* calcd for $C_{38}H_{49}N_8O_{14}S$ 873.3083, found 873.3077.

Compound 27. A mixture of the **15** (2.50 g, 3.1 mmol), (*S*)-2-[(fluorenylmethyl)amino]-3-(3-hydroxyphenyl)propanoic acid (**26**, 2.09 g, 4.0 mmol), and $^{i}Pr_2NEt$ (1.35 mL, 7.44 mol) in DMF (30 mL) was treated with HATU (981 mg, 1.56 mmol) at 0 °C for 2 h. The reaction mixture was diluted with AcOEt and washed with 0.1 M *aq*. HCl, *sat*. *aq*. $NaHCO_3$, H_2O and brine. The organic layer was dried (Na_2SO_4), filtrated and concentrated *in vacuo*. The residue was purified by flash silica gel column chromatography (ϕ 5 × 15 cm, AcOEt/hexane = 33-55%) to afford **27** (3.59 g, 2.67 mol, 86%) as a colorless amorphous solid. ^{1}H NMR (DMSO-d_6, 400 MHz, T = 50 °C) δ 9.07 (d, 1H, NH-5′-uridine, $J_{\text{NH-5′-uridine , H-5′-uridine}}$ = 10.1 Hz), 7.89-7.84 (m, 4H, H-Fmoc), 7.79-7.69 (m, 2H, H-6-uridine, NH-mTyr), 7.61 (t, 1H, H-Ph, $J_{\text{H-Ph, H-Phe}}$ = 8.5 Hz), 7.42-7.23 (m, 9H, H-Ph, H-Fmoc, NH-DABA), 7.14 (dd, 1H, H-5-*m*Tyr, $J_{\text{5-}m\text{Tyr, 4-}m\text{Tyr}}$ = 8.3 Hz, $J_{\text{5-}m\text{Tyr, 6-}m\text{Tyr}}$ = 8.3 Hz), 6.91-6.84 (m, 2H, H-2-*m*Tyr, H-6-*m*Tyr), 6.69 (d, 1H, H-4-*m*Tyr, $J_{\text{4-}m\text{Tyr, 5-}m\text{Tyr}}$ = 8.3 Hz), 6.23 (d, 1H, H-1′-uridine, $J_{\text{H-1′-uridine, H-2′-uridine}}$ = 7.2 Hz), 6.20 (d, 1H, H-5′-uridine, $J_{\text{H-5′-uridine, NH-5′-uridine}}$ = 10.1 Hz), 5.87 (d, 1H, H-5-uridine, $J_{\text{H-5-uridine, H-6-uridine}}$ = 8.7 Hz), 5.33 (m, 2H, H-NCH_2OBn), 4.93-4.81 (m, 1H, H-β-DABA), 4.58-4.40 (m, 6H, H-2′-uridine, H-3′-uridine, H-Fmoc, H-α-mTyr), 4.56 (s, 2H, H-CH_2Ph), 4.25-4.17 (m, 1H, H-α-DABA), 2.98 (s, 3H, NCH_3), 2.71-2.62 (m, 2H, H-β-*m*Tyr), 1.34 (s, 9H, ^{t}Bu), 1.26-1.14 (m, 3H, Si[CH(CH_3)$_2$]$_3$), 1.07-0.97 (m, 21H, Si[CH(CH_3)$_2$]$_3$, H-γ-DABA),

0.86 (s, 9H, SiC($\underline{C}H_3$)$_3$), 0.76 (s, 9H, SiC($\underline{C}H_3$)$_3$), 0.07 (s, 3H, ^{t}BuSi(CH_3)$_2$), 0.04 (m, 3H, ^{t}BuSi(CH_3)$_2$), −0.01 (m, 3H, ^{t}BuSi(CH_3)$_2$), −0.11 (m, 3H, ^{t}BuSi(CH_3)$_2$); ESIMS-LR *m/z* calcd for $C_{72}H_{104}N_6NaO_{13}Si_3$ 1367.69, found 1368.5; $[\alpha]^{20}_D$ +17.4 (*c* 1.00, $CHCl_3$).

Compound 28. A solution of **27** (2.63 g, 2.00 mmol) in CH_2Cl_2 (120 mL) was treated with 1 M BCl_3 in CH_2Cl_2 (20 mL, 20 mmol) at −78 °C for 30 min followed by at 0 °C for 15 min. After *sat*. *aq*. $NaHCO_3$ was added to the mixture, the resulting biphasic mixture was vigorously stirred for 15 min. The organic layer was separated and washed with *sat*. *aq*. $NaHCO_3$, H_2O and brine. The organic layer was dried (Na_2SO_4) and filtrated. The residue was treated with a solution of HCl in AcOEt (4 M, 1.1 mL, 4.4 mmol) for 30 min. Hexane (200 mL) was added to the solution, which was concentrated *in vacuo* to one-third in volume. Hexane (100 mL) was added to the solution and was concentrated *in vacuo*. The precipitates were collected by filtration, washed with ether, and dried to afford **28** (1.31 g, quant.) as a pale brown solid. This compound was directory used to the next reaction without further purification. ^{1}H NMR (DMSO-d_6, 400 MHz, T = 50 °C) δ10.04 (s, 1H, NH-5′-uridine), 7.87 (d, 2H, NH-DABA, $J_{\text{NH-DABA, H-α-DABA}}$ = 9.6 Hz), 7.67-6.37 (m, 13H, Fmoc, H-2, 4, 5, 6-*m*Tyr, NH-DABA), 7.60 (m, 1H, NH-*m*Tyr), 6.19 (m, 1H, H-1′-uridine), 5.20 (m, 1H, H-5-uridine), 4.92 (m, 1H, H-β-DABA), 4.57 (m, 1H, H-α-DABA), 4.10 (m, 7H, Fmoc, H-3′, 4′, 5′, H-α-*m*Tyr), 2.95 (s, 3H, NCH_3), 2.66 (m, 2H,

H-β-*m*Tyr), 1.24 (m, 3H, H-γ-DABA), 1.23-0.77 (m, 39H, Si[C*H*(CH_3)$_2$]$_3$, Si[CH(C*H*$_3$)$_2$]$_3$, SiC(C*H*$_3$)$_3$), 0.07 (m, 3H, ^{t}BuSi(C*H*$_3$)$_2$), 0.04 (m, 3H, ^{t}BuSi(C*H*$_3$)$_2$), –0.06 (m, 3H, ^{t}BuSi(C*H*$_3$)$_2$), –0.19 (m, 3H, ^{t}BuSi(C*H*$_3$)$_2$); ESIMS-LR *m/z* 1125.6 [(M+Na)$^+$]; ESIMS-HR *m/z* calcd for $C_{59}H_{89}N_6O_{10}Si_3$ 1125.5942, found 1125.5940; $[\alpha]^{20}_D$ +8.6 (*c* 1.00, $CHCl_3$).

(*S*)-{[1-(*tert*-Butoxy)-3-(1*H*-indol-3-yl)-1-oxopropan-2-yl]carbamoyl}glycine (29a). 2-Chlorotrityl chloride resin (300 mg, 0.48 mmol) was placed in a 10 mL polypropylene syringe fitted with a polyethylene filter disc. The resin was washed with CH_2Cl_2 (2 mL), and a solution of Fmoc-Gly (428 mg, 1.4 mmol) and ^{i}Pr$_2$NEt (505 μL, 2.9 mmol) in CH_2Cl_2 was then added. After the mixture was agitated at room temperature for 2 h, the solvent and reagents were removed by suction. The resin bound to the Fmoc-amino acid was subjected to the following washing treatments with CH_2Cl_2/MeOH/^{i}Pr$_2$NEt (17/2/1, 2 mL × 3), DMF (2 mL × 3) and CH_2Cl_2 (2 mL × 3). The Fmoc group was removed with piperidine/DMF (1/4, 5 min, then 1/9, 15 min). The resin was washed with DMF (2 mL×3) and CH_2Cl_2 (2 mL×3). A solution of 1,1′-carbonyldiimidazole (234 mg, 1.4 mmol) and *N*-methylmorphline (319 μL, 2.9 mmol) in CH_2Cl_2 (2 mL) was added to the resin. After the mixture was agitated at room temperature for 1 min, the solvent and reagents were removed by suction. This procedure was repeated

for 5 times. The resin was washed with CH_2Cl_2 (2 mL × 3). Then, a solution of L-Trp-O^{t}Bu·HCl (142 mg, 0.48 mmol) and ^{i}Pr$_2$NEt (251 μL, 1.4 mmol) in CH_2Cl_2 was added, the mixture was agitated at room temperature for 3 h. The resin was washed with DMF (2 mL × 3) and CH_2Cl_2 (2 mL × 3). Completion of the reaction was confirmed by Kaiser test. The resin was treated with 5% TFA/CH_2Cl_2 to cleave the urea-dipeptide, and the filtrate was partitioned between CH_2Cl_2 and H_2O. The organic phase was washed with brine, dried (Na_2SO_4), filtered and concentrated *in vacuo* to afford **29a** (43 mg, 0.11 mmol, 23%) as a white solid. This material was used for the next reaction without further purification. ESIMS-LR *m/z* calcd for $C_{18}H_{23}N_3NaO_5$ 384.15, found 383.7.

{[(*S*)-1-(*tert*-Butoxy)-3-(1*H*-indol-3-yl)-1-oxopropan-2-yl]carbamoyl}-L-alanine (29b). In a manner similar to the synthesis of **29a**, **29b** (123 mg, 0.33 mmol, 69%) was obtained as a white solid using L-Trp-O^{t}Bu・HCl (142 mg, 0.48 mmol). ESIMS-LR *m/z* calcd for $C_{19}H_{25}N_3NaO_5$ 398.17, found 397.9.

{[(*S*)-1-(*tert*-Butoxy)-3-(1*H*-indol-3-yl)-1-oxopropan-2-yl]carbamoyl}-L-leucine (29c). In a manner similar to the synthesis of **29a**, **29c** (92 mg, 0.22 mmol, 46%) was obtained as a white solid using Fmoc-Leu (509 mg, 1.4 mmol). ESIMS-LR *m/z* calcd for $C_{22}H_{31}N_3NaO_5$ 440.22, found 439.8.

{[(*S*)-1-(*tert*-Butoxy)-3-(1*H*-indol-3-yl)-1-oxopropan-2-yl]carbamoyl}-L-isoleucine (29d). In a manner similar to the synthesis of **29a**, **29d** (54 mg, 0.13 mmol, 54%) was obtained as a white solid using Fmoc-Ile (254 mg, 0.72 mmol). ESIMS-LR *m/z* calcd for $C_{22}H_{31}N_3NaO_5$ 440.22, found 440.1.

{[(*S*)-1-(*tert*-Butoxy)-3-(1*H*-indol-3-yl)-1-oxopropan-2-yl]carbamoyl}-L-valine (29e). In a manner similar to the synthesis of **29a**, **29e** (58 mg, 0.14 mmol, 58%) was obtained as a white solid using Fmoc-Val (244 mg, 0.72 mmol). ESIMS-LR *m/z* calcd for $C_{21}H_{29}N_3NaO_5$ 426.20, found 426.0.

***N*-{[(*S*)-1-(*tert*-Butoxy)-3-(1*H*-indol-3-yl)-1-oxopropan-2-yl]carbamoyl}-*S*-trityl-L-cysteine (29f).** In a manner similar to the synthesis of **29a**, **29f** (251 mg, 0.38 mmol, 80%) was obtained as a white solid using Fmoc-Cys(Trt) (843 mg, 1.4 mmol). ESIMS-LR *m/z* calcd for $C_{38}H_{39}N_3NaO_5S$ 672.25, found 671.6.

{[(*S*)-1-(*tert*-Butoxy)-3-(1*H*-indol-3-yl)-1-oxopropan-2-yl]carbamoyl}-L-methionine (29g). In a manner similar to the synthesis of **29a**, **29g** (66 mg, 0.15 mmol, 63%) was obtained as a white solid using Fmoc-Met (267 mg, 0.72 mmol). ESIMS-LR *m/z* calcd for $C_{21}H_{29}N_3NaO_5S$ 458.17, found 458.1.

{[(*S*)-1-(*tert*-Butoxy)-3-(1*H*-indol-3-yl)-1-oxopropan-2-yl]carbamoyl}-L-phenylalanine (29h). In a manner similar to the synthesis of **29a**, **29h** (72 mg, 0.16 mmol, 67%)

was obtained as a white solid using Fmoc-Phe (279 mg, 0.72 mmol). ESIMS-LR *m/z* calcd for $C_{25}H_{29}N_3NaO_5$ 474.20, found 474.1.

(*S*)-2-{3-[(*S*)-1-(*tert*-Butoxy)-3-(1*H*-indol-3-yl)-1-oxopropan-2-yl]ureido}-3-[4-(*tert*-butoxy)phenyl]propanoic acid (29i). In a manner similar to the synthesis of **29a**, **29i** (67 mg, 0.13 mmol, 54%) was obtained as a white solid using Fmoc-Tyr(O^{t}Bu) (331 mg, 0.72 mmol). ESIMS-LR *m/z* calcd for $C_{29}H_{37}N_3NaO_6$ 546.26, found 546.0.

***N*α-[{(*S*)-1-(*tert*-Butoxy)-3-(1*H*-indol-3-yl)-1-oxopropan-2-yl]carbamoyl}-1-(*tert*-butoxycarbonyl)-L-tryptophan (29j).** In a manner similar to the synthesis of **29a**, **29j** (69 mg, 0.12 mmol, 50%) was obtained as a white solid using Fmoc-Trp(Boc) (379 mg, 0.72 mmol). ESIMS-LR *m/z* calcd for $C_{32}H_{38}N_4NaO_7$ 474.20, found 613.0.

***N*α-{[(*S*)-1-(*tert*-Butoxy)-3-(1*H*-indol-3-yl)-1-oxopropan-2-yl]carbamoyl}-*N*-trityl-L-histidine (29k)**. In a manner similar to the synthesis of **29a**, **29k** (113 mg, 0.16 mmol, 33%) was obtained as a white solid using Fmoc-His(Trt) (892 mg, 1.4 mmol). ESIMS-LR *m/z* calcd for $C_{41}H_{42}N_5O_5$ 684.32, found 683.9.

(*S*)-4-(*tert*-Butoxy)-2-{3-[(*S*)-1-(*tert*-butoxy)-3-(1*H*-indol-3-yl)-1-oxopropan-2-yl]-ureido}-4-oxobutanoic acid (29l). In a manner similar to the synthesis of **29a**, **29l** (145 mg, 0.22 mmol, 46%) was obtained as a white solid using Fmoc-Asp(O^{t}Bu) (592 mg, 1.4 mmol). ESIMS-LR *m/z* calcd for $C_{24}H_{33}N_3NaO_7$ 498.22, found 498.1.

(*S*)-5-(*tert*-Butoxy)-2-{3-[(*S*)-1-(tert-butoxy)-3-(1*H*-indol-3-yl)-1-oxopropan-2-yl]ureido}-5-oxopentanoic acid (29m). In a manner similar to the synthesis of **29a**, **29m** (144 mg, 0.29 mmol, 60%) was obtained as a white solid using Fmoc-Glu(O^{t}Bu) (638 mg, 1.4 mmol). ESIMS-LR *m/z* calcd for $C_{25}H_{35}N_3NaO_7$ 512.24, found 511.8.

***N*2-{[(*S*)-1-(*tert*-Butoxy)-3-(1*H*-indol-3-yl)-1-oxopropan-2-yl]carbamoyl}-*N*6-(*tert*-butoxycarbonyl)-L-lysine (29n).** In a manner similar to the synthesis of **29a**, **29n** (74 mg, 0.14 mmol, 58%) was obtained as a white solid using Fmoc-Lys(Boc) (337 mg, 0.72 mmol). ESIMS-LR *m/z* calcd for $C_{27}H_{40}N_4NaO_7$ 555.28, found 555.1.

***N*2-{[(*S*)-1-(*tert*-Butoxy)-3-(1*H*-indol-3-yl)-1-oxopropan-2-yl]carbamoyl}-*N*ω-[(2,2,4,6,7-pentamethyl-2,3-dihydrobenzofuran-5-yl)sulfonyl]-L-arginine (29o).** In a manner similar to the synthesis of **29a**, **29o** (133 mg, 0.19 mmol, 40%) was obtained as a white solid using Fmoc-Arg(Pbf) (934 mg, 1.4 mmol). ESIMS-LR *m/z* calcd for $C_{35}H_{49}N_6O_8S$ 713.33, found 713.0.

***N*-{[(*S*)-1-(*tert*-Butoxy)-3-(1*H*-indol-3-yl)-1-oxopropan-2-yl]carbamoyl}-*O*-*tert*-butyl-L-serine (29p).** In a manner similar to the synthesis of **29a**, **29p** (64 mg, 0.14 mmol, 58%) was obtained as a white solid using Fmoc-Ser(O^{t}Bu) (276 mg, 0.72 mmol). ESIMS-LR *m/z* calcd for $C_{23}H_{33}N_3NaO_6$ 470.23, found 469.9.

{[(*S*)-1-(*tert*-Butoxy)-3-(1*H*-indol-3-yl)-1-oxopropan-2-yl]carbamoyl}-*O*-*tert*-butyl-L-threonine (29q). In a manner similar to the synthesis of **29a**, **29q** (63 mg, 0.14 mmol, 57%) was obtained as a white solid using Fmoc-Thr(O^{t}Bu) (286 mg, 0.72 mmol). ESIMS-LR *m/z* calcd for $C_{24}H_{35}N_3NaO_6$ 484.24, found 484.0.

***N*2-{[(*S*)-1-(*tert*-Butoxy)-3-(1*H*-indol-3-yl)-1-oxopropan-2-yl]carbamoyl}-*N*4-trityl-L-asparagine (29r).** In a manner similar to the synthesis of **29a**, **29r** (145 mg, 0.22 mmol, 46%) was obtained as a white solid using Fmoc-Asn(Trt) (859 mg, 1.4 mmol). ESIMS-LR *m/z* calcd for $C_{39}H_{40}N_4NaO_6$ 683.28, found 683.2.

***N*2-{[(*S*)-1-(*tert*-Butoxy)-3-(1*H*-indol-3-yl)-1-oxopropan-2-yl]carbamoyl}-*N*5-trityl-L-glutamine (29s)**. In a manner similar to the synthesis of **29a**, **29s** (66 mg, 0.09 mmol, 19%) was obtained as a white solid using Fmoc-Gln(Trt) (880 mg, 1.4 mmol). ESIMS-LR *m/z* calcd for $C_{40}H_{42}N_4NaO_6$ 697.30, found 696.8.

{[(*S*)-1-(*tert*-Butoxy)-3-(1*H*-indol-3-yl)-1-oxopropan-2-yl]carbamoyl}-L-proline (29t). A solution of L-Trp(Boc)·HCl (100 mg, 0.33 mmol) in CH_2Cl_2 (3.3 mL) was added dropwise to a solution of triphosgene (76 mg, 0.25 mmol) and Et_3N (460 μL, 3.3 mmol) at −78 °C, and the mixture was stirred for 7 h. A solution of L-Pro-OH (37 mg, 0.66 mmol) in DMF (mL) was added to the mixture, which was stirred for 17 h. After H_2O was added, the whole mixture was partitioned between AcOEt and 1 M *aq*. HCl. The

organic phase was washed with H_2O and brine, dried (Na_2SO_4), filtered, and concentrated *in vacuo*. The residue was purified by silica gel chromatography to afford **29t** (20 mg, 0.05 mmol, 15%) as a white solid. ^{1}H NMR (DMSO-d_6, 400 MHz) δ 10.82 (s, 1H, NH-δ1-Trp), 7.53 (d, 1H, H-ε3-Trp, $J_{\text{H-ε3-Trp, H-ζ2-Trp}}$ = 9.0 Hz), 7.33 (d, 1H, H-ζ1-Trp, $J_{\text{H-ζ1-Trp, H-η-Trp}}$ = 8.1 Hz) , 7.15 (s, 1H, H-δ1-Trp), 7.06 (dd, 1H, H-η-Trp, $J_{\text{H-η-Trp, H-ζ1-Trp}}$ = $J_{\text{H-η-Trp, H-ζ2-Trp}}$ = 8.1 Hz), 6.97 (dd, 1H, H-ζ2-Trp, $J_{\text{H-ζ2-Trp, H-η-Trp}}$ = 8.1, $J_{\text{H-ζ2-Trp, H-ε3-Trp}}$ = 9.0 Hz), 4.30-3.98 (m, 2H, H-α-Pro, H-α-Trp), 3.17-2.96 (m, 4H, H-β-Trp, H-δ-Pro), 1.93-1.74 (m, 4H, H-β-Pro, H-γ-Pro), 1.27 (s, 9H, ^{t}Bu); ESIMS-LR *m/z* calcd for $C_{21}H_{27}N_3NaO_5$ 424.18, found 424.0.

Compound 30a. A solution of **29a** (68 mg, 0.10 mmol), **28** (56 mg, 0.05 mmol), and ^{i}Pr$_2$NEt (58 μL, 0.33 mmol) in DMF (1 mL) was treated with HBTU (42 mg, 0.11 mmol) at room temperature for 2 h. The mixture was partitioned between AcOEt and 1 M *aq.* HCl and brine. The organic phase was dried (Na_2SO_4), filtered and concentrated *in vacuo*. The residue was purified by silica gel column chromatography to afford **30a** (16 mg, 0.01 mmol, 10%) as a pale yellow syrup. ^{1}H NMR (DMSO-d_6, 400 MHz, T = 50 °C) δ 11.41 (s, 1H, H-N3-uridine), 10.76 (s, 1H, NH-δ1-Trp), 9.40-9.31 (m, 1H, NH-5′-uridine), 8.17-8.04 (m, 1H, DABA-NH), 7.90-7.79 (m, 2H, H-Fmoc), 7.71-7.45 (m, 2H, NH-*m*Tyr, H-ε3-Trp), 7.43-7.20 (m, 5H, H-Fmoc, H-6-uridine, H-ζ1-Trp, H-η-Trp), 7.19-6.60 (m, 6H,

H-2-*m*Tyr, H-4-*m*Tyr, H-5-*m*Tyr, H-6-*m*Tyr, H-δ1-Trp, H-ζ2-Trp), 6.42 (d, 1H, NH-α-Trp, $J_{\text{NH-α-Trp, H-α-Trp}}$ = 8.1 Hz), 6.42-6.29 (m, 1H, NH-Gly), 6.22-6.08 (m, 2H, H-1′-uridine, H-5′-uridine), 5.67 (d, 1H, H-5-uridine, $J_{\text{H-5-uridine, H-6-uridine}}$ = 8.2 Hz), 5.06-4.71 (m, 1H, H-β-DABA), 4.68-4.58 (m, 1H, H-α-DABA), 4.57-4.02 (m, 7H, H-Fmoc, H-α-Trp, H-α-*m*Tyr, H-2′-uridine, H-3′-uridine), 3.68 (br s, 2H, H-α-Gly), 3.08-2.84 (m, 2H, H-β-Trp), 3.02 (s, 3H, NCH_3), 2.81-2.58 (m, 2H, H-β-*m*Tyr), 1.27 (s, 9H, ^{t}Bu), 1.31-1.14 (m, 3H, Si[CH(CH$_3$)$_2$]$_3$), 1.07-0.97 (m, 21H, Si[CH(CH$_3$)$_2$]$_3$, H-γ-DABA), 0.86 (s, 9H, SiC(CH_3)$_3$), 0.80 (s, 9H, SiC(CH_3)$_3$), 0.07 (s, 3H, ^{t}BuSi(CH_3)$_2$), 0.04 (s, 3H, ^{t}BuSi(CH_3)$_2$), –0.01 (s, 3H, ^{t}BuSi(CH_3)$_2$), –0.10 (s, 3H, ^{t}BuSi(CH_3)$_2$); ESIMS-LR *m/z* calcd for $C_{77}H_{109}N_9NaO_{14}Si_3$ 1492.73, found 1490.8; $[\alpha]^{20}_D$ –2.0 (*c* 1.00, MeOH).

Compound 30b. In a manner similar to the synthesis of **30a**, **30b** (28 mg, 0.018 mmol, 38%) was obtained as a pale yellow syrup using **29b** (20 mg, 0.05 mmol). ^{1}H NMR (DMSO-d_6, 400 MHz, T = 50 °C) δ 11.44 (s, 1H, H-N3-uridine), 10.77 (s, 1H, NH-δ1-Trp), 9.02 (d, 1H, NH-5′-uridine, $J_{\text{NH-5-uridine, H-5′-uridine}}$ = 8.7 Hz), 8.02 (d, 1H, NH-DABA, $J_{\text{NH-DABA, H-α-DABA}}$ = 9.6 Hz), 7.90-7.80 (m, 2H, H-Fmoc), 7.71-7.45 (m, 2H, NH-*m*Tyr, H-ε3-Trp), 7.43-7.20 (m, 5H, H-Fmoc, H-6-uridine, H-ζ1-Trp, H-η-Trp), 7.20-6.62 (m, 6H, H-2-*m*Tyr, H-4-*m*Tyr, H-5-*m*Tyr, H-6-*m*Tyr, H-δ1-Trp, H-ζ2-Trp), 6.39 (d, 1H, NH-Ala, $J_{\text{NH-Ala, H-α-Ala}}$ = 6.7 Hz), 6.27 (d, 1H, NH-Trp, $J_{\text{NH-Trp, α-Trp}}$ = 7.6 Hz), 6.22-6.05 (m,

2H, H-1′-uridine, H-5′-uridine), 5.64 (d, 1H, H-5-uridine, $J_{\text{H-5-uridine, H-6-uridine}}$ = 7.6 Hz), 4.64-4.05 (m, 9H, H-Fmoc, H-α-DABA, H-α-Ala, H-α-Trp, H-α-*m*Tyr, H-2′-uridine, H-3′-uridine), 3.08-2.92 (m, 5H, H-β-Trp, NCH_3), 2.80-2.58 (m, 2H, H-β-*m*Tyr), 1.28 (s, 9H, ^{t}Bu), 1.32-1.14 (m, 3H, Si[CH(CH_3)$_2$]$_3$), 1.12 (d, 3H, H-β-Ala, $J_{\text{H-β-Ala, H-α-Ala}}$ = 6.7 Hz), 1.07-0.94 (m, 21H, Si[CH(CH_3)$_2$]$_3$, H-γ-DABA), 0.86 (s, 9H, SiC(CH_3)$_3$), 0.80 (s, 9H, SiC(CH_3)$_3$), 0.07 (s, 3H, ^{t}BuSi(CH_3)$_2$), 0.04 (s, 3H, ^{t}BuSi(CH_3)$_2$), 0.00 (s, 3H, ^{t}BuSi(CH_3)$_2$), –0.08 (s, 3H, ^{t}BuSi(CH_3)$_2$); ESIMS-LR *m/z* calcd for $C_{78}H_{111}N_9NaO_{14}Si_3$ 1504.75, found 1504.8; $[\alpha]^{20}_D$ –2.6 (*c* 1.00, MeOH).

Compound 30c. In a manner similar to the synthesis of **30a**, **30c** (26 mg, 0.017 mmol, 17%) was obtained as a pale yellow syrup using **29c** (42 mg, 0.10 mmol). ^{1}H NMR (DMSO-d_6, 400 MHz, T = 50 °C) δ 11.39 (s, 1H, H-N3-uridine), 10.76 (s, 1H, NH-δ1-Trp), 9.21-9.08 (m, 1H, NH-5′-uridine), 8.30-8.24 (m, 1H, DABA-NH), 7.90-7.79 (m, 2H, H-Fmoc), 7.70-7.47 (m, 2H, NH-*m*Tyr, H-ε3-Trp), 7.47-7.19 (m, 5H, H-Fmoc, H-6-uridine, H-ζ1-Trp, H-η-Trp), 7.19-6.59 (m, 6H, H-2-*m*Tyr, H-4-*m*Tyr, H-5-*m*Tyr, H-6-*m*Tyr, H-δ1-Trp, H-ζ2-Trp), 6.38-6.30 (m, 1H, NH-α-Trp), 6.25-6.04 (m, 2H, H-1′-uridine, H-5′-uridine, NH-Leu), 5.66-5.58 (m, 1H, H-5-uridine), 5.06-4.85 (m, 1H, H-β-DABA), 4.57-4.02 (m, 8H, H-α-DABA, H-Fmoc, H-α-Trp, H-α-*m*Tyr, H-2′-uridine, H-3′-uridine), 3.08-2.84 (m, 5H, H-β-Trp, NCH_3), 2.79-2.60 (m, 2H, H-β-*m*Tyr), 1.71-1.12

(m, 6H, H-β-Leu, H-γ-Leu, Si[C*H*$(CH_3)_2]_3$), 1.27 (s, 9H, ^{t}Bu), 1.01-0.92 (m, 21H, Si[C*H*$(CH_3)_2]_3$, H-γ-DABA), 0.92-0.66 (m, 24H, SiC($\underline{CH_3}$)$_3$, H-δ-Leu), 0.80 (s, 9H, SiC($\underline{CH_3}$)$_3$), 0.07 (s, 3H, ^{t}BuSi(CH_3)$_2$), 0.04 (s, 3H, ^{t}BuSi(CH_3)$_2$), 0.01 (s, 3H, ^{t}BuSi(CH_3)$_2$), −0.08 (s, 3H, ^{t}BuSi(CH_3)$_2$); ESIMS-LR *m/z* calcd for $C_{81}H_{117}N_9NaO_{14}Si_3$ 1546.79, found 1547.8; $[\alpha]^{20}_D$ −6.5 (*c* 1.00, MeOH).

Compound 30d. In a manner similar to the synthesis of **30a**, **30d** (27 mg, 0.017 mmol, 18%) was obtained as a pale yellow syrup using **29d** (42 mg, 0.10 mmol). ^{1}H NMR (DMSO-d_6, 400 MHz, T = 50 °C) δ 10.75 (s, 1H, NH-δ1-Trp), 9.09-9.02 (m, 1H, NH-5′-uridine), 8.37-8.25 (m, 1H, DABA-NH), 7.91-7.78 (m, 2H, H-Fmoc), 7.71-7.46 (m, 2H, NH-*m*Tyr, H-ε3-Trp), 7.44-7.22 (m, 5H, H-Fmoc, H-6-uridine, H-ζ1-Trp, H-η-Trp), 7.20-6.62 (m, 6H, H-2-*m*Tyr, H-4-*m*Tyr, H-5-*m*Tyr, H-6-*m*Tyr, H-δ1-Trp, H-ζ2-Trp), 6.38-6.28 (m, 1H, NH-Ile), 6.28-6.07 (m, 3H, NH-α-Trp, H-1′-uridine, H-5′-uridine), 5.67-5.57 (m, 1H, H-5-uridine), 5.91-4.87 (m, 1H, H-β-DABA), 4.63-3.94 (m, 9H, H-α-DABA, H-Fmoc, H-α-Trp, H-α-*m*Tyr, H-2′-uridine, H-3′-uridine, H-α-Ile), 3.06-2.84 (m, 5H, H-β-Trp, NCH_3), 2.77-2.60 (m, 2H, H-β-*m*Tyr), 1.68-1.52 (m, 1H, H-β-Ile), 1.68-1.52 (m, 1H, H-γ-Ile), 1.51-1.33 (m, 1H, H-γ-Ile), 1.32-1.14 (m, 7H, H-γ-Ile, H-δ-Ile, Si[C*H*$(CH_3)_2]_3$), 1.27 (s, 9H, ^{t}Bu), 1.07-0.97 (m, 24H, Si[C*H*$(CH_3)_2]_3$, H-γ-DABA, H-β-Me-Ile), 0.88-0.71 (m, 21H, H-γ-Me-Ile, SiC($\underline{CH_3}$)$_3$), 0.07 (s, 3H, ^{t}BuSi(CH_3)$_2$), 0.03 (s,

3H, ^{t}BuSi(CH_3)$_2$), –0.01 (s, 3H, ^{t}BuSi(CH_3)$_2$), –0.08 (s, 3H, ^{t}BuSi(CH_3)$_2$); ESIMS-LR *m/z* calcd for $C_{81}H_{118}N_9O_{14}Si_3$ 1524.81, found 1525.0; $[\alpha]^{20}_D$ –10.7 (c 1.00, MeOH).

Compound 30e. In a manner similar to the synthesis of **30a**, **30e** (88 mg, 0.06 mmol, 58%) was obtained as a pale yellow syrup using **29e** (40 mg, 0.10 mmol). ^{1}H NMR (DMSO-d_6, 400 MHz, T = 50 °C) δ 11.44 (s, 1H, H-N3-uridine), 10.76 (s, 1H, NH-δ1-Trp), 9.03 (d, 1H, NH-5′-uridine, $J_{\text{NH-5′-uridine, H-5′-uridine}}$ = 9.9 Hz), 8.30-8.25 (m, 1H, DABA-NH), 7.90-7.81 (m, 2H, H-Fmoc), 7.70-7.47 (m, 2H, NH-*m*Tyr, H-ε3-Trp), 7.46-7.21 (m, 5H, H-Fmoc, H-6-uridine, H-ζ1-Trp, H-η-Trp), 7.16-6.62 (m, 6H, H-2-*m*Tyr, H-4-*m*Tyr, H-5-*m*Tyr, H-6-*m*Tyr, H-δ1-Trp, H-ζ2-Trp), 6.34 (d, 1H, NH-Val, $J_{\text{NH-Val, H-α-Val}}$ = 9.4 Hz), 6.30 (d, 1H, NH-α-Trp, $J_{\text{NH-α-Trp, H-α-Trp}}$ = 7.6 Hz), 6.18 (d, 2H, H-1′-uridine, $J_{\text{H-1′-uridine, H-2′-uridine}}$ = 7.2 Hz), 6.18 (d, 2H, H-5′-uridine, $J_{\text{H-5′-uridine, NH-5′-uridine}}$ = 9.9 Hz), 5.65 (d, 1H, H-5-uridine, $J_{\text{H-5-uridine, H-6-uridine}}$ = 7.2 Hz), 5.01-4.89 (m, 1H, H-β-DABA), 4.64-4.55 (m, 1H, H-α-DABA), 4.55-4.04 (m, 7H, H-Fmoc, H-α-Trp, H-α-*m*Tyr, H-2′-uridine, H-3′-uridine), 4.04-3.94 (m, 1H, H-α-Val),3.04-2.91 (m, 2H, H-β-Trp), 2.98 (s, 3H, H-NCH_3), 2.80-2.55 (m, 2H, H-β-*m*Tyr), 1.29 (s, 9H, ^{t}Bu), 1.30-1.14 (m, 3H, Si[CH(CH_3)$_2$]$_3$), 1.07-0.97 (m, 21H, Si[CH(CH_3)$_2$]$_3$, H-γ-DABA), 0.91-0.71 (s, 24H, SiC(CH_3)$_3$, H-γ-Val), 0.07 (s, 3H, ^{t}BuSi(CH_3)$_2$), 0.04 (s, 3H, ^{t}BuSi(CH_3)$_2$), 0.01 (s,

3H, ^{t}BuSi(CH_3)$_2$), –0.08 (s, 3H, ^{t}BuSi(CH_3)$_2$); ESIMS-LR *m/z* calcd for $C_{80}H_{115}N_9NaO_{14}Si_3$ 1532.78, found 1531.7; $[\alpha]^{20}_D$ –10.2 (c 1.00, MeOH).

Compound 30f. In a manner similar to the synthesis of **30a**, **30f** (14 mg, 0.008 mmol, 16%) was obtained as a pale yellow syrup using **29f** (65 mg, 0.10 mmol). ^{1}H NMR (DMSO-d_6, 400 MHz, T = 50 °C) δ 11.44 (s, 1H, H-N3-uridine), 10.74 (s, 1H, NH-δ1-Trp), 9.58 (d, 1H, NH-5′-uridine, $J_{\text{NH-5′-uridine, H-5′-uridine}}$ = 10.3 Hz), 8.18 (m, 1H, DABA-NH, $J_{\text{NH-DABA, H-α-DABA}}$ = 9.6 Hz), 7.90-7.82 (m, 2H, H-Fmoc), 7.71-7.45 (m, 2H, NH-*m*Tyr, H-ε3-Trp), 7.43-7.61 (m, 26H, H-Fmoc, H-6-uridine, H-ζ1-Trp, H-η-Trp, H-2-*m*Tyr, H-4-*m*Tyr, H-5-*m*Tyr, H-6-*m*Tyr, H-δ1-Trp, H-ζ2-Trp, Trt), 6.54 (d, 1H, NH-Cys, $J_{\text{NH-Cys, H-α-Cys}}$ = 8.1 Hz), 6.46 (d, 1H, NH-α-Trp, $J_{\text{NH-α-Trp, H-α-Trp}}$ = 8.1 Hz), 6.23-6.14 (m, 2H, H-1′-uridine, H-5′-uridine), 5.55 (d, 1H, H-5-uridine, $J_{\text{H-5-uridine, H-6-uridine}}$ = 9.0 Hz), 4.97-4.82 (m, 1H, H-β-DABA), 4.74-4.65 (m, 1H, H-α-DABA), 4.58-4.05 (m, 8H, H-Fmoc, H-α-Cys, H-α-Trp, H-α-*m*Tyr, H-2′-uridine, H-3′-uridine), 3.08-2.93 (m, 2H, H-β-Trp), 2.96 (s, 3H, NCH_3), 2.81-2.61 (m, 2H, H-β-*m*Tyr), 2.36-2.28 (m, 2H, H-β-Cys),1.26 (s, 9H, ^{t}Bu), 1.31-1.14 (m, 3H, Si[CH(CH$_3$)$_2$]$_3$), 1.08-0.94 (m, 21H, Si[CH(CH$_3$)$_2$]$_3$, H-γ-DABA), 0.82 (s, 9H, SiC(CH_3)$_3$), 0.79 (s, 9H, SiC(CH_3)$_3$), 0.06 (s, 3H, ^{t}BuSi(CH_3)$_2$), 0.01-–0.04 (m, 6H, ^{t}BuSi(CH_3)$_2$), –0.10 (m, 3H, ^{t}BuSi(CH_3)$_2$);

ESIMS-LR *m/z* calcd for $C_{97}H_{125}N_9NaO_{14}SSi_3$ 1778.83, found 1779.6; $[\alpha]^{20}_D$ –3.9 (*c* 1.00, MeOH).

Compound 30g. In a manner similar to the synthesis of **30a**, **30g** (92 mg, 0.06 mmol, 59%) was obtained as a pale yellow syrup using **29g** (44 mg, 0.10 mmol). ^{1}H NMR (DMSO-d_6, 400 MHz, T = 50 °C) δ 11.39 (s, 1H, H-N3-uridine), 10.72 (s, 1H, NH-δ1-Trp), 9.25-9.17 (m, 1H, NH-5′-uridine), 8.28-8.17 (m, 1H, DABA-NH), 7.86-7.75 (m, 2H, H-Fmoc), 7.67-7.41 (m, 2H, NH-*m*Tyr, H-ε3-Trp), 7.40-7.16 (m, 5H, H-Fmoc, H-6-uridine, H-ζ1-Trp, H-η-Trp), 7.15-6.57 (m, 6H, H-2-*m*Tyr, H-4-*m*Tyr, H-5-*m*Tyr, H-6-*m*Tyr, H-δ1-Trp, H-ζ2-Trp), 6.40 (d, 1H, NH-Met, $J_{\text{NH-α-Met, H-α-Met}}$ = 7.6 Hz), 6.21 (d, 1H, NH-α-Trp, $J_{\text{NH-α-Trp, H-α-Trp}}$ = 7.6 Hz), 6.16-6.05 (m, 2H, H-1′-uridine, H-5′-uridine), 5.61 (d, 1H, H-5-uridine, $J_{\text{H-5-uridine, H-6-uridine}}$ = 7.2 Hz), 4.97-4.83 (m, 1H, H-β-DABA), 4.61-4.51 (m, 1H, H-α-DABA), 4.49-4.02 (m, 8H, H-Fmoc, H-α-Met, H-α-Trp, H-α-*m*Tyr, H-2′-uridine, H-3′-uridine), 3.03-2.88 (m, 5H, H-β-Trp, NCH_3), 2.74-2.55 (m, 2H, H-β-*m*Tyr), 2.40-2.25 (m, 2H, H-γ-Met), 1.95 (s, 3H, H-SCH_3), 1.88-1.71 (m, 1H, H-β-Met), 1.70-1.57 (m, 1H, H-β-Met), 1.24 (s, 9H, ^{t}Bu), 1.28-1.10 (m, 3H, Si[CH(CH_3)$_2$]$_3$), 1.06-0.90 (m, 21H, Si[CH(CH_3)$_2$]$_3$, H-γ-DABA), 0.81 (s, 9H, SiC(C$\underline{H_3}$)$_3$), 0.76 (s, 9H, SiC(C$\underline{H_3}$)$_3$), 0.07 (s, 3H, ^{t}BuSi(CH_3)$_2$), –0.01 (s, 3H, ^{t}BuSi(CH_3)$_2$), –0.04 (s, 3H,

^{t}BuSi(CH_3)$_2$), –0.10 (s, 3H, ^{t}BuSi(CH_3)$_2$); ESIMS-LR *m/z* calcd for $C_{80}H_{115}N_9NaO_{14}SSi_3$ 1564.75, found 1564.5; $[\alpha]^{20}_D$ –5.2 (*c* 1.00, MeOH).

Compound 30h. In a manner similar to the synthesis of **30a**, **30h** (80 mg, 0.05 mmol, 51%) was obtained as a pale yellow syrup using **29h** (45 mg, 0.10 mmol). ^{1}H NMR (DMSO-d_6, 400 MHz, T = 50 °C) δ 11.34 (s, 1H, H-N3-uridine), 10.75 (s, 1H, NH-δ1-Trp), 9.31-9.24 (m, 1H, NH-5′-uridine), 8.38-8.30 (m, 1H, DABA-NH), 7.90-7.80 (m, 2H, H-Fmoc), 7.69-7.51 (m, 1H, H-ε3-Trp), 7.49 (d, 1H, NH-*m*Tyr, $J_{\text{NH-α-}m\text{Tyr, H-α-}m\text{Tyr}}$ = 8.1 Hz), 7.43-7.20 (m, 5H, H-Fmoc, H-6-uridine, H-ζ1-Trp, H-η-Trp), 7.19-6.60 (m, 11H, H-δ-Phe, H-ε-Phe, H-ζ-Phe, H-2-*m*Tyr, H-4-*m*Tyr, H-5-*m*Tyr, H-6-*m*Tyr, H-δ1-Trp, H-ζ2-Trp), 6.41-6.29 (m, 2H, NH-α-Trp, NH-Phe), 6.22-6.12 (m, 2H, H-1′-uridine, H-5′-uridine), 5.44 (d, 1H, H-5-uridine, $J_{\text{H-5-uridine, H-6-uridine}}$ = 7.2 Hz), 5.01-4.89 (m, 1H, H-β-DABA), 4.67-4.55 (m, 1H, H-α-DABA), 4.54-4.06 (m, 8H, H-Fmoc, H-α-Phe, H-α-Trp, H-α-*m*Tyr, H-2′-uridine, H-3′-uridine), 3.04-2.86 (m, 7H, H-β-Phe, H-β-Trp, NCH_3), 2.80-2.62 (m, 2H, H-β-*m*Tyr), 1.26 (s, 9H, ^{t}Bu), 1.29-1.15 (m, 3H, Si[C*H*(CH$_3$)$_2$]$_3$), 1.07-0.96 (m, 21H, Si[C*H*(CH$_3$)$_2$]$_3$, H-γ-DABA), 0.86 (s, 9H, SiC(CH_3)$_3$), 0.79 (s, 9H, SiC(CH_3)$_3$), 0.08 (s, 3H, ^{t}BuSi(CH_3)$_2$), 0.06 (s, 3H, ^{t}BuSi(CH_3)$_2$), –0.01 (s, 3H, ^{t}BuSi(CH_3)$_2$), –0.11 (s, 3H, ^{t}BuSi(CH_3)$_2$); ESIMS-LR *m/z* calcd for $C_{84}H_{115}N_9NaO_{14}Si_3$ 1580.78, found 1580.6; $[\alpha]^{20}_D$ +10.6 (*c* 1.00, MeOH).

Compound 30i. In a manner similar to the synthesis of **30a**, **30i** (37 mg, 0.02 mmol, 22%) was obtained as a pale yellow syrup using **29i** (52 mg, 0.10 mmol). ^{1}H NMR (DMSO-d_6, 400 MHz, T = 50 °C) δ 11.38 (s, 1H, H-N3-uridine), 10.75 (s, 1H, NH-δ1-Trp), 9.33-9.26 (m, 1H, NH-5′-uridine), 8.37-8.25 (m, 1H, DABA-NH), 7.90-7.81 (m, 2H, H-Fmoc), 7.68-7.45 (m, 2H, NH-*m*Tyr, H-ε3-Trp), 7.45-6.60 (m, 15H, H-Fmoc, H-6-uridine, H-ζ1-Trp, H-η-Trp, H-2-*m*Tyr, H-4-*m*Tyr, H-5-*m*Tyr, H-6-*m*Tyr, H-δ1-Trp, H-ζ2-Trp, H-δ-Tyr, H-ε-Tyr), 6.47-6.29 (m, 2H, NH-α-Trp, NH-Tyr), 6.23-6.13 (m, 2H, H-1′-uridine, H-5′-uridine), 5.53-5.44 (m, 1H, H-5-uridine), 5.03-4.89 (m, 1H, H-β-DABA), 4.68-4.55 (m, 1H, H-α-DABA), 4.55-4.02 (m, 8H, H-Fmoc, H-α-Tyr, H-α-Trp, H-α-*m*Tyr, H-2′-uridine, H-3′-uridine), 3.06-2.82 (m, 7H, H-β-Trp, H-β-Tyr, NCH_3), 2.77-2.60 (m, 2H, H-β-*m*Tyr), 1.26 (s, 9H, ^{t}Bu), 1.26 (s, 9H, ^{t}Bu), 1.33-1.13 (m, 3H, Si[CH(CH_3)$_2$]$_3$), 1.11-0.95 (m, 21H, Si[CH(CH_3)$_2$]$_3$, H-γ-DABA), 0.86 (s, 9H, SiC(CH_3)$_3$), 0.79 (s, 9H, SiC(CH_3)$_3$), 0.08 (s, 3H, ^{t}BuSi(CH_3)$_2$), 0.05 (s, 3H, ^{t}BuSi(CH_3)$_2$), –0.01 (s, 3H, ^{t}BuSi(CH_3)$_2$), –0.11 (s, 3H, ^{t}BuSi(CH_3)$_2$); ESIMS-LR *m/z* calcd for $C_{88}H_{123}N_9NaO_{15}Si_3$ 1652.834, found 1652.2; $[\alpha]^{20}_D$ +1.5 (*c* 1.00, MeOH).

Compound 30j. In a manner similar to the synthesis of **30a**, **30j** (62 mg, 0.03 mmol, 36%) was obtained as a pale yellow syrup using **29j** (59 mg, 0.10 mmol). ^{1}H NMR (DMSO-d_6, 400 MHz, T = 50 °C) δ 11.24 (s, 1H, H-N3-uridine), 10.74 (s, 1H, NH-δ1-

Trp), 9.35-9.25 (m, 1H, NH-5′-uridine), 8.44-8.34 (m, 1H, DABA-NH), 7.90-7.78 (m, 2H, H-Fmoc), 7.71-6.60 (m, 18H, NH-*m*Tyr, H-ε3-Trp, H-Fmoc, H-6-uridine, H-δ1-Trp, H-ζ2-Trp, H-ζ1-Trp, H-η-Trp, H-2-*m*Tyr, H-4-*m*Tyr, H-5-*m*Tyr, H-6-*m*Tyr), 6.43 (d, 1H, NH-α-Trp, $J_{\text{NH-α-Trp, H-α-Trp}}$ = 8.1 Hz), 6.33 (d, 1H, NH-α-Trp, $J_{\text{NH-α-Trp, H-α-Trp}}$ = 8.1 Hz), 6.22-6.12 (m, 2H, H-1′-uridine, H-5′-uridine), 5.36-5.29 (m, 1H, H-5-uridine), 5.02-4.88 (m, 1H, H-β-DABA), 4.67-4.06 (m, 9H, H-α-DABA, H-Fmoc, H-α-Trp, H-α-*m*Tyr, H-2′-uridine, H-3′-uridine), 3.09-2.80 (m, 7H, H-β-Trp, NCH_3), 2.81-2.57 (m, 2H, H-β-*m*Tyr), 1.62 (s, 9H, Boc-^{t}Bu), 1.21 (s, 9H, ^{t}Bu), 1.28-1.15 (m, 3H, Si[CH(CH_3)$_2$]$_3$), 1.07-0.93 (m, 21H, Si[CH(CH_3)$_2$]$_3$, H-γ-DABA), 0.85 (s, 9H, SiC(CH_3)$_3$), 0.79 (s, 9H, SiC(CH_3)$_3$), 0.07 (s, 3H, ^{t}BuSi(CH_3)$_2$), 0.04 (s, 3H, ^{t}BuSi(CH_3)$_2$), –0.01 (s, 3H, ^{t}BuSi(CH_3)$_2$), –0.11 (s, 3H, ^{t}BuSi(CH_3)$_2$); ESIMS-LR *m/z* calcd for $C_{91}H_{124}N_{10}NaO_{16}Si_3$ 1719.84, found 1719.6; $[\alpha]^{20}_{D}$ +4.7 (*c* 1.00, MeOH).

Compound 30k. In a manner similar to the synthesis of **30a**, **30k** (23 mg, 0.012 mmol, 12%) was obtained as a pale yellow syrup using **29k** (68 mg, 0.10 mmol). ^{1}H NMR (DMSO-d_6, 400 MHz, T = 50 °C) δ 11.60 (s, 1H, H-N3-uridine), 10.74 (s, 1H, NH-δ1-Trp), 9.22 (d, 1H, NH-5′-uridine, $J_{\text{NH-5-uridine, H-5′-uridine}}$ = 9.4 Hz), 8.23 (4, 1H, DABA-NH, $J_{\text{DABA-NH, H-α-DABA}}$ = 9.4 Hz), 7.92-7.72 (m, 2H, H-Fmoc), 7.71-6.57 (m, 30H, NH-*m*Tyr, H-ε3-Trp, H-Fmoc, H-6-uridine, H-δ1-Trp, H-ζ2-Trp, H-ζ1-Trp, H-η-Trp, H-2-*m*Tyr, H-

4-*m*Tyr, H-5-*m*Tyr, H-6-*m*Tyr, H-δ-His, H-ε-His, Trt), 6.51 (d, 1H, NH-α-Trp, $J_{\text{NH-α-Trp, H-α-Trp}}$ = 7.6 Hz), 6.30 (d, 1H, NH-α-His, $J_{\text{NH-α-His, H-α-His}}$ = 7.6 Hz), 6.20-6.08 (m, 2H, H-1′-uridine, H-5′-uridine), 5.54 (d, 1H, H-5-uridine, $J_{\text{H-5-uridine, H-6-uridine}}$ = 7.6 Hz), 5.02-4.86 (m, 1H, H-β-DABA), 4.64-4.01 (m, 9H, H-α-DABA, H-Fmoc, H-α-His, H-α-Trp, H-α-*m*Tyr, H-2′-uridine, H-3′-uridine), 3.07-2.56 (m, 9H, H-β-Trp, H-β-*m*Tyr, H-β-His, NCH_3), 1.22 (s, 9H, ^{t}Bu), 1.29-1.13 (m, 3H, Si[CH(CH_3)$_2$]$_3$), 1.09-0.96 (m, 21H, Si[CH(CH_3)$_2$]$_3$, H-γ-DABA), 0.83 (s, 9H, SiC(CH_3)$_3$), 0.79 (s, 9H, SiC(CH_3)$_3$), 0.04 (s, 3H, ^{t}BuSi(CH_3)$_2$), 0.00 (s, 3H, ^{t}BuSi(CH_3)$_2$), –0.02 (s, 3H, ^{t}BuSi(CH_3)$_2$), –0.11 (s, 3H, ^{t}BuSi(CH_3)$_2$); ESIMS-LR *m/z* calcd for $C_{100}H_{128}N_{11}O_{14}Si_3$ 1490.89, found 1792.1; $[\alpha]^{20}_D$ –0.5 (*c* 1.00, MeOH).

Compound 30l. In a manner similar to the synthesis of **30a**, **30l** (15 mg, 0.009 mmol, 18%) was obtained as a pale yellow syrup using **29l** (47 mg, 0.10 mmol). ^{1}H NMR (DMSO-d_6, 400 MHz, T = 50 °C) δ 11.42 (s, 1H, H-N3-uridine), 10.75 (s, 1H, NH-δ1-Trp), 9.38 (d, 1H, NH-5′-uridine, $J_{\text{NH-5-uridine, H-5′-uridine}}$ = 9.4 Hz), 8.12 (d, 1H, DABA-NH, $J_{\text{DABA-NH, H-α-DABA}}$ = 9.0 Hz), 7.90-7.79 (m, 2H, H-Fmoc), 7.68-7.46 (m, 2H, NH-*m*Tyr, H-ε3-Trp), 7.43-7.21 (m, 5H, H-Fmoc, H-6-uridine, H-ζ1-Trp, H-η-Trp), 7.19-6.62 (m, 6H, H-2-*m*Tyr, H-4-*m*Tyr, H-5-*m*Tyr, H-6-*m*Tyr, H-δ1-Trp, H-ζ2-Trp), 6.58-6.49 (m, 1H, NH-Asp), 6.45 (d, 1H, NH-α-Trp, $J_{\text{NH-α-Trp, H-α-Trp}}$ = 8.1 Hz), 6.18 (d, 1H, H-1′-

uridine, $J_{\text{H-1′-uridine, H-2′-uridine}}$ = 7.2 Hz), 6.14 (d, 1H, H-5′-uridine, $J_{\text{H-5′-uridine, NH-5-uridine}}$ = 9.4 Hz), 5.63 (d, 1H, H-5-uridine, $J_{\text{H-5-uridine, H-6-uridine}}$ = 8.1 Hz), 4.99-4.85 (m, 1H, H-β-DABA), 4.66-3.93 (m, 9H, H-α-DABA, H-Fmoc, H-α-Asp, H-α-Trp, H-α-*m*Tyr, H-2′-uridine, H-3′-uridine), 3.08-2.92 (m, 5H, H-β-Trp, NCH_3), 2.80-2.39 (m, 4H, H-β-*m*Tyr, H-β-Asp), 1.35 (s, 9H, ^{t}Bu), 1.26 (s, 9H, ^{t}Bu), 1.30-1.13 (m, 3H, Si[CH(CH_3)$_2$]$_3$), 1.08-0.93 (m, 21H, Si[CH(CH_3)$_2$]$_3$, H-γ-DABA), 0.85 (s, 9H, SiC(C$\underline{H_3}$)$_3$), 0.80 (s, 9H, SiC(C$\underline{H_3}$)$_3$), 0.06 (s, 3H, ^{t}BuSi(CH_3)$_2$), 0.03 (s, 3H, ^{t}BuSi(CH_3)$_2$), 0.00 (s, 3H, ^{t}BuSi(CH_3)$_2$), –0.09 (s, 3H, H-^{t}BuCSi(CH_3)$_2$); ESIMS-LR *m/z* calcd for $C_{83}H_{119}N_9NaO_{16}Si_3$ 1604.80, found 1605.9; $[\alpha]^{20}_D$ –0.3 (*c* 1.00, MeOH).

Compound 30m. In a manner similar to the synthesis of **30a**, **30m** (26 mg, 0.016 mmol, 16%) was obtained as a pale yellow syrup using **29m** (50 mg, 0.10 mmol). ^{1}H NMR (DMSO-d_6, 400 MHz, T = 50 °C) δ 11.42 (s, 1H, H-N3-uridine), 10.77 (s, 1H, NH-δ1-Trp), 9.36 (d, 1H, NH-5′-uridine, $J_{\text{NH-5-uridine, H-5′-uridine}}$ = 10.3 Hz), 8.27 (d, 1H, DABA-NH, $J_{\text{DABA-NH, H-α-DABA}}$ = 8.5 Hz), 7.92-7.76 (m, 2H, H-Fmoc), 7.71-7.45 (m, 2H, NH-*m*Tyr, H-ε3-Trp), 7.45-7.20 (m, 5H, H-Fmoc, H-6-uridine, H-ζ1-Trp, H-η-Trp), 7.20-6.57 (m, 6H, H-2-*m*Tyr, H-4-*m*Tyr, H-5-*m*Tyr, H-6-*m*Tyr, H-δ1-Trp, H-ζ2-Trp), 6.58-6.49 (d, 1H, NH-Glu, $J_{\text{NH-α-Glu, H-α-Glu}}$ = 8.5 Hz), 6.28 (d, 1H, NH-α-Trp, $J_{\text{NH-α-Trp, H-α-Trp}}$ = 8.1 Hz), 6.21-6.12 (m, 2H, H-1′-uridine, H-5′-uridine), 5.64 (d, 1H, H-5-uridine, $J_{\text{H-5-}}$

$_{\text{uridine, H-6-uridine}}$ = 7.6 Hz), 5.00-4.87 (m, 1H, H-β-DABA), 4.67-3.93 (m, 9H, H-α-DABA, H-Fmoc, H-α-Glu, H-α-Trp, H-α-*m*Tyr, H-2′-uridine, H-3′-uridine), 3.08-2.91 (m, 5H, H-β-Trp, NCH_3), 2.80-2.58 (m, 2H, H-β-*m*Tyr), 2.24-2.08 (m, 2H, H-γ-Glu), 1.92-1.75 (m, 2H, H-β-Glu), 1.71-1.58 (m, 2H, H-β-Glu), 1.38 (s, 9H, ^{t}Bu), 1.28 (s, 9H, ^{t}Bu), 1.31-1.13 (m, 3H, Si[CH(CH_3)$_2$]$_3$), 1.09-0.92 (m, 21H, Si[CH(CH_3)$_2$]$_3$, H-γ-DABA), 0.85 (s, 9H, SiC(CH_3)$_3$), 0.80 (s, 9H, SiC(CH_3)$_3$), 0.06 (s, 3H, ^{t}BuSi(CH_3)$_2$), 0.03 (s, 3H, ^{t}BuSi(CH_3)$_2$), –0.01 (s, 3H, ^{t}BuSi(CH_3)$_2$), –0.09 (s, 3H, ^{t}BuSi(CH_3)$_2$); ESIMS-LR *m/z* calcd for $C_{83}H_{119}N_9NaO_{16}Si_3$ 1618.81, found 1619.5; $[\alpha]^{20}_D$ –2.3 (*c* 1.00, MeOH).

Compound 30n. In a manner similar to the synthesis of **30a**, **30n** (25 mg, 0.015 mmol, 15%) was obtained as a pale yellow syrup using **29n** (53 mg, 0.10 mmol). ^{1}H NMR (DMSO-d_6, 400 MHz, T = 50 ℃) δ 11.43 (s, 1H, H-N3-uridine), 10.76 (s, 1H, NH-δ1-Trp), 9.31-9.20 (m, 1H, NH-5′-uridine), 8.24-8.17 (m, 1H, DABA-NH), 7.90-7.80 (m, 2H, H-Fmoc), 7.70-7.48 (m, 2H, NH-*m*Tyr, H-ε3-Trp), 7.43-7.19 (m, 6H, H-Fmoc, H-6-uridine, H-ζ1-Trp, H-η-Trp, NH-ε-Lys), 7.19-6.63 (m, 6H, H-2-*m*Tyr, H-4-*m*Tyr, H-5-*m*Tyr, H-6-*m*Tyr, H-δ1-Trp, H-ζ2-Trp), 6.36 (d, 1H, NH-α-Trp, $J_{\text{NH-α-Trp, H-α-Trp}}$ = 8.5 Hz), 6.23 (d, 1H, NH-α-Lys, $J_{\text{NH-α-Lys, H-α-Lys}}$ = 7.6 Hz), 6.20-6.12 (m, 2H, H-1′-uridine, H-5′-uridine), 5.64 (d, 1H, H-5-uridine, $J_{\text{H-5-uridine, H-6-uridine}}$ = 8.5 Hz), 4.97-4.87 (m, 1H, H-β-DABA), 4.65-4.56 (m, 1H, H-α-DABA), 4.54-4.03 (m, 8H, H-Fmoc, H-α-Lys, H-α-Trp,

H-α-*m*Tyr, H-2′-uridine, H-3′-uridine), 3.04-2.92 (m, 5H, H-β-Trp, NCH_3), 2.90-2.80 (m, 2H, H-ε-Lys), 2.77-2.61 (m, 2H, H-β-*m*Tyr), 1.62-1.4 (m, 1H, H-β-Lys), 1.36 (s, 9H, Boc), 1.27 (s, 9H, ^{t}Bu), 1.43-1.13 (m, 8H, H-β-Lys, H-γ-Lys, H-δ-Lys, Si[CH(CH_3)$_2$]$_3$), 1.08-0.92 (m, 21H, Si[CH(CH_3)$_2$]$_3$, H-γ-DABA), 0.85 (s, 9H, SiC($\underline{CH_3}$)$_3$), 0.80 (s, 9H, SiC($\underline{CH_3}$)$_3$), 0.07 (s, 3H, ^{t}BuSi(CH_3)$_2$), 0.03 (s, 3H, ^{t}BuSi(CH_3)$_2$), –0.01 (s, 3H, ^{t}BuSi(CH_3)$_2$), –0.09 (s, 3H, ^{t}BuSi(CH_3)$_2$); ESIMS-LR *m/z* calcd for $C_{86}H_{126}N_{10}NaO_{16}Si_3$ 1661.86, found 1661.1; $[\alpha]^{20}_D$ –0.2 (*c* 1.00, MeOH).

Compound 30o. In a manner similar to the synthesis of **30a**, **30o** (55 mg, 0.03 mmol, 60%) was obtained as a pale yellow syrup using **29o** (36 mg, 0.05 mmol). ^{1}H NMR (DMSO-d_6, 400 MHz, T = 50 °C) δ 11.45 (s, 1H, H-N3-uridine), 10.75 (s, 1H, NH-δ1-Trp), 9.41-9.32 (m, 1H, NH-5′-uridine), 8.26-8.16 (m, 1H, DABA-NH), 7.91-7.78 (m, 2H, H-Fmoc), 7.69-7.45 (m, 2H, NH-*m*Tyr, H-ε3-Trp), 7.45-7.20 (m, 5H, H-Fmoc, H-6-uridine, H-ζ1-Trp, H-η-Trp), 7.19-6.59 (m, 6H, H-2-*m*Tyr, H-4-*m*Tyr, H-5-*m*Tyr, H-6-*m*Tyr, H-δ1-Trp, H-ζ2-Trp), 6.56-6.35 (m, NH-α-Arg), 6.27 (d, 1H, NH-α-Trp, $J_{\text{NH-α-Trp, H-α-Trp}}$ = 7.6 Hz), 6.18-6.09 (m, 2H, H-1′-uridine, H-5′-uridine), 5.66-5.59 (m, 1H, H-5-uridine), 4.97-4.86 (m, 1H, H-β-DABA), 4.68-4.57 (m, 1H, H-α-DABA), 4.57-4.05 (m, 8H, H-Fmoc, H-α-Arg, H-α-Trp, H-α-*m*Tyr, H-2′-uridine, H-3′-uridine), 3.08-2.86 (m, 9H, H-δ-Arg, H-β-Trp, NCH_3, Pbf-CH_2), 2.78-2.61 (m, 2H, H-β-*m*Tyr), 2.43 (m, 3H,

Pbf-CH_3), 2.01 (m, 3H, Pbf-CH_3), 1.68-1.49 (m, 1H, H-β-Arg), 1.41 (s, 3H, Pbf-CH_3), 1.28 (s, 9H, ^{t}Bu), 1.48-1.14 (m, 6H, β-Arg), Si[CH(CH$_3$)$_2$]$_3$), 1.07-0.95 (m, 24H, Si[CH(CH$_3$)$_2$]$_3$, H-γ-DABA, Pbf-CH_3), 0.83 (s, 9H, SiC(CH_3)$_3$), 0.79 (s, 9H, SiC(CH_3)$_3$), 0.05 (s, 3H, ^{t}BuSi(CH_3)$_2$), 0.01 (s, 3H, ^{t}BuSi(CH_3)$_2$), –0.01 (s, 3H, ^{t}BuSi(CH_3)$_2$), –0.10 (s, 3H, ^{t}BuSi(CH_3)$_2$); ESIMS-LR *m/z* calcd for $C_{94}H_{134}N_{12}NaO_{17}Si_3$ 1841.89, found 1842.7; $[\alpha]^{20}_D$ –2.4 (*c* 1.00, MeOH).

Compound 30p. In a manner similar to the synthesis of **30a**, **30p** (84 mg, 0.054 mmol, 54%) was obtained as a pale yellow syrup using **29p** (45 mg, 0.10 mmol). ^{1}H NMR (DMSO-d_6, 400 MHz, T = 50 °C) δ 11.43 (s, 1H, H-N3-uridine), 10.75 (s, 1H, NH-δ1-Trp), 9.58-9.47 (m, 1H, NH-5′-uridine), 8.06-7.97 (m, 1H, DABA-NH), 7.90-7.79 (m, 2H, H-Fmoc), 7.69-7.57 (m, 1H, H-ε3-Trp), 7.51 (m, 2H, NH-*m*Tyr, $J_{\text{NH-}m\text{Trp, H-}\alpha\text{-}m\text{Tyr}}$ = 8.1 Hz), 7.43-7.18 (m, 5H, H-Fmoc, H-6-uridine, H-ζ1-Trp, H-η-Trp), 7.17-6.63 (m, 6H, H-2-*m*Tyr, H-4-*m*Tyr, H-5-*m*Tyr, H-6-*m*Tyr, H-δ1-Trp, H-ζ2-Trp), 6.58 (d, 1H, NH-α-Trp, $J_{\text{NH-α-Trp, H-α-Trp}}$ = 7.6 Hz), 6.35 (d, 1H, NH-Ser, 7.2 Hz), 6.20-6.08 (m, 2H, H-1′-uridine, H-5′-uridine), 5.61 (d, 1H, H-5-uridine, $J_{\text{H-5-uridine, H-6-uridine}}$ = 8.1 Hz), 4.97-4.86 (m, 1H, H-β-DABA), 4.80-4.69 (m, 1H, H-α-DABA), 4.60-4.05 (m, 8H, H-Fmoc, H-α-Ser, H-α-Trp, H-α-*m*Tyr, H-2′-uridine, H-3′-uridine), 3.56-3.46 (m, 1H, H-β-Ser), 3.39-3.31 (m, 1H, H-β-Ser), 3.03-2.93 (m, 5H, H-β-Trp, NCH_3), 2.80-2.57 (m, 2H, H-β-*m*Tyr),

1.26 (s, 9H, ^{t}Bu), 1.29-1.13 (m, 3H, Si[C*H*(CH_3)$_2$]$_3$), 1.08-0.96 (m, 30H, ^{t}Bu, Si[C*H*(CH_3)$_2$]$_3$, H-γ-DABA), 0.84 (s, 9H, SiC(C*H*$_3$)$_3$), 0.79 (s, 9H, SiC(C*H*$_3$)$_3$), 0.06 (s, 3H, ^{t}BuSi(C*H*$_3$)$_2$), 0.02 (s, 3H, ^{t}BuSi(C*H*$_3$)$_2$), –0.01 (s, 3H, ^{t}BuSi(C*H*$_3$)$_2$), –0.11 (s, 3H, ^{t}BuSi(C*H*$_3$)$_2$); ESIMS-LR *m/z* calcd for $C_{82}H_{119}N_9NaO_{15}Si_3$ 1576,80, found 1576.7; $[\alpha]^{20}_D$ +7.2 (*c* 1.00, MeOH).

Compound 30q. In a manner similar to the synthesis of **30a**, **34q** (66 mg, 0.042 mmol, 42%) was obtained as a pale yellow syrup using **29q** (46 mg, 0.10 mmol). ^{1}H NMR (DMSO-d_6, 400 MHz, T = 50 °C) δ 11.43 (s, 1H, H-N3-uridine), 10.75 (s, 1H, NH-δ1-Trp), 9.36-9.25 (m, 1H, NH-5′-uridine), 7.99-7.91 (m, 1H, DABA-NH), 7.91-7.75 (m, 2H, H-Fmoc), 7.71-7.45 (m, 2H, NH-*m*Tyr, H-ε3-Trp), 7.44-7.20 (m, 5H, H-Fmoc, H-6-uridine, H-ζ1-Trp, H-η-Trp), 7.19-6.60 (m, 6H, H-2-*m*Tyr, H-4-*m*Tyr, H-5-*m*Tyr, H-6-*m*Tyr, H-δ1-Trp, H-ζ2-Trp), 6.30-6.05 (d, 4H, NH-α-Trp, NH-Thr, H-1′-uridine, H-5′-uridine), 5.61 (d, 1H, H-5-uridine, $J_{\text{H-5-uridine, H-6-uridine}}$ = 8.1 Hz), 4.98-4.82 (m, 1H, H-β-DABA), 4.74-4.62 (m, 1H, H-α-DABA), 4.60-4.04 (m, 8H, H-Fmoc, H-α-Thr, H-α-Trp, H-α-*m*Tyr, H-2′-uridine, H-3′-uridine), 3.96-3.84 (m, 1H, H-β-Thr), 3.08-2.84 (m, 5H, H-β-Trp, NC*H*$_3$), 2.82-2.59 (m, 2H, H-β-*m*Tyr), 1.27 (s, 9H, ^{t}Bu), 1.31-1.14 (m, 3H, Si[C*H*(CH_3)$_2$]$_3$), 1.12-0.97 (m, 30H, Si[C*H*(CH_3)$_2$]$_3$, H-γ-DABA, ^{t}Bu), 0.94 (d, 3H, H-γ-Thr, $J_{\text{H-γ-Thr, H-β-Thr}}$ = 6.3 Hz), 0.85 (s, 9H, SiC(C*H*$_3$)$_3$), 0.80 (s, 9H, SiC(C*H*$_3$)$_3$), 0.08 (s,

3H, ^{t}BuSi(CH_3)$_2$), 0.04 (s, 3H, ^{t}BuSi(CH_3)$_2$), 0.00 (s, 3H, ^{t}BuSi(CH_3)$_2$), –0.09 (s, 3H, ^{t}BuSi(CH_3)$_2$); ESIMS-LR *m/z* calcd for $C_{83}H_{122}N_9O_{15}Si_3$ 1568.83, found 1568.9; $[\alpha]^{20}_D$ –8.0 (*c* 1.00, MeOH).

Compound 30r. In a manner similar to the synthesis of **30a**, **30r** (63 mg, 0.036 mmol, 71%) was obtained as a pale yellow syrup using **29r** (33 mg, 0.05 mmol). ^{1}H NMR (DMSO-d_6, 400 MHz, T = 50 °C) δ 11.36 (s, 1H, H-N3-uridine), 10.74 (s, 1H, NH-δ1-Trp), 9.60-9.39 (m, 1H, NH-5′-uridine), 8.51 (s, 1H, NH-γ-Asn), 8.04-7.92 (m, 1H, DABA-NH), 7.92-7.73 (m, 2H, H-Fmoc), 7.71-7.46 (m, 2H, NH-*m*Tyr, H-ε3-Trp), 7.43-6.44 (m, 27H, H-Fmoc, H-6-uridine, H-ζ1-Trp, H-η-Trp, NH-α-Trp, NH-α-Asn, Trt, H-2-*m*Tyr, H-4-*m*Tyr, H-5-*m*Tyr, H-6-*m*Tyr, H-δ1-Trp, H-ζ2-Trp), 7.19-6.60 (m, 6H, H-2-*m*Tyr, H-4-*m*Tyr, H-5-*m*Tyr, H-6-*m*Tyr, H-δ1-Trp, H-ζ2-Trp), 6.42 (d, 1H, NH-α-Trp, $J_{\text{NH-α-Trp, H-α-Trp}}$ = 8.1 Hz), 6.25-6.03 (m, 2H, H-1′-uridine, H-5′-uridine), 5.59-5.48 (m, 1H, H-5-uridine), 4.98-4.75 (m, 1H, H-β-DABA), 4.71-4.57 (m, 1H, H-α-DABA), 4.57-3.90 (m, 7H, H-Fmoc, H-α-Asn, H-α-Trp, H-α-*m*Tyr, H-2′-uridine, H-3′-uridine), 3.09-2.81 (m, 5H, H-β-Trp, NCH_3), 2.80-2.28 (m, 4H, H-β-*m*Tyr, H-β-Asn), 1.26 (s, 9H, ^{t}Bu), 1.30-1.13 (m, 3H, Si[CH(CH$_3$)$_2$]$_3$), 1.08-0.92 (m, 21H, Si[CH(CH$_3$)$_2$]$_3$, H-γ-DABA), 0.89-0.73 (m, 18H, SiC(CH_3)$_3$), 0.08 (s, 3H, ^{t}BuSi(CH_3)$_2$), 0.01 (s, 3H, ^{t}BuSi(CH_3)$_2$),

–0.01 (s, 3H, ^{t}BuSi(CH_3)$_2$), –0.12 (s, 3H, ^{t}BuSi(CH_3)$_2$); ESIMS-LR *m/z* calcd for $C_{98}H_{126}N_{10}NaO_{15}Si_3$ 1789.86, found 1790.7; $[\alpha]^{20}_D$ +2.7 (*c* 1.00, MeOH).

Compound 30s. In a manner similar to the synthesis of **30a**, **30s** (26 mg, 0.014 mmol, 29%) was obtained as a pale yellow syrup using **29s** (66 mg, 0.10 mmol). ^{1}H NMR (DMSO-d_6, 400 MHz, T = 50 °C) δ 11.61 (s, 1H, H-N3-uridine), 10.75 (s, 1H, NH-δ1-Trp), 9.23 (d, 1H, NH-5′-uridine, $J_{\text{NH-5-uridine, H-5′-uridine}}$ = 10.3 Hz), 8.24 (d, 1H, DABA-NH, $J_{\text{DABA-NH, H-α-DABA}}$ = 9.0 Hz), 7.92-7.77 (m, 2H, H-Fmoc), 7.70-7.43 (m, 2H, NH-*m*Tyr, H-ε3-Trp), 7.43-7.20 (m, 5H, H-Fmoc, H-6-uridine, H-ζ1-Trp, H-η-Trp), 7.19-6.59 (m, 22H, NH-ε-Gln, H-2-*m*Tyr, H-4-*m*Tyr, H-5-*m*Tyr, H-6-*m*Tyr, H-δ1-Trp, H-ζ2-Trp, Trt), 6.51 (d, 1H, NH-a-Gln, $J_{\text{NH-α-Gln, H-α-Gln}}$ = 7.6 Hz), 6.31 (d, 1H, NH-α-Trp, $J_{\text{NH-α-Trp, H-α-Trp}}$ = 7.6 Hz), 6.20-6.08 (m, 2H, H-1′-uridine, H-5′-uridine), 5.55 (d, 1H, H-5-uridine, $J_{\text{H-5-uridine, H-6-uridine}}$ = 7.6 Hz), 5.03-4.87 (m, 1H, H-β-DABA), 4.68-4.58 (m, 1H, H-α-DABA), 4.65-3.93 (m, 9H, H-α-DABA, H-α-Gln, H-Fmoc, H-α-Trp, H-α-*m*Tyr, H-2′-uridine, H-3′-uridine), 3.07-2.56 (m, 11H, H-β-Trp, NCH_3, H-β-*m*Tyr, H-β-Gln, H-γ-Gln), 1.22 (s, 9H, ^{t}Bu), 1.29-1.13 (m, 3H, Si[C*H*(CH$_3$)$_2$]$_3$), 1.11-0.96 (m, 21H, Si[C*H*(CH$_3$)$_2$]$_3$, H-γ-DABA), 0.83 (s, 9H, SiC(CH_3)$_3$), 0.80 (s, 9H, SiC(CH_3)$_3$), 0.05 (s, 3H, ^{t}BuSi(CH_3)$_2$), 0.01 (s, 3H, ^{t}BuSi(CH_3)$_2$), –0.01 (s, 3H, ^{t}BuSi(CH_3)$_2$), –0.11 (s, 3H,

^{t}BuSi(CH_3)$_2$); ESIMS-LR *m/z* calcd for $C_{99}H_{128}N_{10}NaO_{15}Si_3$ 1803.88, found 1804.7; $[\alpha]^{20}_D$ −1.7 (*c* 1.00, MeOH).

Compound 30t. In a manner similar to the synthesis of **30a**, **30t** (40 mg, 0.026 mmol, 53%) was obtained as a pale yellow syrup using **29t** (20 mg, 0.05 mmol). ^{1}H NMR (DMSO-d_6, 400 MHz, T = 50 °C) δ 11.44 (s, 1H, H-N3-uridine), 10.73 (s, 1H, NH-δ1-Trp), 9.06-8.93 (m, 1H, NH-5′-uridine), 8.23-8.14 (m, 1H, DABA-NH), 7.90-7.81 (m, 2H, H-Fmoc), 7.67-7.47 (m, 2H, NH-*m*Tyr, H-ε3-Trp), 7.43-7.21 (m, 5H, H-Fmoc, H-6-uridine, H-ζ1-Trp, H-η-Trp), 7.17-6.62 (m, 6H, H-2-*m*Tyr, H-4-*m*Tyr, H-5-*m*Tyr, H-6-*m*Tyr, H-δ1-Trp, H-ζ2-Trp), 6.22-6.11 (m, 2H, H-1′-uridine, H-5′-uridine), 5.97-5.88 (m, 1H, NH-α-Trp), 5.67 (d, 1H, H-5-uridine, $J_{\text{H-5-uridine, H-6-uridine}}$ = 7.2 Hz), 4.98-4.86 (m, 1H, H-β-DABA), 4.58-4.05 (m, 9H, H-α-DABA, H-Fmoc, H-α-Pro, H-α-Trp, H-α-*m*Tyr, H-2′-uridine, H-3′-uridine), 3.14-2.57 (m, 9H, H-β-Trp, H-δ-Pro, H-β-*m*Tyr, NCH_3), 1.98-1.70 (m, 4H, H-β-Pro, H-γ-Pro), 1.29 (s, 9H, ^{t}Bu), 1.31-1.15 (m, 3H, Si[CH(CH$_3$)$_2$]$_3$), 1.07-0.98 (m, 21H, Si[CH(CH$_3$)$_2$]$_3$, H-γ-DABA), 0.86 (s, 9H, SiC(CH_3)$_3$), 0.80 (s, 9H, SiC(CH_3)$_3$), 0.07 (s, 3H, ^{t}BuSi(CH_3)$_2$), 0.04 (s, 3H, ^{t}BuSi(CH_3)$_2$), 0.00 (s, 3H, ^{t}BuSi(CH_3)$_2$), −0.09 (s, 3H, ^{t}BuSi(CH_3)$_2$); ESIMS-LR *m/z* calcd for $C_{80}H_{113}N_9NaO_{14}Si_3$ 1530.76, found 1530.5; $[\alpha]^{20}_D$ −22.7 (*c* 1.00, MeOH).

Compound 25a. A solution of **30a** (10 mg, 6.8 μmol) in MeCN (136 μL) was treated with 3HF·Et_3N (44 μL, 270 mmol) at room temperature for 3 d. Trimethylsilanol (70 μL, 630 μmol) was added to the reaction mixture, which was further stirred for 1 h. The mixture was concentrated *in vacuo*, and the residue was treated with 20% Et_2NH/MeCN (250 μL) at room temperature for 1 h. The mixture was concentrated *in vacuo*, and the residue was triturated with Et_2O. The solvent was removed by decantation, and the resulting precipitate was treated with 80% *aq*. TFA (250 μL) at room temperature for 3 h. After toluene was added, the mixture was concentrated *in vacuo*. The residue was triturate with Et_2O and the solvent was removed by decantation. The precipitate was purified by ODS column chromatography (MeCN/H_2O = 10-30%, containing 0.1% TFA) to afford **25a** (1.5 mg, 1.6 μmol, 24% over 3 steps) as a yellow powder. ^{1}H NMR (DMSO-d_6, 400 MHz, T = 50 °C, 3:2 mixture of rotamers, selected date for the major rotamer) δ11.37 (s, 1H, H-N3-uridine), 10.77 (s, 1H, NH-δ1-Tr), 9.58-9.44 (m, 1H, NH-5′-uridine), 9.45-9.26 (m, 2H, NH-*m*Tyr), 8.63-8.54 (m, 1H, DABA-NH), 7.62 (d, 1H, H-ε3-Trp, $J_{\text{H-ε3-Trp, H-ζ2-Trp}}$ = 7.8 Hz), 7.42-6.71 (m, 9H, H-6-uridine, H-ζ1-Trp, H-η-Trp, H-2-*m*Tyr, H-4-*m*Tyr, H-5-*m*Tyr, H-6-*m*Tyr, H-δ1-Trp, H-ζ2-Trp), 6.47-6.32 (m, 2H, NH-Gly, NH-α-Trp), 6.17-6.01 (m, 1H, H-1′-uridine), 5.74-5.64 (m, 1H, H-5′-uridine), 5.47 (d, 1H, H-5-uridine, $J_{\text{H-5-uridine, H-6-uridine}}$ = 7.8 Hz), 4.97-4.84 (m, 1H, H-β-DABA), 4.76-

4.56 (m, 1H, H-α-DABA), 4.46-4.27 (m, 2H, H-α-Tyr, H-α-Trp), 4.41-3.91 (m, 2H, H-2′-uridine, H-3′-uridine), 3.74-3.63 (m, 2H, H-α-Gly), 3.17-2.79 (m, 4H, H-β-Trp, H-β-*m*Tyr), 2.90 (s, 3H, NCH_3), 1.22-1.15 (m, 3H, H-γ-DABA); ESIMS-LR *m/z* 806.3 [(M+H)$^+$]; ESIMS-HR *m/z* calcd for $C_{37}H_{44}N_9O_{12}$ 806.3104, found 806.3048; $[\alpha]^{20}_D$ +3.4 (*c* 0.12, MeOH).

Compound 25b. In a manner similar to the synthesis of **25a**, **25b** (0.5 mg, 0.5 μmol, 7.4% over 3 steps) was obtained as a pale yellow powder using **30b** (10 mg, 6.7 μmol). ^{1}H NMR (DMSO-d_6, 400 MHz, T = 50 °C, 3:2 mixture of rotamers, selected date for the major rotamer) δ 11.34 (s, 1H, H-N3-uridine), 10.77 (s, 1H, NH-δ1-Trp), 9.43-9.30 (m, 2H, NH-5′-uridine, NH-*m*Tyr), 8.29-8.18 (m, 1H, DABA-NH), 7.55-7.47 (m, 1H, H-ε3-Trp), 7.37-6.56 (m, 9H, H-6-uridine, H-ζ1-Trp, H-η-Trp, H-2-*m*Tyr, H-4-*m*Tyr, H-5-*m*Tyr, H-6-*m*Tyr, H-δ1-Trp, H-ζ2-Trp), 6.47-6.36 (m, 1H, NH-Ala), 6.26-6.16 (m, 1H, NH-α-Trp), 6.15-6.04 (m, 1H, H-1′-uridine), 5.59-5.46 (m, 1H, H-5′-uridine), 5.39-5.32 (m, 1H, H-5-uridine), 4.98-4.88 (m, 1H, H-β-DABA), 4.81-4.67 (m, 1H, H-α-DABA), 4.66-4.28 (m, 2H, H-α-*m*Tyr, H-α-Trp), 4.22-3.87 (m, 3H, H-α-Ala, H-2′-uridine, H-3′-uridine), 3.13-2.78 (m, 7H, H-β-Trp, H-β-*m*Tyr, NCH_3), 1.33-1.00 (m, 6H, H-γ-DABA, H-β-Ala); ESIMS-LR *m/z* 820.4 [(M+H)$^+$]; ESIMS-HR *m/z* calcd for $C_{38}H_{46}N_9O_{12}$ 820.3260, found 820.3256; $[\alpha]^{20}_D$ −1.7 (*c* 0.02, MeOH).

Compound 25c. In a manner similar to the synthesis of **25a**, **25c** (1.8 mg, 1.8 μmol, 27% over 3 steps) was obtained as a pale yellow powder using **30c** (10 mg, 6.6 μmol). ^{1}H NMR (DMSO-d_6, 400 MHz, T = 50 °C, 3:2 mixture of rotamers, selected date for the major rotamer) δ11.38 (s, 1H, H-N3-uridine), 10.77 (s, 1H, NH-δ1-Trp), 9.44-9.14 (m, 3H, NH-5′-uridine, NH-*m*Tyr), 8.08-7.85 (m, 1H, DABA-NH), 7.70-7.59 (m, 1H, H-ε3-Trp), 7.56-6.53 (m, 9H, H-6-uridine, H-ζ1-Trp, H-η-Trp, H-2-*m*Tyr, H-4-*m*Tyr, H-5-*m*Tyr, H-6-*m*Tyr, H-δ1-Trp, H-ζ2-Trp), 6.43-6.31 (m, 1H, NH-Leu), 6.21-6.02 (m, 2H, NH-α-Trp, H-1′-uridine), 5.72-5.66 (m, 1H, H-5′-uridine), 5.53-5.48 (m, 1H, H-5-uridine), 4.98-4.88 (m, 1H, H-β-DABA), 4.80-4.73 (m, 1H, H-α-DABA), 4.70-4.24 (m, 3H, H-α-*m*Tyr, H-α-Trp, H-α-Leu), 4.21-3.96 (m, 2H, H-2′-uridine, H-3′-uridine), 3.12-2.82 (m, 7H, H-β-Trp, H-β-*m*Tyr, NCH_3), 1.70-1.14 (m, 3H, H-β-Leu, H-γ-Leu), 1.14-1.00 (m, 3H, H-γ-DABA), 0.95-0.71 (m, 6H, H-δ-Leu); ESIMS-LR *m/z* 862.5 [(M+H)$^+$]; ESIMS-HR *m/z* calcd for $C_{41}H_{52}N_9O_{12}$ 862.3730, found 862.3748; $[\alpha]^{20}_D$ −1.7 (*c* 0.15, MeOH).

Compound 25d. In a manner similar to the synthesis of **25a**, **25d** (1.0 mg, 1.0 μmol, 15% over 3 steps) was obtained as a pale yellow powder using **30d** (10 mg, 6.6 μmol). ^{1}H NMR (DMSO-d_6, 400 MHz, T = 50 °C, 3:2 mixture of rotamers, selected date for the major rotamer) δ11.40 (s, 1H, H-N3-uridine), 10.77 (s, 1H, NH-δ1-Trp), 9.47-9.27 (m,

2H, NH-*m*Tyr), 9.14-9.05 (m, 1H, NH-5′-uridine), 8.32-8.21 (m, 1H, DABA-NH), 8.13-7.85 (m, 1H, H-ε3-Trp), 7.55-6.52 (m, 9H, H-6-uridine, H-ζ1-Trp, H-η-Trp, H-2-*m*Tyr, H-4-*m*Tyr, H-5-*m*Tyr, H-6-*m*Tyr, H-δ1-Trp, H-ζ2-Trp), 6.41-6.30 (m, 1H, NH-Ile) 6.29-6.17 (m, 1H, NH-Trp), 6.15-6.03 (m, 1H, H-1′-uridine), 5.73-5.67 (m, 1H, H-5′-uridine), 5.56-5.49 (m, 1H, H-5-uridine), 5.00-4.87 (m, 1H, H-β-DABA), 4.81-4.69 (m, 1H, H-α-DABA), 4.68-4.29 (m, 3H, H-α-*m*Tyr, H-α-Trp, H-α-Ile), 4.12-3.95 (m, 2H, H-2′-uridine, H-3′-uridine), 3.15-2.80 (m, 7H, H-β-Trp, H-β-*m*Tyr, NCH_3), 1.63-1.53 (m, 1H, H-β-Ile), 1.50-1.35 (m, 2H, H-γ-Ile), 1.14-0.98 (m, 3H, H-γ-DABA), 0.92-0.67 (m, 6H, H-γ-Ile, H-δ-Ile); ESIMS-LR *m/z* 862.6 [$(M+H)^+$]; ESIMS-HR *m/z* calcd for $C_{41}H_{52}N_9O_{12}$ 862.3730, found 862.3748; $[\alpha]^{20}_D$ +1.9 (*c* 0.07, MeOH).

Compound 25e. In a manner similar to the synthesis of **25a**, **25e** (2.2 mg, 2.3 μmol, 18% over 3 steps) was obtained as a pale yellow powder using **30e** (20 mg, 13 μmol). ^{1}H NMR (DMSO-d_6, 400 MHz, T = 50 °C, 3:2 mixture of rotamers, selected date for the major rotamer) δ11.40 (s, 1H, H-N3-uridine), 10.77 (s, 1H, NH-δ1-Trp), 9.53-9.22 (m, 2H, NH-*m*Tyr), 9.10 (m, 1H, NH-5′-uridine, $J_{\text{NH-5′-uridine, H-5′-uridine}}$ = 10.3 Hz), 8.23-8.20 (m, 1H, DABA-NH), 7.63 (d, 1H, H-ε3-Trp, $J_{\text{H-ε3-Trp, H-ζ2-Trp}}$ = 7.8 Hz), 7.56-6.52 (m, 9H, H-6-uridine, H-ζ1-Trp, H-η-Trp, H-2-*m*Tyr, H-4-*m*Tyr, H-5-*m*Tyr, H-6-*m*Tyr, H-δ1-Trp, H-ζ2-Trp), 6.41−6.22 (m, 2H, NH-Trp, NH-Val), 6.16-6.04 (d, 1H, H-1-uridine, $J_{1,\,2}$ =

9.6 Hz), 5.74-5.67 (m, 1H, H-5′-uridine, $J_{5',4'}$ = 7.6 Hz), 5.53-5.49 (m, 1H, H-5-uridine), 5.00-4.89 (m, 1H, H-β-DABA), 4.80-4.71 (m, 1H, H-α-DABA), 4.69-4.27 (m, 3H, H-α-*m*Tyr, H-α-Val, H-α-Trp), 4.10-3.95 (m, 2H, H-2′-uridine, H-3′-uridine), 3.10-2.83 (m, 7H, H-β-Trp, H-β-*m*Tyr, NCH_3), 1.97-1.76 (m, 1H, H-β-Val), 1.10 (d, 3H, H-γ-DABA, $J_{\text{H-γ-DABA, H-β-DABA}}$ = 6.9 Hz), 1.00-0.66 (m, 6H, Val-CH_3); ESIMS-LR *m/z* 848.5 [$(M+H)^+$]; ESIMS-HR *m/z* calcd for $C_{40}H_{50}N_9O_{12}$ 848.3573, found 848.3611; $[\alpha]^{20}_D$ −4.1 (*c* 0.19, MeOH).

Compound 25f. In a manner similar to the synthesis of **25a**, **25f** (0.5 mg, 0.5 μmol, 8.7% over 3 steps) was obtained as a pale yellow powder using **30f** (10 mg, 5.7 μmol). ^{1}H NMR (DMSO-d_6, 400 MHz, T = 50 °C, 3:2 mixture of rotamers, selected date for the major rotamer) δ11.37 (s, 1H, H-N3-uridine), 10.77 (s, 1H, NH-δ1-Trp), 9.49-9.22 (m, 3H, NH-5′-uridine, NH-*m*Tyr), 8.36-8.31 (m, 1H, NH-DABA), 7.51 (d, 1H, H-ε3-Trp, $J_{\text{H-ε3-Trp, H-ζ2-Trp}}$ = 8.1 Hz), 7.35-6.52 (m, 10H, H-2, 4, 5, 6, 7-Trp, H-2, 4, 5, 6-*m*Tyr, NH-Cys), 6.44-6.36 (m, 1H, NH-α-Trp), 6.16-6.05 (m, 1H, H-1′-uridine), 5.73-5.66 (d, 1H, H-5′-uridine), 5.52-5.47 (m, 1H, H-5-uridine), 5.00-4.91 (m, 1H, H-β-DABA), 4.84-4.72 (m, 1H, H-α-DABA), 4.70-4.26 (m, 3H, H-α-*m*Tyr, H-α-Trp, H-α-Cys), 4.06-3.97 (m, 2H, H-2′-uridine, H-3′-uridine), 3.11-2.85 (m, 7H, H-β-Trp, H-β-*m*Tyr, NCH_3), 2.72-2.63 (m, 2H, H-β-Cys), 1.12-1.06 (m, 3H, H-γ-DABA); ESIMS-LR *m/z* 852.4 [$(M+H)^+$];

ESIMS-HR *m/z* calcd for $C_{38}H_{46}N_9O_{12}S$ 852.2981, found 852.3046; $[\alpha]^{20}_D$ +8.7 (*c* 0.02, MeOH).

Compound 25g. In a manner similar to the synthesis of **25a**, **25g** (2.3 mg, 2.3 μmol, 18% over 3 steps) was obtained as a pale yellow powder using **30g** (20 mg, 13 μmol). ^{1}H NMR (DMSO-d_6, 400 MHz, T = 50 °C, 3:2 mixture of rotamers, selected date for the major rotamer) δ11.37 (s, 1H, H-N3-uridine), 10.78 (m, 1H, NH-δ1-Trp), 9.50-9.24 (m, 3H, NH-5′-uridine, NH-*m*Tyr), 8.36-8.23 (m, 1H, DABA-NH), 7.51 (d, 1H, H-ε3-Trp, $J_{\text{H-ε3-Trp, H-ζ2-Trp}}$ = 8.1 Hz), 7.36-6.56 (m, 9H, H-6-uridine, H-ζ1-Trp, H-η-Trp, H-2-*m*Tyr, H-4-*m*Tyr, H-5-*m*Tyr, H-6-*m*Tyr, H-δ1-Trp, H-ζ2-Trp), 6.51-6.42 (m, 1H, NH-Met), 6.25-6.16 (m, 1H, NH-α-Trp), 6.15-6.03 (m, 1H, H-1′-uridine), 5.73-5.68 (m, 1H, H-5′-uridine), 5.52-5.47 (m, 1H, H-5-uridine), 4.99-4.88 (m, 1H, H-β-DABA), 4.82-4.72 (m, 1H, H-α-DABA), 4.70-4.27 (m, 3H, H-α-*m*Tyr, H-α-Trp, H-α-Met), 4.25-4.18 (m, 2H, H-2′-uridine, H-3′-uridine), 3.15-2.82 (m, 9H, H-β-Trp, H-β-*m*Tyr, NCH_3, H-γ-Met), 2.00 (s, 3H, SCH_3), 1.90-1.61 (m, 2H, H-β-Met), 1.14-1.02 (m, 3H, H-γ-DABA); ESIMS-LR *m/z* 880.4 [$(M+H)^+$]; ESIMS-HR *m/z* calcd for $C_{40}H_{50}N_9O_{12}S$ 880.3294, found 880.3288; $[\alpha]^{20}_D$ −1.1 (*c* 0.21, MeOH).

Compound 25h. In a manner similar to the synthesis of **25a**, **25h** (3.4 mg, 3.4 μmol, 26% over 3 steps) was obtained as a pale yellow powder using **30h** (20 mg, 13 μmol). ^{1}H

NMR (DMSO-d_6, 400 MHz, T = 50 °C, 3:2 mixture of rotamers, selected date for the major rotamer) δ11.32 (s, 1H, H-N3-uridine), 10.76 (s, 1H, NH-δ1-Trp), 9.60 (d, 1H, NH-5′-uridine, $J_{\text{NH-5′-uridine, H-5′-uridine}}$ = 9.0 Hz), 9.49-9.24 (m, 2H, NH-*m*Tyr), 8.36 (d, 1H, DABA-NH, $J_{\text{DABA-NH, H-α-DABA}}$ = 9.0 Hz), 7.50 (d, 1H, H-ε3-Trp, $J_{\text{H-ε3-Trp, H-ζ2-Trp}}$ = 7.6 Hz), 7.35-6.54 (m, 14H, H-6-uridine, H-δ-Phe, H-ε-Phe, H-ζ-Phe, H-ζ1-Trp, H-η-Trp, H-2-*m*Tyr, H-4-*m*Tyr, H-5-*m*Tyr, H-6-*m*Tyr, H-δ1-Trp, H-ζ2-Trp), 6.43-6.29 (m, 2H, NH-Phe, NH-α-Trp), 6.18-6.08 (m, 1H, H-1′-uridine), 5.71-5.66 (m, 1H, H-5′-uridine), 5.42-5.37 (m, 1H, H-5-uridine), 4.99-4.89 (m, 1H, H-β-DABA), 4.83-4.83 (m, 1H, H-α-DABA), 4.72-4.30 (m, 3H, H-α-*m*Tyr, H-α-Trp, H-α-Phe), 4.08-3.90 (m, 2H, H-2′-uridine, H-3′-uridine), 3.07-2.80 (m, 9H, H-β-Trp, H-β-Phe, H-β-*m*Tyr, NCH_3), 1.10 (d, 3H, H-γ-DABA, $J_{\text{H-γ-DABA, H-β-DABA}}$ = 6.7 Hz); ESIMS-LR *m/z* 896.4 [(M+H)$^+$]; ESIMS-HR *m/z* calcd for $C_{44}H_{50}N_9O_{12}$ 896.3573, found 896.3593; $[\alpha]^{20}_{D}$ +0.52 (*c* 0.31, MeOH).

Compound 25i. In a manner similar to the synthesis of **25a**, **25i** (2.6 mg, 2.5 μmol, 21% over 3 steps) was obtained as a pale yellow powder using **30i** (20 mg, 12 μmol). ^{1}H NMR (DMSO-d_6, 400 MHz, T = 50 °C, 3:2 mixture of rotamers, selected date for the major rotamer) δ11.34 (s, 1H, H-N3-uridine), 10.75 (s, 1H, NH-δ1-Trp), 9.62 (d, 1H, NH-5′-uridine, $J_{\text{NH-5′-uridine, H-5′-uridine}}$ = 10.3 Hz), 9.45-9.29 (m, 2H, NH-*m*Tyr), 8.29 (d, 1H, NH-DABA, $J_{\text{DABA-NH, H-α-DABA}}$ = 10.3 Hz), 7.50 (d, 1H, H-ε3-Trp, $J_{\text{H-ε3-Trp, H-ζ2-Trp}}$ =

7.6 Hz), 7.34-7.54 (m, 13H, H-6-uridine, H-ζ1-Trp, H-η-Trp, H-2-*m*Tyr, H-4-*m*Tyr, H-5-*m*Tyr, H-6-*m*Tyr, H-δ1-Trp, H-ζ2-Trp, H-δ-Tyr, H-ε-Tyr), 6.40-6.26 (m, 2H, NH-α-Trp, NH-Tyr), 6.17-6.07 (m, 1H, H-1′-uridine), 5.71-5.67 (m, 1H, H-5′-uridine), 5.46-5.41 (m, 1H, H-5-uridine), 4.98-4.88 (m, 1H, H-β-DABA), 4.82-4.75 (m, 1H, H-α-DABA), 4.70-4.22 (m, 3H, H-α-*m*Tyr, H-α-Tyr, H-α-Trp), 4.01-3.90 (m, 2H, H-2′-uridine, H-3′-uridine), 3.10-2.54 (m, 7H, H-β-Trp, H-β-*m*Tyr, NCH_3, H-β-Tyr), 1.09 (d, 3H, H-γ-DABA, $J_{\text{H-γ-DABA, H-β-DABA}}$ = 7.2 Hz); ESIMS-LR *m/z* 912.5 [$(M+H)^+$]; ESIMS-HR *m/z* calcd for $C_{44}H_{50}N_9O_{13}$ 912.3523, found 912.3546; $[\alpha]^{20}_D$ +3.6 (*c* 0.23, MeOH).

Compound 25j. In a manner similar to the synthesis of **25a**, **25j** (3.2 mg, 3.1 μmol, 26% over 3 steps) was obtained as a pale yellow powder using **30j** (20 mg, 12 μmol). ^{1}H NMR (DMSO-d_6, 400 MHz, T = 50°C, 3:2 mixture of rotamers, selected date for the major rotamer) δ11.32 (s, 1H, H-N3-uridine), 10.75 (m, 1H, NH-δ1-Trp), 9.68 (d, 1H, NH-5′-uridine, $J_{\text{NH-5′-uridine, H-5′-uridine}}$ = 9.9 Hz), 9.54-9.18 (m, 2H, NH-*m*Tyr), 8.38-8.25 (m, 1H, DABA-NH), 7.61 (d, 1H, H-ε3-Trp, $J_{\text{H-ε3-Trp, H-ζ2-Trp}}$ = 8.1 Hz), 7.55-6.54 (m, 14H, H-6-uridine, H-ζ1-Trp, H-η-Trp, H-2-*m*Tyr, H-4-*m*Tyr, H-5-*m*Tyr, H-6-*m*Tyr, H-δ1-Trp, H-ζ2-Trp), 6.48-6.27 (m, 2H, NH-α-Trp), 6.20-6.07 (m, 2H, NH-α-Trp), 5.96-5.90 (m, 1H, H-1′-uridine), 5.72-5.66 (m, 1H, H-5′-uridine), 5.36-5.31 (m, 1H, H-5-uridine), 4.99-4.89 (m, 1H, H-β-DABA), 4.83-4.75 (m, 1H, H-α-DABA), 4.74-4.30 (m, 3H, H-α-*m*Tyr,

H-α-Trp), 4.01-3.92 (m, 2H, H-2′-uridine, H-3′-uridine), 3.14-2.80 (m, 9H, H-β-Trp, H-β-*m*Tyr, NCH_3), 1.07 (d, 3H, H-γ-DABA, $J_{\text{H-γ-DABA, H-β-DABA}}$ = 7.2 Hz); ESIMS-LR *m/z* 935.5 [(M+H)$^+$]; ESIMS-HR *m/z* calcd for $C_{46}H_{51}N_{10}O_{12}$ 935.3882, found 935.3696; $[\alpha]^{20}_{D}$ +9.6 (*c* 0.28, MeOH).

Compound 25k. In a manner similar to the synthesis of **25a**, **25k** (2.4 mg, 2.4 μmol, 43% over 3 steps) was obtained as a pale yellow powder using **30k** (10 mg, 5.6 μmol). ^{1}H NMR (DMSO-d_6, 400 MHz, T = 50 °C, 3:2 mixture of rotamers, selected date for the major rotamer) δ11.37 (s, 1H, H-N3-uridine), 10.78 (s, 1H, NH-δ1-Trp), 9.57-9.25 (m, 1H, NH-5′-uridine), 8.96-8.78 (m, 2H, NH-*m*Tyr), 8.44-7.77 (m, 2H, DABA-NH, H-ε-His), 7.77-6.53 (m, 13H, H-6-uridine, H-ζ1-Trp, H-η-Trp, H-2-*m*Tyr, H-4-*m*Tyr, H-5-*m*Tyr, H-6-*m*Tyr, H-δ1-Trp, H-ζ2-Trp, H-ε3-Trp, H-δ-His, NH-α-His, NH-ε-His), 6.31 (d, 1H, NH-α-Trp, $J_{\text{NH-α-Trp, H-α-Trp}}$ = 7.6 Hz), 6.15-6.03 (m, 1H, H-1′-uridine), 5.63-5.58 (m, 1H, H-5′-uridine), 5.49-5.40 (m, 1H, H-5-uridine), 4.98-4.82 (m, 1H, H-β-DABA), 4.80-4.10 (m, 4H, H-α-DABA, H-α-*m*Tyr, H-α-Trp, H-α-His), 4.10-3.82 (m, 2H, H-2′-uridine, H-3′-uridine), 3.13-2.57 (m, 9H, H-β-Trp, H-β-*m*Tyr, H-β-His, NCH_3), 1.21-1.13 (m, 3H, H-γ-DABA); ESIMS-LR *m/z* 886.3 [(M+H)$^+$]; ESIMS-HR *m/z* calcd for $C_{41}H_{48}N_{11}O_{12}$ 886.3478, found 886.3484; $[\alpha]^{20}_{D}$ –0.9 (*c* 0.21, MeOH).

Compound 25l. In a manner similar to the synthesis of **25a**, **25l** (1.5 mg, 1.5 μmol, 24% over 3 steps) was obtained as a pale yellow powder using **30l** (10 mg, 6.3 μmol). ^{1}H NMR (DMSO-d_6, 400 MHz, T = 50 °C, 3:2 mixture of rotamers, selected date for the major rotamer) δ11.36 (s, 1H, H-N3-uridine), 10.75 (s, 1H, NH-δ1-Trp), 9.58-9.24 (m, 3H, NH-5′-uridine, NH-*m*Tyr), 8.16-7.83 (m, 1H, DABA-NH), 7.54-7.47 (m, 1H, H-ε3-Trp), 7.36-6.53 (m, 10H, H-6-uridine, H-ζ1-Trp, H-η-Trp, H-2-*m*Tyr, H-4-*m*Tyr, H-5-*m*Tyr, H-6-*m*Tyr, H-δ1-Trp, H-ζ2-Trp, NH-Asp), 6.44-6.37 (m, 1H, NH-α-Trp), 6.14-6.03 (m, 1H, H-1′-uridine), 5.73-5.67 (m, 1H, H-5′-uridine), 5.51-5.45 (m, 1H, H-5-uridine), 4.96-4.27 (m, 5H, H-β-DABA, H-α-DABA, H-α-*m*Tyr, H-α-Asp, H-α-Trp), 4.08-3.94 (m, 2H, H-2′-uridine, H-3′-uridine), 3.15-2.80 (m, 7H, H-β-Trp, H-β-*m*Tyr, NCH_3), 2.70-2.62 (m, 2H, H-β-Asp), 1.21-1.14 (m, 3H, H-γ-DABA); ESIMS-LR *m/z* 864.4 [(M+H)$^+$]; ESIMS-HR *m/z* calcd for $C_{39}H_{46}N_9O_{14}$ 864.3159, found 864.3103; $[\alpha]^{20}_D$ −1.7 (*c* 0.12, MeOH).

Compound 25m. In a manner similar to the synthesis of **25a**, **25m** (1.3 mg, 1.3 μmol, 21% over 3 steps) was obtained as a pale yellow powder using **30m** (10 mg, 6.3 μmol). ^{1}H NMR (DMSO-d_6, 400 MHz, T = 50 °C, 3:2 mixture of rotamers, selected date for the major rotamer) δ 11.36 (s, 1H, H-N3-uridine), 10.77 (s, 1H, NH-δ1-Trp), 9.52-9.21 (m, 3H, NH-5′-uridine, NH-*m*Tyr), 8.18-7.82 (m, 1H, DABA-NH), 7.51 (d, 1H, H-ε3-Trp,

$J_{\text{H-ε3-Trp, H-ζ2-Trp}}$ = 7.6 Hz), 7.36-6.51 (m, 9H, H-6-uridine, H-ζ1-Trp, H-η-Trp, H-2-*m*Tyr, H-4-*m*Tyr, H-5-*m*Tyr, H-6-*m*Tyr, H-δ1-Trp, H-ζ2-Trp), 6.50-6.35 (m, 1H, NH-Glu), 6.28-6.19 (m, 1H, NH-α-Trp), 6.13-6.04 (m, 1H, H-1′-uridine), 5.73-5.61 (m, 1H, H-5′-uridine), 5.50-5.42 (m, 1H, H-5-uridine), 4.99-4.83 (m, 1H, H-β-DABA), 4.82-4.28 (m, 4H, H-α-DABA, H-α-*m*Tyr, H-α-Trp, H-α-Glu), 4.20-4.07 (m, 2H, H-2′-uridine, H-3′-uridine), 3.14-2.82 ((m, 7H, H-β-Trp, H-β-*m*Tyr, NCH_3), 2.25-2.13 (m, 2H, H-β-Gln), 1.89-1.72 (m, 2H, H-γ-Gln), 1.71-1.57 (m, 2H, H-γ-Gln), 1.13-0.98 (m, 3H, H-γ-DABA); ESIMS-LR *m/z* 878.3 [(M+H)$^+$]; ESIMS-HR *m/z* calcd for $C_{40}H_{48}N_9O_{14}$ 878.3315, found 878.3329; $[\alpha]^{20}_D$ +1.7 (*c* 0.10, MeOH).

Compound 25n. In a manner similar to the synthesis of **25a**, **25n** (5.5 mg, 5.5 μmol, 47% over 3 steps) was obtained as a pale yellow powder using **30n** (20 mg, 12 μmol). ^{1}H NMR (DMSO-d_6, 400 MHz, T = 50 °C, 3:2 mixture of rotamers, selected date for the major rotamer) δ11.39 (s, 1H, H-N3-uridine), 10.79 (s, 1H, NH-δ1-Trp), 9.58-9.18 (m, 3H, NH-5′-uridine, NH-*m*Tyr), 8.15-7.86 (m, 1H, DABA-NH), 7.78-7.57 (m, 1H, H-ε3-Trp), 7.38-6.52 (m, 9H, H-6-uridine, H-ζ1-Trp, H-η-Trp, H-2-*m*Tyr, H-4-*m*Tyr, H-5-*m*Tyr, H-6-*m*Tyr, H-δ1-Trp, H-ζ2-Trp), 6.48-6.39 (m, 1H, NH-α-Lys), 6.26-6.19 (m, 1H, NH-α-Trp), 6.10-6.03 (m, 1H, H-1′-uridine), 5.75-5.70 (m, 1H, H-5′-uridine), 5.52-5.45 (m, 1H, H-5-uridine), 4.98-4.84 (m, 1H, H-β-DABA), 4.82-4.74 (m, 1H, H-α-DABA),

4.71-4.30 (m, 3H, H-α-*m*Tyr, H-α-Trp, H-α-Lys), 4.18-4.07 (m, 2H, H-2′-uridine, H-3′-uridine), 3.12-2.82 (m, 7H, H-β-Trp, H-β-*m*Tyr, NCH_3), 2.80-2.63 (m, 2H, H-ε-Lys), 1.63-1.20 (m, 6H, H-β-Lys, H-γ-Lys, H-δ-Lys), 1.42 (m, 2H, NH_2-Lys), 1.28 (m, 2H, H-γ-Lys), 1.09 (d, 3H, H-γ-DABA, $J_{\text{H-γ-DABA, H-β-DABA}}$ = 6.7 Hz); ESIMS-LR *m/z* 877.5 [$(M+H)^+$]; ESIMS-HR *m/z* calcd for $C_{41}H_{53}N_{10}O_{12}$ 877.3839, found 877.3905; $[\alpha]^{20}_D$ +0.1 (*c* 0.52, MeOH).

Compound 25o. In a manner similar to the synthesis of **25a**, **25o** (1.4 mg, 1.4 μmol, 25% over 3 steps) was obtained as a pale yellow powder using **30o** (10 mg, 5.5 μmol). ^{1}H NMR (DMSO-d_6, 400 MHz, T = 50 °C, 3:2 mixture of rotamers, selected date for the major rotamer) δ 11.39 (s, 1H, H-N3-uridine), 10.77 (s, 1H, NH-δ1-Trp), 9.61-9.20 (m, 3H, NH-5′-uridine, NH-*m*Tyr), 8.07-7.86 (m, 1H, DABA-NH), 7.57-7.41 (m, 1H, H-ε3-Trp), 7.38-6.55 (m, 9H, H-6-uridine, H-ζ1-Trp, H-η-Trp, H-2-*m*Tyr, H-4-*m*Tyr, H-5-*m*Tyr, H-6-*m*Tyr, H-δ1-Trp, H-ζ2-Trp), 6.52-6.40 (m, 1H, NH-α-Arg), 6.32-6.26 (m, 1H, NH-α-Trp), 6.10-6.05 (m, 1H, H-1′-uridine), 5.75-5.69 (m, 1H, H-5′-uridine), 5.49-5.42 (m, 1H, H-5-uridine), 4.97-4.74 (m, 1H, H-β-DABA), 4.74-4.58 (m, 1H, H-α-DABA), 4.51-4.11 (m, 3H, H-α-mTyr, H-α-Trp, H-α-Arg), 4.00-3.88 (m, 2H, H-2′-uridine, H-3′-uridine), 3.15-2.81 (m, 7H, H-β-Trp, H-β-*m*Tyr, NCH_3), 2.70-2.65 (m, 2H, H-δ-Arg), 1.66-1.35 (m, 4H, H-β–Aργ, H-γ-Arg), 1.11-1.00 (m, 3H, H-γ-DABA); ESIMS-LR *m/z*

905.5 [(M+H)$^+$]; ESIMS-HR *m/z* calcd for $C_{41}H_{53}N_{12}O_{12}$ 905.3900, found 905.3150; $[\alpha]^{20}_D$ +3.4 (*c* 0.11, MeOH).

Compound 25p. In a manner similar to the synthesis of **25a**, **25p** (1.8 mg, 1.9 μmol, 15% over 3 steps) was obtained as a pale yellow powder using **30p** (20 mg, 13 μmol). ^{1}H NMR (DMSO-d_6, 400 MHz, T = 50 °C, 3:2 mixture of rotamers, selected date for the major rotamer) δ11.36 (s, 1H, H-N3-uridine), 10.76 (s, 1H, NH-δ1-Trp), 9.46-9.21 (m, 3H, NH-5′-uridine, NH-*m*Tyr), 8.23-7.83 (m, 1H, DABA-NH), 7.57-7.40 (m, 1H, H-ε3-Trp), 7.37-6.52 (m, 9H, H-6-uridine, H-ζ1-Trp, H-η-Trp, H-2-*m*Tyr, H-4-*m*Tyr, H-5-*m*Tyr, H-6-*m*Tyr, H-δ1-Trp, H-ζ2-Trp), 6.49-6.33 (m, 2H, NH-Ser, NH-α-Trp), 6.15-6.02 (m, 1H, H-1′-uridine), 5.77-5.60 (m, 1H, H-5′-uridine), 5.55-5.42 (m, 1H, H-5-uridine), 5.07-3.84 (m, 7H, H-β-DABA, H-α-DABA, H-α-Ser, H-α-*m*Tyr, H-α-Trp, H-2′-uridine, H-3′-uridine), 3.07-2.79 (m, 9H, H-β-Trp, H-β-Ser, H-β-*m*Tyr, NCH_3), 1.30-0.99 (m, 3H, H-γ-DABA); ESIMS-LR *m/z* 836.2 [(M+H)$^+$]; ESIMS-HR *m/z* calcd for $C_{38}H_{46}N_9O_{13}$ 836.3210, found 836.3187; $[\alpha]^{20}_D$ +1.3 (*c* 0.15, MeOH).

Compound 25q. In a manner similar to the synthesis of **25a**, **25q** (2.9 mg, 3.0 μmol, 27% over 3 steps) was obtained as a pale yellow powder using **30q** (20 mg, 11 μmol). ^{1}H NMR (DMSO-d_6, 400 MHz, T = 50 °C, 3:2 mixture of rotamers, selected date for the major rotamer) δ11.37 (s, 1H, H-N3-uridine), 10.75 (s, 1H, NH-δ1-Trp), 9.48-9.20 (m,

3H, NH-5′-uridine, NH-*m*Tyr), 8.15-7.81 (m, 1H, DABA-NH), 7.52 (d, 1H, H-ε3-Trp, $J_{\text{H-ε3-Trp, H-ζ2-Trp}}$ = 8.1 Hz), 7.36-6.48 (m, 10H, H-6-uridine, H-ζ1-Trp, H-η-Trp, H-2-*m*Tyr, H-4-*m*Tyr, H-5-*m*Tyr, H-6-*m*Tyr, H-δ1-Trp, H-ζ2-Trp, NH-Thr), 6.54 (d, 1H, NH-Thr, $J_{\text{NH-Thr, α-Thr}}$ = 7.8 Hz), 6.38 (d, 1H, NH-α-Trp, $J_{\text{NH-α-Trp, H-α-Trp}}$ = 8.1 Hz), 6.11-6.04 (m, 1H, H-1′-uridine), 5.72-5.67 (m, 1H, H-5′-uridine), 5.51-5.46 (m, 1H, H-5-uridine), 4.98-4.87 (m, 1H, H-β-DABA), 4.82-4.74 (m, 1H, H-α-DABA), 4.73-4.27 (m, 3H, H-α-*m*Tyr, H-α-Trp, H-α-Thr), 4.14-3.74 (m, 3H, H-β-Thr, H-2′-uridine, H-3′-uridine), 3.13-2.80 (m, 7H, H-β-Trp, H-β-*m*Tyr, NCH_3), 1.11 (d, 3H, H-γ-Thr, $J_{\text{H-γ-Thr, H-β-Thr}}$ = 7.2 Hz), 1.01-0.95 (m, 3H, H-γ-DABA); ESIMS-LR *m/z* 850.5 [$(M+H)^+$]; ESIMS-HR *m/z* calcd for $C_{39}H_{48}N_9O_{13}$ 850.3366, found 850.3347; $[\alpha]^{20}_D$ −1.9 (*c* 0.26, MeOH).

Compound 25r. In a manner similar to the synthesis of **25a**, **25r** (0.5 mg, 0.5 μmol, 10% over 3 steps) was obtained as a pale yellow powder using **30r** (10 mg, 5.6 μmol). ^{1}H NMR (DMSO-d_6, 400 MHz, T = 50 °C, 3:2 mixture of rotamers, selected date for the major rotamer) δ11.47 (s, 1H, H-N3-uridine), 10.81 (s, 1H, NH-δ1-Trp), 9.65-9.39 (m, 3H, NH-5′-uridine, NH-*m*Tyr), 8.21-7.87 (m, 3H, NH-DABA, NH-γ-Asn), 7.55-7.46 (m, 1H, H-ε3-Trp), 7.36-6.40 (m, 9H, H-6-uridine, H-ζ1-Trp, H-η-Trp, H-2-*m*Tyr, H-4-*m*Tyr, H-5-*m*Tyr, H-6-*m*Tyr, H-δ1-Trp, H-ζ2-Trp, NH-α-Asn, , NH-α-Trp), 6.17-6.00 (m, 1H, H-1′-uridine), 5.75-5.56 (m, 1H, H-5′-uridine), 5.50-5.38 (m, 1H, H-5-uridine),

4.99-4.84 (m, 1H, H-β-DABA), 4.81-4.22 (m, 4H, H-α-DABA, H-α-*m*Tyr, H-α-Asn, H-α-Trp), 4.06-3.86 (m, 2H, H-2′-uridine, H-3′-uridine), 3.17-2.26 (m, 7H, H-β-Trp, H-β-*m*Tyr, NCH_3, H-β-Asn), 1.11-0.96 (m, 3H, H-γ-DABA); ESIMS-LR *m/z* 863.4 [(M+H)$^+$]; ESIMS-HR *m/z* calcd for $C_{39}H_{47}N_{10}O_{13}$ 863.3319, found 863.3333; $[\alpha]^{20}_D$ +2.1 (*c* 0.02, MeOH).

Compound 25s. In a manner similar to the synthesis of **25a**, **25s** (1.2 mg, 1.2 μmol, 21% over 3 steps) was obtained as a pale yellow powder using **30s** (10 mg, 5.6 μmol). ^{1}H NMR (DMSO-d_6, 400 MHz, T = 50 °C, 3:2 mixture of rotamers, selected date for the major rotamer) δ11.37 (s, 1H, H-N3-uridine), 10.77 (s, 1H, NH-δ1-Trp), 9.55-9.23 (m, 3H, NH-5′-uridine, NH-*m*Tyr), 8.17-7.83 (m, 1H, DABA-NH), 7.54-7.44 (m, 1H, H-ε3-Trp), 7.37-6.51 (m, 11H, H-6-uridine, H-ζ1-Trp, H-η-Trp, H-2-*m*Tyr, H-4-*m*Tyr, H-5-*m*Tyr, H-6-*m*Tyr, H-δ1-Trp, H-ζ2-Trp, NH-δ-Gln), 6.49-6.37 (m, 1H, NH-α-Gln), 6.29-6.22 (m, 1H, NH-α-Trp), 6.11-6.05 (m, 1H, H-1′-uridine), 5.73-5.67 (m, 1H, H-5′-uridine), 5.50-5.44 (m, 1H, H-5-uridine), 5.16-4.28 (m, 5H, H-β-DABA, H-α-DABA, H-α-*m*Tyr, H-α-Trp, H-α-Gln), 4.19-4.07 (m, 2H, H-2′-uridine, H-3′-uridine), 3.13-2.81 (m, 7H, H-β-Trp, H-β-*m*Tyr, NCH_3), 2.17-1.99 (m, 2H, H-γ-Gln), 1.86-1.72 (m, 1H, H-β-Gln), 1.70-1.55 (m, 1H, H-β-Gln), 1.13-1.00 (m, 3H, H-γ-DABA); ESIMS-LR *m/z*

877.4 [(M+H)$^+$]; ESIMS-HR *m/z* calcd for $C_{40}H_{49}N_{10}O_{13}$ 877.3475, found 877.3601; $[\alpha]^{20}_D$ +10.7 (*c* 0.12, MeOH).

Compound 25t. In a manner similar to the synthesis of **25a**, **25t** (2.2 mg, 2.3 μmol, 18% over 3 steps) was obtained as a pale yellow powder using **30t** (20 mg, 13 μmol). ^{1}H NMR (DMSO-d_6, 400 MHz, T = 50 °C, 3:2 mixture of rotamers, selected date for the major rotamer) δ11.39 (s, 1H, H-N3-uridine), 10.73 (s, 1H, NH-δ1-Trp), 9.54-9.23 (m, 3H, NH-5′-uridine, NH-*m*Tyr), 8.10-7.82 (m, 1H, DABA-NH), 7.59-7.48 (m, 1H, H-ε3-Trp), 7.37-6.47 (m, 9H, H-6-uridine, H-ζ1-Trp, H-η-Trp, H-2-*m*Tyr, H-4-*m*Tyr, H-5-*m*Tyr, H-6-*m*Tyr, H-δ1-Trp, H-ζ2-Trp, NH-α-Trp), 6.17-6.02 (m, 1H, H-1′-uridine), 5.73-5.65 (m, 1H, H-5′-uridine), 5.57-5.48 (m, 1H, H-5-uridine), 4.96-4.85 (m, 1H, H-β-DABA), 4.78-4.20 (m, 4H, H-α-DABA, H-α-*m*Tyr, H-α-Trp, H-α-Pro), 4.09-3.91 (m, 2H, H-2′-uridine, H-3′-uridine), 3.20-2.78 (m, 9H, H-δ-Pro, H-β-Trp, H-β-*m*Tyr, NCH_3), 2.05-1.66 (m, 4H, H-β-Pro, H-γ-Pro), 1.13-0.99 (m, 3H, H-γ-DABA); ESIMS-LR *m/z* 846.4 [(M+H)$^+$]; ESIMS-HR *m/z* calcd for $C_{40}H_{48}N_9O_{12}$ 846.3417, found 846.3422; $[\alpha]^{20}_D$ −6.1 (*c* 0.19, MeOH).

Fluorescence-based MraY assay. Reactions were carried out in a 384-well microplate. A solution containing 10 μM of UDP-MurNAc-dansylpentapeptide in 20 μL of an assay buffer (50 mM Tris-HCl (pH 7.6), 50 mM KCl, 25 mM $MgCl_2$, 0.2% Triton

X-100, 8% glycerol, 50 μM C55-P) was prepared. The reaction was initiated by the addition of *Staphylococcus aureus* MraY enzyme (55 ng/5 μL/well). After 3 h incubation at room temperature, the formation of dansylated lipid I was monitored by fluorescence enhancement (excitation at 355 nm, emission at 535 nm) by using infinite M200 microplate reader (Tecan). The inhibitory effects of each compound were determined in the MraY assays described above. The mixtures contained 2% dimethyl sulfoxide in order to increase the solubility of the compounds.

Evaluation of antibacterial activity. Minimum inhibitory concentrations (MICs) were determined by a microdilution broth method as recommended by the CLSI[54] with cation-adjusted Mueller-Hinton broth (CA-MHB). Serial two-fold dilutions of each compound were made in appropriate broth, and the strains were inoculated with 5 x 10^5 cfu/mL in 96-well plates (each 0.1 mL/well). The plates were incubated at 37 °C for 18 h and then MICs were determined.

Evaluation of cytotoxicity. Cytotoxic activity of the compounds against HepG2 cells was measured using Cell Counting Kit-8 according to manufacturer's protocol. Briefly, HepG2 cells (1×10^5 cells/well) in a 96 well plate were cultures in D-MEM (Low Glucose) medium containing 10% fetal bovine serum in the presence of test compounds at 37 °C

for 24 h under 5% CO_2 atmosphere. A solution of Cell Counting Kit-8 reagent in medium (1:10) was added. The plates were incubated at 37 °C for 2 h under 5% CO_2 atmosphere, then 450 nm absorbance was measured.

Modelling of complex structures of 2 bound to $MraY_{SA}$ and $MraY_{PA}$. The target amino acid sequences of $MraY_{SA}$ and $MraY_{PA}$ were retrieved from the UniProtKB database [accession number: Q6GHQ3 ($MraY_{SA}$), Q9HVZ8 ($MraY_{PA}$)]. X-ray crystal structure of $MraY_{Aa}$ in complex with muraymaicin D2 (PDB ID: 5CKR) was used as a template structure. The three-dimensional structures of $MraY_{SA}$ and $MraY_{PA}$ were generated by using SWISS-MODEL server, and each generated structure was superimposed on the template structure. The template structure was separated into protein and ligand structures, then, the ligand structures were combined with modeled structures to build initial complex structures. Finally, each complex structure was energy minimized using MacroModel with a GB/SA water solvent model to generate complex structure shown in Figure 5. All calculations were performed using OPLS3 force field, and heavy atoms of side chain of Phe262, Lys70, Asp196, Asn255, and uracil moiety of ligand were restrained during the calculation. Coordinates have been included in Supporting Information.

Continuous *in vitro* cultivation with 2 in *P. aeruginosa*. Continuous cultivation with MRD was performed using Muller Hinton broth II (MHB-II, Becton, Dickinson and Company, USA) containing sub-MIC of MRD (4 mg/L). The parent strain was used *P. aeruginosa* PAO1 (Day 0) and cultivated in MHB-II containing **2** overnight at 37 °C. Each 1 μL (approximately 1 x 10^6 CFU) of cell culture was inoculated into 1 ml of fresh MHB-II (1:1000, vol/vol) containing sub-MIC of MRD and incubated overnight at 37°C. This step was continued for 30 days, and strains derived from each day were determined MIC of MRD with reference to CLSI guidelines.[55]

Whole genome sequencing. The experiment was conducted in a manner similar to a procedure previously described. The genomic DNA of *P. aeruginosa* PAO1 (Day 0) and the MRD-resistant mutants derived at Days 1, 2, and 30 during continuous cultivation with sub-MIC of MRD (4 mg/L) was isolated using DNeasy Blood and Tissue Kit (Qiagen, Hilden, Germany). The isolated DNA was sequenced by MiSeq (Illumina, San Diego, CA) using Nextera XT DNA Library Prep Kit (Illumian). For the assembly, the contig was mapped with 300-bp paired-end reads to the genome of the parent strain followed by the polishing using CLC Genomic Workbench (Qiagen). Genome annotations were using DFAST based on PROKKA.[56] Comprehensive genetic comparison between *P. aeruginosa* PAO1 (Day 0) and the MRD-resistant mutants were

performed, and non-synonymous mutations were detected by CLC Genomic Workbench by sorting the obtained contig count frequency was more than 70%.

Supporting Information

The Supporting Information is available free of charge at https://pubs.acs.org/doi/xxxxxxxx. Preparation of compounds, ^{1}H, ^{13}C NMR spectrum of compounds, Chromatograms of LC-MS analysis, Data of cell viability assay, Data of MraY inhibitory assay, Coordinates of $MraY_{SA}$ and $MraY_{PA}$ docked with **2**, and Structures with SMILES codes (CSV).

Corresponding Author

Satoshi Ichikawa - Faculty of Pharmaceutical Sciences, Hokkaido University, Kita-12, Nishi-6, Kita-ku, Sapporo 060-0812, Japan, Center for Research and Education on Drug Discovery, Faculty of Pharmaceutical Sciences, Hokkaido University, Kita-12, Nishi-6, Kita-ku, Sapporo 060-0812, Japan, Global Station for Biosurfaces and Drug Discovery, Global Institution for Collaborative Research and Education (GI-CoRE), Hokkaido University, Kita-12, Nishi-6, Kita-ku, Sapporo 060-0812, Sapporo, Japan

Yuma Terasawa - Faculty of Pharmaceutical Sciences, Hokkaido University, Kita-12, Nishi-6, Kita-ku, Sapporo 060-0812, Japan

Chisato Sataka - Faculty of Pharmaceutical Sciences, Hokkaido University, Kita-12, Nishi-6, Kita-ku, Sapporo 060-0812, Japan

Toyotaka Sato - Department of Microbiology, Sapporo Medical University School of Medicine, South-1, West-17, Chuo-ku, Sapporo, 060-8556, Japan

Kazuki Yamamoto - Faculty of Pharmaceutical Sciences, Hokkaido University, Kita-12, Nishi-6, Kita-ku, Sapporo 060-0812, Japan

Yukari Fukushima - Division of Bioresources, Hokkaido University Research Center for Zoonosis Control, Sapporo, 001-0020, Japan, Global Station for Zoonosis Control, Global Institution for Collaborative Research and Education (GI-CoRE), Hokkaido University, Kita-20, Nishi-10, Kita-ku, Sapporo, 001-0020, Japan

Chie Nakajima - Division of Bioresources, Hokkaido University Research Center for Zoonosis Control, Sapporo, 001-0020, Japa*n,* Global Station for Zoonosis Control, Global Institution for Collaborative Research and Education (GI-CoRE), Hokkaido University, Kita-20, Nishi-10, Kita-ku, Sapporo, 001-0020, Japan

Yasuhiko Suzuki - Division of Bioresources, Hokkaido University Research Center for Zoonosis Control, Sapporo, 001-0020, Japa*n,* Global Station for Zoonosis Control, Global Institution for Collaborative Research and Education (GI-CoRE), Hokkaido University, Kita-20, Nishi-10, Kita-ku, Sapporo, 001-0020, Japan

Akira Katsuyama - Faculty of Pharmaceutical Sciences, Hokkaido University, Kita-12, Nishi-6, Kita-ku, Sapporo 060-0812, Japan, Center for Research and Education on Drug Discovery, Faculty of Pharmaceutical Sciences, Hokkaido University, Kita-12, Nishi-6, Kita-ku, Sapporo 060-0812, Japan

Takanori Matsumaru - Faculty of Pharmaceutical Sciences, Hokkaido University, Kita-12, Nishi-6, Kita-ku, Sapporo 060-0812, Japan, Center for Research and Education on Drug Discovery, Faculty of Pharmaceutical Sciences, Hokkaido University, Kita-12, Nishi-6, Kita-ku, Sapporo 060-0812, Japan. Current affiliation: Department of Chemistry, Faculty of Science and Technology, Keio University, Hiyoshi 3-14-1, Minatokita-ku, Yokohama, 223-8522, Japan

Fumika Yakushiji - Faculty of Pharmaceutical Sciences, Hokkaido University, Kita-12, Nishi-6, Kita-ku, Sapporo 060-0812, Japan, Center for Research and Education on Drug Discovery, Faculty of Pharmaceutical Sciences, Hokkaido University, Kita-12, Nishi-6, Kita-ku, Sapporo 060-0812, Japan

Shin-ichi Yokota - Department of Microbiology, Sapporo Medical University School of Medicine, South-1, West-17, Chuo-ku, Sapporo, 060-8556, Japan

Author Contributions

All authors have given approval to the final version of the manuscript.

Notes

The authors declare no competing financial interest.

Acknowledgement

We thank Ms. Chihiro Inagaki, Mr. Kousuke Nakamura, and Mr. Naoto Tokoro for initial investigation for the synthesis of **2**. This research was supported in part by JSPS KAKENHI Grant-in-Aid for Scientific Research (B) (Grant Number 16H05097 and 19H03345 to S.I.), Grant-in Aid for Scientific Research on Innovative Areas “Frontier Research on Chemical Communications” (No 18H04599 and 20H04757 to S.I.), JSPS KAKENHI Grant-in-Aid for Research for Young Scientist (Grant Number JP19K16648 to T.S.), Takeda Foundation, The Tokyo Biomedical Research Foundation and was partly supported by Hokkaido University, Global Facility Center (GFC), Pharma Science Open Unit (PSOU), funded by MEXT under "Support Program for Implementation of New Equipment Sharing System", Platform Project for Supporting Drug Discovery and Life

Science Research (Basis for Supporting Innovative Drug Discovery and Life Science Research (BINDS)) from AMED under Grant Number JP18am0101093j0002, AMED under Grant Number JP19ak0101118h0001, Japan Initiative for Global Research Network on Infectious Diseases (J-GRID) from the Ministry of Education, Culture, Sport, Science, and Technology in Japan, and MEXT for the Joint Research Program of the Research Center for Zoonosis Control, Hokkaido University.

Abbreviations

Alloc, allyloxycarbonyl; BOM, benzyloxymethyl; HATU, 1-[bis(dimethylamino)methylene]-1*H*-1,2,3-triazolo[4,5-*b*]pyridinium 3-oxide hexafluorophosphate; HepG2, human hepatocellular carcinoma; MIC, minimum inhibitory concentration; MraY, phospho-MurNAc-pentapeptide transferase; MRD, mureidomycn; MRY, muraymycin; *m*Tyr, *m*-tyrosine; NppA1A2BCD, nucleoside peptide permease; PCD, pacidamycin; SAR, structure-activity relationship

References

1. Hagiya, H.; Tanaka, T.; Takimoto, K.; Yoshida, H.; Yamamoto, N.; Akeda, Y.; Tomono, K. Non-nosocomial healthcare-associated left-sided *Pseudomonas aeruginosa* endocarditis: a case report and literature review. *BMC Infect*. *Dis*. **2016**, *16*, 431-437.
2. Marcus, N.; Ashkenazi, S.; Samra, Z.; Cohen, A.; Livni, G. Community-acquired *Pseudomonas aeruginosa* urinary tract infections in children hospitalized in a tertiary center: relative frequency, risk factors, antimicrobial resistance and treatment. *Infection* **2008**, *36*, 421-426.
3. Obritsch, M. D.; Fish, D. N.; MacLaren, R.; Jung, R. Nosocomial infections due to multidrug-resistant *Pseudomonas aeruginosa*: epidemiology and treatment options. *Pharmacotherapy* **2005**, *25*, 1353-1364.
4. Sonmezer, M. C.; Ertem, G.; Erdinc, F. S.; Kaya Kilic, E.; Tulek, N.; Adiloglu, A.; Hatipoglu, C. Evaluation of risk factors for antibiotic resistance in patients with nosocomial infections caused by. *Pseudomonas aeruginosa*. *Can*. *J*. *Infect Dis Med*. *Microbiol* **2016**, *2016*, 1-9.
5. Tam, V. H.; Chang, K. T.; Abdelraouf, K.; Brioso, C. G.; Ameka, M.; McCaskey, L. A.; Weston, J. S.; Caeiro, J. P.; Garey, K. W. Prevalence, resistance mechanisms, and susceptibility of multidrug-resistant bloodstream

isolates of *Pseudomonas aeruginosa*. *Antimicrob. Agents Chemother.* **2010**, *54*, 1160-1164.

6. Page, M. G.; Heim, J. Prospects for the next anti-Pseudomonas drug. *Curr. Opin. Pharmacol.* **2009**, *9*, 558-565.
7. Scheld, M.; Spellberg, B.; Bartlett, J. Bad Bugs, No drugs: no ESKAPE! An update from the Infectious Diseases Society of America. *Clin. Infect. Dis.* **2009**, *48*, 1-12.
8. Payne, D. J.; Gwynn, M. N.; Holms, D. J.; Pompliano, D. L. Drugs for bad bugs: confronting the challenges of antibacterial discovery. *Nature Rev. Drug Discov*. **2007**, *6*, 29-40.
9. Talbot, G. H.; Bradley, J.; Edwards, J. E. Jr.; Gilbert, D.; Scheld, M.; Bartlett, J. G. Bad Bugs Need Drugs: An update on the development pipeline from the antimicrobial availability task force of the Infectious Diseases Society of America. *Clin. Infect. Dis*. **2006**, *42*, 657-668.
10. Overbye, K. M.; Barrett. J. F. Antibiotics: where did we go wrong? *Drug Discov. Today* **2005**, *10*, 45-52.
11. Monagham, R. L.; Barrett, J. F. Antibacterial drug discovery-then, now and the genomics future. *Biochem. Pharmacol*. **2006**, *71*, 901-909.

12. Walsh, C. Where will new antibiotics come from? *Nature Rev. Microbiol*. **2003**, *1*, 65-70.

13. Winn, M.; Goss, R. J. M.; Kimura, K.-I.; Bugg, T. D. H. Antimicrobial nucleoside antibiotics targeting cell wall assembly: Recent advances in structure–function studies and nucleoside biosynthesis. *Nat. Prod. Rep*. **2010**, *27*, 279-304.

14. Kimura, K.-I.; Bugg, T. D. H. Recent advances in antimicrobial nucleoside antibiotics targeting cell wall biosynthesis. *Nat. Prod. Rep*. **2003**, *20*, 252-273.

15. a) Inukai, M.; Isono, F.; Takahashi, R.; Enokita, S.; Sakaida Y.; Haneishi, T. Mureidomycins A-D, novel peptidyl nucleoside antibiotics with spheroplast forming activity. I. Taxonomy, fermentation, isolation and physicochemical properties. *J. Antibiot.* **1989**, *42*, 662-666. b) Isono, F.; Katayama, T.; Inukai, M.; Haneishi, T. Mureidomycins A-D, novel peptidylnucleoside antibiotics with spheroplast forming activity. III. Biological properties. *J. Antibiot.* **1989**, *42*, 674-679. c) Isono, F.; Inukai, M.; Takahashi, S.; Haneishi, T.; Kinoshita, T.; Kuwano, H. Mureidomycins A-D, novel peptidyl nucleoside antibiotics with spheroplast forming activity. II. Structural elucidation. *J. Antibiot.* **1989**, *42*, 667-673. d) Isono, F.; Sakaida, Y.; Takahashi, S.; Kinoshita, T.; Nakamura, T.; Inukai, M. Mureidomycins E and F, minor components of mureidomycins. *J. Antibiot.* **1993**, *46*, 1203-1207.

16. Chaterjee, S.; Nadkami, S. R.; Vijayakumar, E. K. S.; Patel, M. V.; Ganguli, B. N. Napsamycins, new Pseudomonas active antibiotics of the mureidomycin family from Streptomyces sp. HIL Y-82,11372. *J. Antibiot*. **1994**, *47*, 595-598.

17. a) Karwowski, J. P.; Jackson, M.; Theriault, R. J.; Chen, R. H.; Barlow. G. J. Maus, M. L. Pacidamycins, a novel series of antibiotics with anti-Pseudomonas aeruginosa activity. I. Taxonomy of the producing organism and fermentation. *J. Antibiot*. **1989**, *42*, 506-511. b) Chen, R. H.; Buko, A. M.; Whittern, D. N.; McAlpine, J. B. Pacidamycins, a novel series of antibiotics with anti-Pseudomonas aeruginosa activity. II. Isolation and structural elucidation. *J. Antibiot.*, **1989**, *42*, 512-520. c) Fernandes, P. B.; Swanson, R. N.; Hardy, D. J.; Hanson, C. W. Coen, L.; Rasmussen, R. R.; Chen, R. H. Pacidamycins, a novel series of antibiotics with anti-Pseudomonas aeruginosa activity. III. Microbiologic profile. *J. Antibiot.* **1989**, *42*, 521-526. d) Fronko, R. M.; Lee, J. C.; Galazzo, J. G.; Chamberland, S.; Malouin, F.; Lee, M. D. New pacidamycins produced by *Streptomyces coeruleorubidus*, NRRL 18370**.** *J. Antibiot.* **2000**, *53*, 1405-1410.

18. a) Xie, X. Y.; Chen, R. X.; Si, S. Y.; Sun, C. H. Xu, H. Z. A new nucleosidyl-peptide antibiotic, sansanmycin. *J. Antibiot*. **2007**, *60*, 158-162. b) Xie, X. Y.; Xu, H. Z.; Si,

S. Y.; Sun, C. H. Chen, R. X. Sansanmycins B and C, new components of sansanmycins. *J. Antibiot*. **2008**, *61*, 237-240.

19. Isono, F.; Inukai, M. Mureidomycin A, a new inhibitor of bacterial peptidoglycan synthesis. *Antimicrob. Agents Chemother*. **1991**, *35*, 234-236.

20. Inukai, M.; Isono, F.; Takatsuki, A. Selective inhibition of the bacterial translocase reaction in peptidoglycan synthesis by mureidomycins. *Antimicrob. Agents Chemother*. **1993**, *37*, 980-983.

21. a) Bugg, T. D. H.; Lloyd, A. J.; Roper, D. I. Phospho-MurNAc-pentapeptide translocase (MraY) as a target for antibacterial agents and antibacterial proteins. *Infect*. *Dis*. *Drug Targets* **2006**, *6*, 85-106. b) Kimura, K.; Bugg, T. D. H. Recent advances in antimicrobial nucleoside antibiotics targeting cell wall biosynthesis. *Nat. Prod. Rep*. **2003**, *20*, 252-273.

22. Bouhss, A.; Mengin-Lecreulx, D.; Le Beller, D.; Van Heijenoort, J. Topological analysis of the MraY protein catalyzing the first membrane step of peptidoglycan synthesis. *Mol. Microbiol*. **1999**, *34*. 576-585.

23. Bouhss, A.; Trunkfield, A. E.; Bugg, T. D.; Mengin-Lecreulx, D. The biosynthesis of peptidoglycan lipid-linked intermediates. *FEMS Microbiol. Rev.* **2008**, *32*, 208-33.

24. Al-Dabbagh, B.; Henry, X.; El Ghachi, M.; Auger, G.; Blanot, D.; Parquet, C.; Mengin-Lecreulx, D.; Bouhss, A. Active site mapping of MraY, a member of the polyprenyl-phosphate *N*-acetylhexosamine 1-phosphate transferase superfamily, catalyzing the first membrane step of peptidoglycan biosynthesis. *Biochemistry* **2008**, *47*, 8919-8928.

25. Review of MraY inhibitors; a) Fer, M. J.; Le Corre, L.; Pietrancosta, N.; Evard-Todeschi, N.; Olatunji, S.; Bouhss, A.; Calvet-Vitale, S.; Gravier-Pelletier, C. Bacterial transferase MraY, a source of inspiration towards new antibiotics. *Curr. Med. Chem*. **2018**, *25*, 6013-6029. b) Katsuyama, A.; Ichikawa, S. Synthesis and medicinal chemistry of muraymycins nucleoside antibiotics. *Chem. Pharm. Bull.* **2018**, *66*, 123-131. c) Wiegmann, D.; Koppermann, S.; Wirth, M.; Niro, G.; Leyerer, K.; Ducho, C. Muraymycin nucleoside-peptide antibiotics: uridine-derived natural products as lead structures for the development of novel antibacterial agents. *Beilstein J. Org. Chem.* **2016**, *12*, 769-795. d) Bugg, T. D. H.; Rodolis, M. T.; Mihalyi, A.; Jamshidi, S. Inhibition of phospho-MurNAc-pentapeptide translocase (MraY) by nucleoside natural product antibiotics, bacteriophage ϕX174 lysis protein E, and cationic antibacterial peptides. *Bioorg. Med. Chem.* **2016**, *24*, 6340-6347. e) Ichikawa, S. Function-oriented synthesis: how to design simplified analogues of antibacterial

nucleoside natural products? *Chem. Rec.* **2016**, *16*, 1106-1115. f) Ichikawa, S.; Yamaguchi, M.; Matsuda, A. Antibacterial nucleoside natural products inhibiting phosphor-MurNAc-pentapeptide translocase; chemistry and structure-activity relationship. *Curr. Med. Chem*. **2015**, *22*, 3951-3979. g) Winn, M.; Goss, R. J. M.; Kimura, K.; Bugg, T. D. H. Antimicrobial nucleoside antibiotics targeting cell wall assembly: Recent advances in structure–function studies and nucleoside biosynthesis. *Nat. Prod. Rep.* **2010**, *27*, 279-304. h) Ichikawa, S.; Matsuda, A. Nucleoside natural products and related analogs with potential therapeutic properties as antibacterial and antiviral agents. *Expert Opin. Ther. Pat.* **2007**, *17*, 487-498. i) Bugg, T. D. H.; Lloyd, A. J.; Roper, D. I. Phospho-MurNAc-pentapeptide translocase (MraY) as a target for antibacterial agents and antibacterial proteins. *Infect*. *Dis*. *Drug Targets* **2006**, *6*, 85-106. j) Kimura, K.; Bugg, T. D. H. Recent advances in antimicrobial nucleoside antibiotics targeting cell wall biosynthesis. *Nat. Prod. Rep*. **2003**, *20*, 252-273.

26. a) Mistry, Anita.; Warren, M. S.; Cusick, J. K.; Karkhoff-Schweizer, R. R. Lomovskaya, O.; Schweizer. H. P. High-level pacidamycin resistance in *Pseudomonas aeruginosa* is mediated by an Opp oligopeptide permease encoded by the *opp-fabI* operon. *Antimicrob. Agents Chemther.* **2013**, *57*, 5565-5571. b) Pletzer, D.; Braun, Y.; Dubiley, S.; Lafon, C.; Kohler, T.; Page, M. G. P.; Mourez, M.;

Severinov, K.; Weingart, Helge. The *Pseudomonas aeruginosa* PA14 ABC transporter NppA1A2BCD is required for uptake of peptidyl nucleoside antibiotics. *J. Bacteriol.* **2015**, *197*, 2217-2228.

27. Okamoto, K.; Sakagami, M.; Feng, F.; Togame, H.; Takemoto, H.; Ichikawa, S.; Matsuda A. Total synthesis of pacidamycin D by $Cu^{(I)}$-catalyzed oxy enamide formation. *Org. Lett.* **2011**, *13,* 5240-5243.

28. Okamoto, K.; Sakagami, M.; Feng, F.; Togame, H.; Takemoto, H.; Ichikawa, S.; Matsuda A. Total synthesis and biological evaluation of pacidamycin D and its 3′-hydroxy analogue. *J. Org. Chem*. **2012**, *77*, 1367-1377.

29. Gentle, C. A.; Harrison, S. A.; Inukai, M.; Bugg, T. D. H. Structure-function studies on nucleoside antibiotic mureidomycin A: synthesis of 5'-functionalized uridine models**.** *J. Chem. Soc. Perkin Trans. 1* **1999**, 1287-1294.

30. Bozzoli, A.; Kazmierski, W.; Kennedy, G.; Pasquarello, A.; Pecunioso, A. A solid-phase approach to analogues of the antibiotic mureidomycin**.** *Bioorg. Med. Chem. Lett*. **2000**, *10*, 2759-2763.

31. Boojamra, C. G.; Lemoine, R. C.; Lee, J. C.; Léger, R.; Stein, K. A.; Vernier, N. G.; Magon, A.; Lomovskaya, O.; Martin, P. K.; Chamberland, S.; Lee, M. D.; Hecker, S.

J.; Lee, V. J. Stereochemical elucidation and total synthesis of dihydropacidamycin D, a semisynthetic pacidamycin. *J. Am. Chem. Soc.* **2001**, *123*, 870-874.

32. Lemoine, R. C.; Magon, A.; Hecker, S. Synthesis of base-modified dihydropacidamycins. *Bioorg. Med. Chem. Lett*. **2002**, *12*, 1121-1123.

33. Boojamra, C. G.; Lemoine, R. C.; Blais, J.; Vernier, N. G.; Stein, K. A.; Magon, A.; Chamberland, S.; Hecker, S. J.; Lee, V. J. Synthetic dihydropacidamycin antibiotics: a modified spectrum of activity for the pacidamycin class. *Bioorg. Med. Chem. Lett*. **2003**, *13*, 3305-3309.

34. Howard, N. I.; Bugg, T. D. H. Synthesis and activity of 5'-uridinyl dipeptide analogues mimicking the amino terminal peptide chain of nucleoside antibiotic mureidomycin A. *Bioorg. Med. Chem.* **2003**, *11*, 3083-3099.

35. Sun, D. Q.; Jones, V.; Carson, E. I.; Lee, R. E. B.; Scherman, M. S.; McNeil, M. R.; Lee, R. E. Solid-phase synthesis and biological evaluation of a uridinyl branched peptide urea library. *Bioorg. Med. Chem. Lett.* **2007**, *17*, 6899-6904.

36. Gruschow, S.; Rackham, E. J.; Elkins, B.; Newill, P.; Hill, L. M.; Goss, R. J. M. New pacidamycin antibiotics through precursor-directed biosynthesis. *ChemBioChem* **2009**, *10*, 355-360.

37. Roy, A. D.; Grüschow, S.; Cairns, N.; Goss, R. J. M. Gene expression enabling synthetic diversification of natural products: chemogenetic generation of pacidamycin analogs. *J. Am. Chem. Soc*. **2010**, *132*, 12243-12245.

38. Okamoto, K.; Sakagami, M.; Feng, F.; Fumiyo, T.; Kouichi, U.; Togame, H.; Takemoto, H.; Ichikawa, S.; Matsuda A. Synthesis of pacidamycin analogue via an Ugi-multicomponent reaction. *Bioorg. Med. Chem*. *Lett.* **2012**, *22*, 4810-4815.

39. Tran, A. T.; Watson, E. E.; Pujari, V.; Conroy, T.; Dowman, L. J.; Giltrap, A. M.; Pang, A.; Wong, W. R.; Linington, R. G.; Mahapatra, S.; Saunders, J. S. Charman, A.; West, N. P. Bugg, T. D. H.; Tod, J.; Dowson, C. G.; Roper, D. I.; Crick, D. C.; Britton, W. J.; Payne, R. J. Sansanmycin natural product analogues as potent and selective anti-mycobacterials that inhibit lipid I biosynthesis. *Nat. Commun*. **2017**, *8*, 14414.

40. Mashalidis, E. H.; Kaeser, B.; Terasawa, Y.; Katsuyama, A.; Kwon, D.-Y.; Lee, K.; Hong, J.; Ichikawa, S.; Lee, S.-Y. Chemical logic of MraY inhibition by antibacterial nucleoside natural products. *Nat. Commun*. **2019**, 10, 2917.

41. Chiba, T.; Hosono, H.; Nakagawa, K.; Asaka, M.; Takeda, H.; Matsuda, A.; Ichikawa, S. Total synthesis of syringolin A and its improvement of biological activity. *Angew. Chem. Int. Ed.* **2014**, *126*, 4936-4939.

42. Stachyra, T.; Dini, C.; Ferrari, P.; Bouhss, A.; van Heijenoort, J.; Mengin-Lecreulx, D.; Blanot, D.; Biton, J.; Le Beller, D. Fluorescence detection-based functional assay for high-throughput screening for MraY. *Antimicrob. Agents Chemother.* **2004**, *48*, 897-902.

43. Katsuyama, A.; Sato, K.; Yakushiji, F.; Matsumaru, T.; Ichikawa, S. Solid-phase modular synthesis of Park nucleotide and lipid I and lipid II analogues. *Chem. Phar. Bull*. **2018**, *66*, 84-95.

44. Chung, B. C.; Mashalidis, E. H.; Tanino, T.; Kim, M.; Matsuda, A.; Hong, Ji.; Ichikawa, S.; Lee, Seok-Yong. Structural insights into inhibition of lipid I production in bacterial cell wall synthesis. *Nature*, **2016**, *533,* 557-561.

45. Chung, B. C.; Zhao, J.; Gillespie, R. A.; Kwon, D.-Y.; Guan, Z.; Hong, J.; Zhou, P.; Lee, S.-Y. Crystal structure of MraY, an essential membrane enzyme for bacterial cell wall synthesis. *Science* **2013**, *341*, 1012–1016.

46. Waterhouse, A., Bertoni, M., Bienert, S., Studer, G., Tauriello, G., Gumienny, R., Heer, F.T., de Beer, T.A.P., Rempfer, C., Bordoli, L., Lepore, R., Schwede, T. SWISS-MODEL: homology modelling of protein structures and complexes. *Nucleic Acids Res.* **2018**, *46*, W296-W303.

47. Takeoka, Y.; Tanino, T.; Sekiguchi, M.; Yonezawa, S.; Sakagami, M.; Takahashi, F.; Togame, H.; Tanaka, Y.; Takemoto, H.; Ichikawa, S.; Matsuda, A. Expansion of antibacterial spectrum of muraymycins toward *Pseudomonas aeruginosa*. *ACS Med. Chem. Lett.* **2014**, *5*, 556-560.

48. Tanino, T.; Al-Dabbagh, B.; Mengin-Lecreulx, D.; Bouhss, A.; Oyama, H.; Ichikawa, S.; and Matsuda, A. Mechanistic analysis of muraymycin analogues: a guide to the design of MraY inhibitors. *J. Med. Chem.* **2011**, *54*, 8421-8439.

49. a) Brandish, P. E.; Burnham, M. K.; Lonsdale, J. T.; Southgate, R.; Inukai, M.; Bugg, T. D. H. Slow binding inhibition of phospho-*N*-acetylmuramyl-pentapeptide-translocase (*Escherichia coli*) by mureidomycin A. *J. Biol. Chem*. **1996**, *271*, 7609-7614. b) Brandish, P. E.; Kimura, K.; Inukai, M.; Southgate, R.; Lonsdale, J. T.; Bugg, T. D. H. Modes of action of tunicamycin, liposidomycin B, and mureidomycin A: inhibition of phospho-*N*-acetylmuramyl-pentapeptide translocase from *Escherichia coli*. *Antimicrob. Agents. Chemother*. **1996**, *40*, 1640-1644.

50. Gentle, C. A.; Bugg, T. D. H. Role of the enamide linkage of nucleoside antibiotic mureidomycin A: synthesis and reactivity of enamide-containing analogues *J. Chem. Soc. Perkin Trans*. 1, **1999**, 1279–1286.

51. Gotoh, N.; Murata, T.; Ozaki, T.; Kimura, T.; Kondo, A.; Nishino, T. Intrinsic resistance of *Escherichia coli* to mureidomycin A and C due to expression of the multidrug efflux system AcrAB-TolC: comparison with the efflux systems of mureidomycin-susceptible *Pseudomonas aeruginosa*. *J. Infect. Chemother.* **2003**, *9*, 101-103.

52. Rodolis, M. T.; Mihalyi, A.; Ducho, C.; Eitel, K.; Gust, B.; Gos, R. J. M.; Bugg, T. D. H. Mechanism of action of the uridyl peptide antibiotics: an unexpected link to a protein-prptein interaction site in translocase MraY. *Chem. Commun*. **2014**, *50*, 13203-13025.

53. Bernhardt, T. G.; Roof, W. D.; Young, R. Genetic evidence that the bacteriophage ϕX174 lysis protein inhibits cell wall synthesis. *Proc. Natl. Acad. Sci. U. S. A.* 2000, *97*, 4297-4302.

54. Bernhardt, T. G.; Struck, D.; Young, K. R. The lysis protein E of ϕX174 is a specific inhibitor of the MraY-catalyzed step in peptidoglycan synthesis. *J. Biol. Chem.* 2001, *276*, 6093-6097.

55. Clinical and Laboratory Standards Institute. 2017. Performance standards for antimicrobial susceptibility testing; 27th informational supplement .CLSI M100-S27. Clinical and Laboratory Standards Institute, Wayne, PA.

56. Tanizawa, Y.; Fujisawa, T.; Kaminuma, E.; Nakamura, Y.; Arita, M. DFAST and DAGA: web-based integrated genome annotation tools and resources. *Biosci Microbiota Food Health* **2016**, *35*, 173-184.

Table of Contents graphic

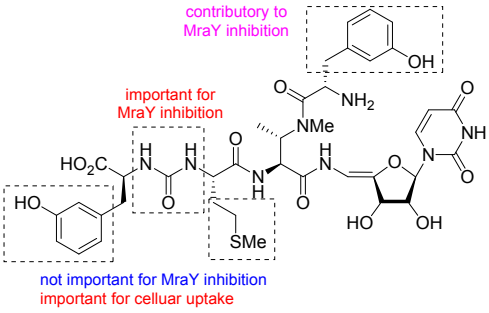

3'-hydroxymureidomycin A

IC_{50} for $MraY_{SA}$	**1.2 nM**
MIC for P. aeruginosa PAO1	**4-16 μg/mL**